Characterization of Tropical Agricultural Soil Microbiomes After Biochar Amendment

by

Julian Yu

A Dissertation Presented in Partial Fulfillment
of the Requirements for the Degree
Doctor of Philosophy

Approved April 2020 by the
Graduate Supervisory Committee:

C. Ryan Penton, Co-Chair
Hinsby Cadillo-Quiroz, Co-Chair
Ferran Garcia-Pichel
Sharon Hall

ARIZONA STATE UNIVERSITY

May 2020

ABSTRACT

Modern agriculture faces multiple challenges: it must produce more food for a growing global population, adopt more efficient and sustainable management strategies, and adapt to climate change. One potential component of a sustainable management strategy is the application of biochar to agricultural soils. Biochar is the carbon-rich product of biomass pyrolysis, which contains large proportions of aromatic compounds that influence its stability in soil. Concomitant with carbon sequestration, biochar has the potential to increase soil fertility through increasing soil pH, moisture and nutrient retention. Changes in the soil physical and chemical properties can result in shifts in the soil microbiome, which are the proximate drivers of soil processes. This dissertation aims to determine the compositional and functional changes in the soil microbial community in response to the addition of a low-volatile matter biochar. First, the impact of biochar on the bacterial community was investigated in two important agricultural soils (Oxisol and Mollisol) with contrasting fertility under two different cropping systems (conventional sweet corn and zero-tillage napiergrass) one month and one year after the initial addition. This study revealed that the effects of biochar on the bacterial community were most pronounced in the Oxisol under napiergrass cultivation, however soil type was the strongest determinant of the bacterial community. A follow-up study was conducted using shotgun metagenomics to probe the functional community of soil microcosms, which contained Oxisol soil under napiergrass two years after the initial addition of biochar. Biochar significantly increased total carbon in the soils but had little impact on other soil properties. Theses analyses showed that biochar-amended soil microcosms exhibited significant shifts in the functional community and key metabolic pathways

related to carbon turnover and denitrification. Given the distinct alterations to the biochar-amended community, deoxyribose nucleic acid (DNA) stable isotope probing was used to target the active populations. These analyses revealed that biochar did not significantly shift the active community in soil microcosms. Overall, these results indicate that the impact of biochar on the active soil community is transient in nature. Yet, biochar may still be a promising strategy for long-term carbon sequestration in agricultural soils.

DEDICATION

I dedicate this work to my family who first taught me the value of education and critical thought. To my wonderful parents and grandma, thank you for doing everything in your power to give me the opportunities I have had in life, anything is achievable knowing I have you. To my sister Tiffany and brother Henry, thank you for your invaluable advice and consistent encouragement. Thank you Jonathan, for all your love and support throughout this odyssey. To my beloved nephew Owen, I hope this inspires you to explore the world around you and to become the person you desire to be.

A special thanks to all my friends for the love, company and laughs. I would like to thank Alexandria Page for your never-ending friendship, for listening to all my ramblings, and for sending cards and gifts. To Nicole Jaycox, thank you for all of your support, for cheering me on and for bringing me meals when I was too busy to cook. Thank you, you all make me enormously happy.

ACKNOWLEDGMENTS

I take this opportunity to express my deepest gratitude to number of people that have contributed to my personal and professional development during this endeavor. First, I would like to thank my advisor, Dr. Christopher Ryan Penton, who is abundantly helpful and offered invaluable assistance, support, and guidance from the very beginning of this research as well as giving me extraordinary experiences throughout this work. I am deeply appreciative of the opportunities you gave me to present my research nationally and internationally. I thank you for allowing me the independence throughout my research as well as introducing me to a number of collaborators to work with.

I would like to express my gratitude to my supervisory committee Dr. Hinsby Cadillo-Quiroz, Dr. Sharon Hall and Dr. Ferran Garcia-Pichel for their all their helpful feedback and suggestions throughout my research. I would also like to acknowledge the generosity and friendship of the Cadillo lab members: Steffen Büssecker, Mark Reynolds, Analissa Sarno, Mike Pavia. Analissa, thank you for your assistance on numerous occasions especially with fractionation; Mark and Steffen for training me on the various equipment. Mike, thank you for your helping with the metagenomics and for indulging all of my coffee breaks. I would also like to thank Dr. Damien Finn and Dr. Rajeev Misra, it is always nice to bounce ideas and I appreciate the guidance, editing assistance, and for advice on achieving my PhD and career goals.

This project would not be possible without Dr. Susan Crow, Lauren Deem and Dr. Jonathan Deenik at the University of Manoa. Thank you for maintaining the field experiment, sample collection and running the soil chemical analysis, input on the experiment and all the helpful question and feedback.

I would like to acknowledge the United States Department of Agriculture National Institute of Food and Agriculture (USDA-NIFA 2012-67020-30234), and USDA-NIFA Hatch project (HAW01130-H) managed by the College of Tropical Agriculture and Human Resources. I would also like to acknowledge financial support from Arizona State University School of Life Sciences for awarding me the Completion Fellowship, as well as teaching assistantships and conference travel grants.

TABLE OF CONTENTS

Page

LIST OF TABLES viii

LIST OF FIGURES x

LIST OF ABBREVIATIONS xii

CHAPTER

1 INTRODUCTION 1

Sustainable Agriculture to Mitigate Climate Change 1

Biochar as a Soil Amendment 2

Biochar Effects on the Soil Microbiome 5

Dissertation Framework 8

2 BIOCHAR APPLICATION INFLUENCES MICROBIAL ASSEMBLAGE COMPLEXITY AND COMPOSITION DUE TO SOIL AND BIOENERGY CROP TYPE INTERACTIONS 13

Introduction 13

Materials and Methods 16

Results 21

Discussion and Conclusion 33

3 COMPARATIVE METAGENOMICS REVEALS ENHANCED NUTRIENT CYCLING POTENTIAL AFTER 2 YEARS OF BIOCHAR AMENDMENT IN A TROPICAL OXISOL 41

Introduction 41

Materials and Methods 44

CHAPTER Page

Results 49

Discussion and Conclusion 66

4 DNA-STABLE ISOTOPE PROBING SHOTGUN METAGENOMES REVEALS RESILIENCE OF ACTIVE SOIL MICROBIAL COMMUNITIES TO BIOCHAR AMENDMENT IN AN OXISOL SOIL 75

Introduction 75

Materials and Methods 79

Results 86

Discussion and Conclusion 98

5 CONCLUSION 107

REFERENCES 111

APPENDIX

A MICROBIAL COMMUNITY STRUCTURE AND SOIL METADATA SUPPORTING FINDINGS OF CHAPTER 3 139

B CROP DATA, METAGENOMIC STATISTICS AND RESULTS SUPPORTING FINDS OF CHAPTER 4 152

C METAGENOMIC STATISTICS AND GENOMIC BINNIG RESULTS SUPPORTING FINDINGS OF CHAPTER 5 176

LIST OF TABLES

Table Page

2.1. Diversity Indices According to Soil Type, Cropping System and Biochar Treatment. 22

2.2. Topological Properties of Molecular Ecological Networks of Bacterial Communities under Biochar Amendment. 27

3.1. Soil Characteristics of the Oxisol Used in the Microcosms. 51

4.1. Metagenomic Sequence and Assembly Summary 89

A1. Mean Values and Standard Error of Measured Soil Chemical Properties. 145

A2. Permutational ANOVA (PERMANOVA) of Microbial Community Between Soil, Cropping System, Sampling Period, Biochar Treatment, and the Interactions. 146

A3. ANOVA Table of Aligned Rank Transformed Diversity Indices According to Soil Type, Biochar Treatment, Cropping System, and Sampling Time. 147

A4. Permutational Dispersion (PERMDISP) Test of Homogeneity of Dispersion with Corresponding T-test Results Comparing Biochar and No Biochar Treatments under Each Crop/Soil Type Group 148

A5. Detailed Lineage for Module Hubs and Connectors from Figure 2.2 149

A6. Network Properties of 100 Randomized Networks of the Oxisol and Mollisol Control and Biochar Networks. 151

B1. Sequencing and Assembly Statistics for Each Soil Metagenome 156

B2. Statistics of Metagenomes Analyzed Through MG-RAST 157

Table Page

B3. Alpha Diversity Estimates of Samples Used in This Study Based on rRNA Gene-Encoded Reads 158

B4. Differentially Abundant SEED Subsystems (Levels 1 – 3) Between Biochar-amended and Control Metagenomes. 159

C1. Soil Properties per Plot in Microcosms Incubated with ^{13}C-labeled Perennial Ryegrass. 179

C2. Significant and Nearly Significant Results Differentially Abundant KO Terms Between Biochar-amended and Control Metagenomes. 180

C3. Characteristics of Medium- and High-quality Genome Bins 182

LIST OF FIGURES

Figure Page

2.1. Non-metric Multi-dimensional Scaling (nMDS) Plot Depicting Differences in Bacterial Community Composition.....24

2.2. Topological Roles of Otus Based on Distribution of Nodes on Zi (Within Module) Vs. Pi (among Module) Connectivity Scatter Plot.....28

2.3. Molecular Ecological Network Analysis of the Oxisol.....30

2.4. Molecular Ecological Network Analysis of the Mollisol.....31

3.1. Cumulative CO_2 Production over a 14-day Incubation Period.....52

3.2. Average Metagenomic Coverage.....54

3.3. Shifts in Taxon Abundance as Effects of Biochar Amendment.....57

3.4. Significant Changes in Abundance of Carbohydrates Pathways as an Effect of Biochar Addtion.....60

3.5. Significant Changes in Abundance of Different Pathways in Respiration, Metabolism of Aromatic Compounds, and Secondary Metabolism as an Effect of Biochar Addtion.....62

3.6. Significant Changes in Abundance of Different Pathways for Nutrient Acquistition and Metabolism.....65

4.1. Isopycnic Separation of DNA from Density-gradient Fractionation.....88

4.2. Taxonomic Affiliation of Recovered 16s rRNA Gene Fragments.....90

4.3. Taxonomic and Functional Shifts as an Effect of Biochar Amendment.....91

4.4. Proportion of Abundance of Recovered Populations from Metagenomes.....94

Figure Page

4.5. Metabolic Features of Medium- and High-quality Mags Recovered from Biochar-amended and Control Metagenomes. 95

A1. Layout of Plots at Each Site. 140

A2. Relative Abundance of Phyla in the Oxisol During (a) Pre-plant and (B) Pre-harvest and in the Mollisol During (C) Pre-plant and (D) Pre-harvest. 141

A3. Relative Abundance of Taxa (Class-level) According to Soil Type and Sampling Time. 142

A4. Non-metric Multi-dimensional Scaling (nMDS) Plot Depicting Differences in Bacterial Community Composition. 143

A5. Venn Diagram of Unique and Shared Otus Shared by Soil Type and Biochar Treatment. 144

B1. Boxplots Representing Napiergrass Crop Yield Harvested December 2015. 153

B2. Clustering of Samples and Replicates Based on Seed Subsystem Relative Abundance. 154

B3. Significant Changes in Abundance of Select Pathways Related to N Metabolism 155

C1. Cumulative Gas Production Rate for Microcosms Receiving 13c-perennial Ryegrass over a 14-day Incubation Period 177

C2. Average Coverage of DNA-SIP Metagenomes. 178

LIST OF ABBREVIATIONS

C	Carbon
CEC	Cation exchange capacity
CH_4	Methane
GHG	Greenhouse gases
KEGG	Kyoto Encyclopedia Genes and Genomes
KO	KEGG Orthology
MENA	Molecular ecological network analysis
MG-RAST	Metagenomic RAST (Rapid Annotation Server Tool)
N	Nitrogen
N_2O	Nitrous oxide
nMDS	Nonmetric multidimensional scaling
OTU	Operational taxonomic unit
PCoA	Principle component analysis
QIIME	Quantitative insights into microbial ecology
qPCR	Quantitative real-time polymerase chain reaction
SOC	Soil organic carbon
WHC	Water holding capacity

CHAPTER 1

INTRODUCTION

1.1 Sustainable Agriculture to Mitigate Climate Change

Agriculture lies at the heart of many fundamental global challenges to humanity including food security, environmental degradation and climate change. The agricultural sector is a major contributor to greenhouse gases (GHG), which contributes about 25% of all global GHG emissions from the production of food, feed, and biofuels, including emissions from agriculture-driven land use change (Smith et al., 2014). Soils and plants in terrestrial ecosystems currently absorb the equivalent of about 20% of total anthropogenic GHG emissions, however, this sink is offset by emissions from land use change, which generates methane (CH_4) and nitrous oxide (N_2O) in addition to carbon dioxide (CO_2) (Le Quéré et al., 2014). By 2050 the global population is projected to reach 9.8 billion with increases occurring primarily in developing countries with accelerated urbanization (United Nations, 2017). To feed this growing and urbanized population, global food production must increase by ~70% (Alexandratos and Bruinsma, 2012), putting additional pressure on existing natural resources. Past increases in global agricultural production were facilitated by conversion of natural ecosystems to intensive continuous agricultural land uses with massive inputs of synthetic fertilizers that ultimately confer high environmental costs (Post and Kwon, 2000) leading to negative impacts on soil fertility, soil organic carbon (SOC) and the possible reduction of biomass production over time (Lal, 2015, 2004). Better land stewardship offers the potential for large additional climate mitigation by combining enhanced land sinks with reduced emissions. Integrative solutions are required to re-structure production systems into

'climate smart agriculture' using models of 'sustainable intensification' in order to increase food production from existing farmland in ways that reduce environmental impacts, such as through reductions in GHG emissions and the enhancement of carbon (C) sequestration (Campbell et al., 2014; Garnett et al., 2013; Griscom et al., 2017; Paustian et al., 2016).

1.2 Biochar as a Soil Amendment

1.2.1 *Terra Preta*

The use of biochar, a C-rich product of biomass pyrolysis, as a soil amendment to ameliorate soil quality and increase C storage is modeled on the anthropogenic soils known as *Terra Preta do Indio* (Indian dark earth) found in Amazonia, also referred to as the Amazon Dark Earth (ADE). ADE soils are highly fertile in comparison to the highly weathered surrounding tropical soils, these soils are characterized by higher organic carbon (OC), higher nutrients, higher soil pH, higher cation exchange capacity (CEC), and higher base saturation (Glaser, 2007; Glaser et al., 2001; Lehmann et al., 2003). The most distinguishing feature of the ADE is the high charcoal content in the soil to depths of about 1m, which is approximately 70% higher compared to the adjacent soil (Glaser et al., 2001). Comparison of the SOM composition of ADE with the adjacent soils showed higher amounts of condensed aromatic and carboxylic moieties in ADE, which resulted from the process of charring biomass (Glaser et al., 2003; Glaser and Birk, 2012). The poly-condensed aromatic moieties found in ADE soils are responsible for the prolonged stability against microbial degradation and, after partial degradation, also for the higher nutrient retention (Glaser, 2007; Glaser et al., 2001). Similarly, biochar also contains large amounts of polycyclic aromatic structures that influence its stability in the soil

(Keiluweit et al., 2010; Wiedemeier et al., 2015). Studies of biochar decomposition estimate that the mean resident time varies widely, ranging betweent six to thousands of years, depending on the feedstock (Kuzyakov et al., 2009; Lehmann et al., 2015). Thus, the addition of biochar to soils can sequester C for long periods of time, making this an attractive practice for mitigating climate change. The properties of ADE soils are often seen as proxies for the long-term effects of biochar on soil properties. However, these comparisons must be approached with caution due to their complex history of formation.

1.2.2 Biochar Properties

In addition to long-term C storage, the application of biochar to agricultural land has received increasing attention as a strategy for improving soil fertility. For instance, biochar application has been reported to improve soil quality, water and nutrient retention and crop productivity (Ding et al., 2010; Lehmann et al., 2006). The positive impacts of biochar in soils are often explained by the porosity and sorption capacity, liming capacity and its influence on soil structure (Briones, 2012; Hernandez-Soriano et al., 2016; Jien and Wang, 2013; Laghari et al., 2016; Lehmann et al., 2011; Liang et al., 2006). However, the utility of biochar for any particular application depends on its inherent properties. The heterogeneity of biochar properties are a function of the pyrolysis temperature and feedstock source. The parameters that most affect the total OC, CEC and mineral elements concentration in biochar are due to feedstock type (Barrow, 2012; Mukherjee et al., 2011; Zhao et al., 2013). For example, manure biochar contained more phosphorus (P) than crop residue and grass biochar, conversely, crop and grass biochars contained more potassium (K) than manure (Zhao et al., 2013). On the other hand, biochar surface chemistry, volatile matter content and pH are mainly influenced by

pyrolysis temperature, with pH and recalcitrance increasing and CEC and volatile matter content decreasing with higher pyrolysis temperatures (Bruun et al., 2011; Suliman et al., 2016; Zhao et al., 2013). The ability to tailor biochar, either through feedstock or pyrolysis conditions, offers considerable opportunities for the use of biochar in sustainable agriculture. For example, biochar can be better used as a source of nutrients to increase soil fertility by low pyrolysis temperatures and a high nutrient feedstock (Barrow, 2012). Alternatively, if the purpose is to increase C storage high, pyrolysis temperatures of wood feedstock would be more suitable (Bruun et al., 2011).

In addition to an increase in soil fertility through biochar nutrients, biochar could also be used as a potential additive for nutrient retention. The application of biochar to soils has been shown to increase N retention through the reduction of leaching losses of NH_4^+ and NO_3^- due to sorption (Ding et al., 2010). Due to the physical and chemical properties, solutes and nutrient ions can be adsorbed onto the biochar surface, which is related to the biochar surface area, negative surface charge and charge density (Liang et al., 2006). CEC is a function of the presence of oxygenated functional groups, such as carboxylic and phenolic groups, in the biochar and on the surface. These functional groups increase on the surface of biochar as a consequence of the natural oxidation via biotic and abiotic process (e.g. microbial oxidation or aging). Thus, oxidation of the biochar surface can increase the reactivity of the biochar surface and is responsible for raising the biochar CEC (Sorrenti et al., 2016; Zimmerman, 2010), which can result in increased N retention or stabilization over time(Mia et al., 2017; Zheng et al., 2013).

1.3 Biochar Effects on the Soil Microbiome

1.3.1 Soil microbial communities

Soil microbial communities are highly diverse, in part because soil and their environmental conditions are extremely heterogeneous. At a global scale, soil properties and characteristics, such as pH, nutrient content, and texture, are highly variable between soils and these factors significantly influence the composition of soil microbial communities (Girvan et al., 2003; Lauber et al., 2013). The range of environmental conditions is a product of factors that affect soil formation, such as parent material, climate and biota. In addition, soil encompasses a wide range of microenvironments that differ considerably in their biotic and abiotic characteristics, such as the plant cover (i.e. rhizosphere) and aggregate environments, which can support distinct microbial communities (Bach et al., 2018; Ruamps et al., 2011; Shi et al., 2016; Wilpiszeski et al., 2019). At spatial scales relevant for microbially mediated reactions, soils are primarily composed of microaggregates (<250μm) and macroaggregates (0.25 – 2 mm), which can bind and stabilize SOC or regulate water flow and limit oxygen diffusion, respectively (Carminati et al., 2007; Six et al., 2004, 2000). The resulting distribution of sizes, available water and oxygen of soil aggregates provide heterogeneous niches for microorganisms to occupy, which in turn supports distinct microbial communities and affect their metabolic activities (Rabbi et al., 2016; Wilpiszeski et al., 2019). In addition, other important factors that have strong influences on the structure of bacterial communities including soil pH, SOC and N availability (Cederlund et al., 2014; Lauber et al., 2009). Consequently, soil processes can be directly and indirectly influenced by the soil microbial communities, including cycling of C, N and other mineral nutrients. Soils represent a vast reservoir of microbial life. For example, a single gram of soil can harbor up to 10^{10} bacterial cells and an estimated 10^{4} species (L. F. W. Roesch et al., 2007). As

the soil microbial community plays a crucial role in many ecosystem-level processes, it is important to identify the taxa that are responsible for these processes, their abundance and activity. In-depth knowledge on how agricultural management practices effect the soil microbiome is essential in developing sustainable food production systems. Thus, the properties of the soil microbiome can be used as in indicator for soil quality and fertility due to its sensitivity to perturbations (Nannipieri et al., 2003; Sharma et al., 2010).

1.3.2 Biochar effects on soil bacterial communities

The incorporation of biochar into soil is a promising management strategy for sustainable agriculture owing to its potential to sequester C and improve soil fertility (Jha et al., 2010; Lehmann et al., 2011). As part of a sustainable management practice, biochar addition to soil induces changes in the physicochemical properties which can modify soil microbial abundance, activity and community structure. However, the microbial response to biochar addition depends strongly on soil type and cropping system, as well as the properties of the biochar being added (Anders et al., 2013; Docherty et al., 2015; Girvan et al., 2003; Jenkins et al., 2017; Lehmann et al., 2011). Due to the variety of soils and biochars across different studies, the observed effects of biochar on microbial processes are variable. In short-term experiments (>1 year), increased soil respiration after the addition of biochar produced at lower pyrolysis temperatures (≤500ºC) has been reported (Luo et al., 2011; Smith et al., 2010; Wang et al., 2012). Conversely, decreased or no change in soil respiration has also been observed in short- and longer-term (<1year) experiments, dependent on the application rate (Dempster et al., 2012; Zheng et al., 2016). Changes in soil respiration measurements can indicate stimulation of microorganisms by biochar. Similarly, biochar addition has also been reported to increase

microbial biomass (MB), with the effect size increasing with higher biochar application rates (Xu et al., 2016; Zhang et al., 2014). The inverse has also been reported, MB increased or decreased at lower and high biochar application rates, respectively (Li et al., 2018). Interestingly, these changes in MB were accompanied by increased bacterial diversity (Li et al., 2018).

The effects of biochar on microbial community composition has also been reported with some contradictory findings. It has been suggested that biochar may affect the soil bacterial community via improving soil physicochemical properties (H.-J. Xu et al., 2014). Studies based on 16S rRNA gene analysis observed increased water holding capacity (WHC), MB, pH, respiration rates and N mineralization and increases in the relative abundance of *Proteobacteria*, *Bacteroidetes*, and *Actinobacteria,* while *Acidobacteria*, *Chloroflexi*, and *Gemmatimonadetes* under biochar treatment decreased (Anderson et al., 2011; Xu et al., 2016; Zheng et al., 2016). In pot-experiments, an increased relative abundance of *Bacteroidetes* with biochar addition has been reported, while *Proteobacteria* decreased in root-associated communities (Kolton et al., 2011). Increased soil respiration and increased relative abundance of *Gemmatimonadetes* and *Actinobacteria* in soils that contained natural or added biochar has also been reported (Khodadad et al., 2011). The variability of observed changes in the microbial communities could reflect the differences in soils and management strategies, i.e. agricultural – pastures or cropland compared to forest soils. Indeed, a study across three European sites with identical biochar applications found enrichment of different bacterial phyla across the site and plant cover, increased relative abundance of *Gemmatimonadetes* and *Acidobacteria* Gp6 were observed in short rotation coppice in the United Kingdom,

while relative abundance of *Gemmatimonadetes* and *Proteobacteria* increased in an Italian grassland, and decreased in *Acidobacteria* (Jenkins et al., 2017). Although biochar addition to soils has a significant effect on the bacterial communities, the effects of biochar on the soil community composition may be small compared to the highly variable soil microbiomes that are found in different soils.

Whether the impact of biochar on soil community composition directly shifts the microbial functional potential remains poorly understood as very few have conducted metagenomic studies of biochar amended soils. Despite the variation in biochar effects on soil bacterial communities, several studies showed that the addition of biochar can alter soil community composition as well as lead to a reduction in soil N_2O emissions (Cayuela et al., 2013; Harter et al., 2014; Kuzyakov et al., 2014), CH_4 emissions (Feng et al., 2012), and improved plant growth (Kolton et al., 2017, 2011). However, the dynamics and mechanisms of biochar impacts on soil microbial community function remain poorly understood.

1.4 Dissertation Framework

1.4.1 Significance

In order to strive towards sustainable agricultural practices that promote plant productivity, soil C retention, and reduce GHG emissions, it is imperative that we understand the impacts of biochar addition on the underlying soil microbial community that is the catalyst for biogeochemical cycling and plant growth promotion. Available evidence and indications strongly justify continued research and development efforts in order to understand the benefits and potential as well as the limitations of biochar application in order to expand its use in agricultural land management practices. The

potential to expand biochar application to large-scale agriculture hinges on the beneficial effects on the microbial community which underpins soil biogeochemical processes. While it is established that microbial processes are responsible for SOM mineralization and the associated emissions of CO_2 and other GHGs, the mechanisms and the response to biochar are much less clear. Soil microbial communities are highly responsive to many edaphic factors, climatic and management factors. Changes to soil nutrient concentrations and pH induced by biochar is expected to modulate changes in the activity, abundance, and diversity of the biochar-amended soil microbiome. The impact of biochar on the soil microbiome likely differs from other organic matter additions due to its persistence in the soil. Thus, it is unlikely to serve as a significant long-term source of either energy or cell C, after the decomposition of any initial condensates (Thies et al., 2015). Soil GHG emissions are influenced by management practices and many current mitigation strategies use technologies that can be implemented immediately (Smith et al., 2008). Therefore, it is imperative to understand the direct and indirect influences of biochar amendment to soil function and agricultural productivity and its variable effects under different conditions.

1.4.2 Research Objective

The overarching goal of this project is to determine changes in the taxonomic composition and functional diversity of the microbial community in response to the addition of a low-volatile matter biochar. In addition, we assessed whether amendment with biochar increased C sequestration and the combinatorial impacts of different soil types and bioenergy crops on the responses. Below is a summary of the organization of each chapter.

Chapter 3. In this study, we employ high-throughput sequencing of the *16S rRNA* gene to establish a baseline description of prokaryotic community composition after the first year of biochar addition. In order to understand the practical benefits of biochar amendment we first conducted a field experiment to measure changes in microbial composition and diversity, as well as changes to soil chemical concentrations after the addition of biochar in opposing soil types under two different cropping systems. Previous studies of biochar effects on the soil microbial community have presented variable and sometimes contradictory results owing to the variability of the biochar feedstock, pyrolysis temperature, soil type, and cropping system that the biochar is applied to. We further examine the community using random-matrix theory based molecular network analysis to elucidate robust associations among taxa within the soil microbial community.

Chapter 4. Following the *16S rRNA* gene amplicon analyses, we expanded the survey of the microbial community to examine the functional potential of the Oxisol under napiergrass cultivation after two years of biochar amendment. The results of chapter 3 showed that biochar effects were most pronounced in the low-fertility Oxisol under napiergrass cultivation. Previous studies on the effects of biochar on the soil community revealed important shifts in community composition. However, there remains a lack of information concerning functional gene content and diversity thus limiting our understanding concerning the impacts of biochar on the potential of the soil microbiome to control the fate of soil C and N. Here, we determined whether the observed changes in community composition lasted through the next year, whether a shift in the composition is reflected by shifts in the functional gene diversity of the soil community, and which genes and taxa responded to biochar amendment and their potential effects on soil C and

N cycling. As an important component of soil health, investigations into the functional gene content has important implications for improving soil C sequestration and reduction in GHG emissions.

Chapter 5. The changes in microbial communities in response to biochar has principally been investigated using molecular techniques that have primarily focused on the compositional and diversity of the total community derived from genomic DNA. In order to predict the impact of the microbial community on soil function, it is critical to improve our understanding of the active population within the community. In this chapter, we used stable isotope probing (SIP) coupled with shotgun metagenomics to target the active members of the community and to examine the composition and functional differences in of the active microbial community responding to the addition of biochar. DNA-SIP coupled with shotgun metagenomics offers a way to directly link microbial populations with ecological processes such as plant biomass degradation and reveal the genetic potential of these population with regard to other mechanisms for C and N cycling in soil.

Chapter 6. This chapter summarizes the key findings of the research in chapters 3 – 5.

CHAPTER 2

BIOCHAR APPLICATION INFLUENCES MICROBIAL ASSEMBLAGE COMPLEXITY AND COMPOSITION DUE TO SOIL AND BIOENERGY CROP TYPE INTERACTIONS

Published in: Soil Biology and Biochemistry

2018. Biochar application influences microbial assemblage complexity and composition due to soil and bioenergy crop type interactions. *Soil Biology and Biochemistry*, *117*, 97-107. DOI: 10.1016/j.soilbio.2017.11.017

Coauthors have acknowledged the use of this manuscript in my dissertation

Authors: Julian Yu, Lauren Deem, Susan E. Crow, Jonathan L. Deenik, and C. Ryan Penton

2.1 Introduction

The global conversion of natural ecosystems to intensive, continuous agricultural land use has led to the widespread depletion of soil organic carbon (SOC) stocks (Post and Kwon, 2000) that negatively impacts soil fertility and ultimately may reduce biomass production over time (Lal, 2015). Carbon (C) loss through decomposition in response to deforestation and warmer conditions results in carbon dioxide (CO_2) and methane (CH_4) emissions that can contribute to global atmospheric concentrations of greenhouse gases (GHG) (Lal, 2012, 2004). Thus, developing sustainable agricultural practices and supporting "climate smart soils" that enhance SOC sequestration and potentially offset agricultural sources of greenhouse gas emissions are of critical importance to addressing global food, fuel and fiber needs (Campbell et al., 2014; Paustian et al., 2016).

One potential component of sustainable management is the application of biochar,

a C-rich product of biomass pyrolysis, as a soil amendment. First described within the highly weathered, infertile soils of central Amazonia, patches of persistent, anthropogenic dark-colored soil (*terra preta*), characterized by large reserves of charred materials, have maintained their fertility for several thousand years (Glaser, 2007; Glaser and Birk, 2012). Compared to the surrounding soils, *terra preta* is less acidic, contains higher nutrient concentrations (P, Ca, N, Mg) and remains high in soil organic matter, despite intensive cultivation (Barrow, 2012; Glaser and Birk, 2012). Biochar within the *terra preta* is thought to be key to the observed changes in soil physical and chemical properties, leading to nutrient retention, improved crop yields and thus can potentially address decreases in soil fertility as a potential C sink (Lehmann et al., 2006).

Modeled on the C-rich *terra preta*, biochar amendments were proposed as an approach to ameliorate soil quality (Laird, 2008; Lehmann et al., 2011, 2006). Biochar contains a large portion of aromatic compounds recalcitrant to microbial degradation and thus may enhance long-term C sequestration in terrestrial systems (Laird, 2008; Lehmann et al., 2006; Noyce et al., 2015). However, the sorption and residence time of biochar in soil is dependent on its physical and chemical properties (Keiluweit et al., 2010) and is a result of a combination of feedstock and pyrolysis temperature (Bourke et al., 2007; Deenik et al., 2011). Observed alterations of soil chemical and physical properties with biochar application may result in a shift in the composition of the native soil microbial community, but not necessarily total microbial biomass (Anders et al., 2013; Anderson et al., 2011; Harter et al., 2014; Steinbeiss et al., 2009). By influencing the activity of microbial functional groups, subsequent changes in soil physiochemical properties induced by biochar addition may suppress GHG emissions and further increase the

climate change mitigation potential of the system (Lehmann et al., 2011; Liu et al., 2012; Wang et al., 2012).

As the proximate driver of soil processes underlying C and N cycling, the response of microbial functional groups to biochar addition is critical to understand and anticipate. For example, in one study biochar increased potential nitrogen (N) fixation and enhanced the activity of nitrous oxide (N_2O) reducing bacteria in water-saturated soil microcosms (Harter et al., 2014). In another system, biochar shifted microbial community composition to favor Gram-negative *Proteobacteria* (Anderson et al., 2011; Orr and Ralebitso-Senior, 2014), thus providing a mechanistic explanation for improved N-cycling through complete denitrification (Jones et al., 2013; Mills et al., 2008; Orr and Ralebitso-Senior, 2014). Changes in soil pH and nutrient availability associated with biochar amendment also may select for a subset of the microbial community (Su et al., 2017; Ventura et al., 2007). For example, biochar addition promoted the abundance of *Actinomycetes* with no significant changes in total microbial biomass in temperate forest soils (Anders et al., 2013).

Previously, most studies of the effect of biochar on soil microbial communities focused on biomass and composition change, e.g., species richness and abundance. The recent emergence of random matrix theory-based molecular ecological network analysis revealed robust associations among taxa within the soil microbial community (Barberán et al., 2012; Shi et al., 2016; Zhou et al., 2010). The generation of large environmental sequencing datasets offer an opportunity to identify co-occurrence patterns and interdependent relationships among taxa (e.g. OTUs) within the microbial community (Faust and Raes, 2012; Hallam and McCutcheon, 2015) by analyzing the topology of the

nodes and characteristics of microbial network assemblages. In this study, we determined the effect of biochar amendment on bacterial community composition and assemblage patterns in two contrasting soil types in Hawaii under two cropping systems using a highly replicated targeted sequencing approach. We emphasize the impact of soil type and biochar amendment on bacterial community network architecture and, by doing so, reveal relationships between specific network modules and environmental factors and identify large changes in assemblage composition in response to amendment and cultivation.

2.2 Materials and Methods

2.2.1 Study sites and experimental design

Field trials were conducted on the island of Oahu, Hawaii, United States at the Waimanalo (21°20'15"N; 157°43'30"W) and Poamoho (21°32'30"N; 158°05'15"W) agricultural experimental research stations of the College of Tropical Agriculture and Human Resources, University of Hawaii Manoa. Waimanalo has a mean annual precipitation and mean annual temperature of 95 cm and 23°C (Soil Survey staff, accessed 7/25/2013). The soil, of the Waialua series, is a fertile Mollisol with 55% clay, strong shrink-swell properties, is slightly acidic (pH 6.2) and has a moderately high cation exchange capacity (CEC) (Soil Survey staff, accessed 7/25/2013). Poamoho has a mean annual precipitation and mean annual temperature of 127 cm and 22.5°C (Soil Survey staff, accessed 7/25/2013). The soil, of the Wahiawa series, is an acidic (pH 5.2) Oxisol with 44% clay rich in kaolinite and iron oxides with a low CEC (Soil Survey staff, accessed 7/25/2013).

The biochar, supplied by Diacarbon Energy, Inc. (Burnaby, BC Canada), was

produced at 600°C in a continuous flow reactor, composed of 80% woodchip (spruce, pine and fir) and 20% anaerobic digester residue. Biochar was applied to the field at a 1% rate by volume (45.36 kg/plot). All plots were amended with 10.89 kg/plot of fish bone meal (9.07%N; 2.38%P; 0.63%K; 1.49%Ca; 0.13%Mg). Lime was applied to all plots at Poamoho (13.61 kg/plot) to improve soil pH of the acidic Oxisol for cultivation.

The field experiment consisted of biochar application and corresponding control plots in two cropping systems in two contrasting soil types. Each site had two crops, napiergrass (*Pennisetum perpereum* var. green bana, cultivated as a potential biofuel feedstock) and sweet corn (*Zea mays*, var. Hawaiian Supersweet #9, a regionally important food crop) with eight plots of each crop and two bare plots (Figure A1). Napiergrass and sweet corn plots were planted in December 2013 and February 2014, respectively, planted plots were 4.57 m by 6.10 m and bare plots were 2.29 m by 3.05 m. At each site, four napiergrass plots, four corn plots and one bare plot were randomly chosen for biochar amendment. Napiergrass was planted December 2013 at Waimanalo and Poamoho, approximately 10 cuttings were planted per row with 121.92 cm row spacing. Sweet corn seeds were planted February 2014 and April 2014 at Waimanalo and Poamoho, respectively, with 76 cm spacing between rows. Napiergrass was harvested by ratoon, i.e., a form of zero-tillage management by cutting the grass near the surface leaving the soil and root system intact for vegetative regeneration, every 6 months and corn was conventionally harvested approximately 72 days after planting.

Soils were collected at two sampling times for microbial community analyses. Samples from napiergrass plots and bare plots at both sites were collected December, 2013, 5-13 d after planting, ~1 month after biochar amendment. Poamoho corn plot soils

were collected April 2014, 14 days after biochar amendment and 7 days after planting. Waimanalo corn plots were collected March 2014, 14 days after biochar amendment and planting. All soils from the initial sampling are referred to as "pre-plant" henceforth. The second set of samples was obtained from all plots after the second crop rotation several days before harvesting, approximately one year later. Soils from corn plots were collected October 2014 from Poamoho and November 2014 from Waimanalo. Soils from napiergrass plots and bare plots from both sites were collected December 2014. Soils from the second collection are here on referred to as "pre-harvest". For all soil sampling, each plot was split in half and three half-plot 0-10-cm depth cores (8-cm diameter) were taken randomly and mixed for each sample to create a composite sample. Four of these composite samples were taken per half-plot, for a total of 8 replicates per plot and were transported on dry ice and stored at -80°C until DNA extraction.

2.2.2 Soil chemical analyses

Base cations were determined using a 1M ammonium acetate ($NH_4C_2H_3O_2$) (pH 7) extraction with a soil to $NH_4C_2H_3O_2$ ratio of 1:20 (Sparks et al., 1996), shaken for 30 minutes and filtered through a Whatman 42 filter paper and frozen until analysis for calcium (Ca^{2+}), sodium (Na^{-}), magnesium (Mg^{2+}) and potassium (K^{+}) content (QuikChem 8500 Series Automated Ion Analyzer, Lechat Instruments, Loveland, Colorado). Soil pH was measured (Accumet Research AR20, Fisher Scientific, Waltham, MA, USA) and total soil C and N was analyzed using oxidative combustion (ECS 4010 CHNSO Analyzer, Costech Analytical Technologies Inc., Valencia, CA) (Table A1).

2.2.3 DNA extraction and Illumina MiSeq sequencing

Genomic DNA was extracted from 0.25 g soil using MoBio Powerlyzer

PowerSoil DNA Isolation kits (MoBio Laboratories, Carlsbad, CA, USA). To improve lysis and desorption of DNA from the clay soils, 200 µl of Tris buffer (0.5 M Tris-HCl pH 9) and 200 µl of phosphate buffer (0.2M Na_2HPO_4 pH 8) were added to bead tubes loaded with soil and bead solution, mixed and 60 µl of solution C1 was added, incubated at 70°C for 10 min and frozen at -80°C for 5 min. Extracts were quantified using the Qubit dsDNA high sensitivity assay kit (Life Technologies, Carlsbad, CA, USA) and stored at -20°C until amplification. Amplicon libraries for the 16S *rRNA* gene V4 region were generated using a previous protocol (Kozich et al., 2013). For library preparation, a single PCR was performed per sample on a 96-well plate, product size confirmed on a 2% agarose gel and purified using the SequalPrep Normalization Plate Kit (Invitrogen, Carlsbad, CA, USA). Pooled amplicon libraries were sequenced on Illumina MiSeq instrument using 250-base paired-ends kit at the genomic core facility, Arizona State University.

The 16S *rRNA* gene sequence paired-end reads were demultiplexed on the MiSeq instrument at the time of sequencing. An operational taxonomic unit (OTU) table at 3% dissimilarity was generated using the Quantitative Insights Into Microbial Ecology (QIIME) software (Caporaso et al., 2010). Briefly, the paired reads were joined with a 50 bp overlap and quality filtered (phred 20). Chimeric sequences were filtered using UCHIME and clustering was carried out using open reference OTU picking in QIIME. Sequences were clustered against the 2013 Greengenes database, sequences that failed to hit the reference database were subsequently clustered in de novo mode using the UCLUST implementation in QIIME. The resulting OTU tables were rarified to 13,300 sequences per sample.

2.2.4 Statistical Analysis

Statistical analysis of community composition was performed using PRIMER-6 software (Clarke and Gorley, 2006). Raw OTU abundances were normalized by Hellinger transformation for Bray-Curtis dissimilarity matrices. Soil base cations, moisture, C, N and pH data were log transformed and normalized for the Euclidean resemblance matrix. Significant differences in the microbial community composition between soil, cropping system, sampling period, biochar treatment, and interactions between these factors (Table A2) were tested with Permutational Multivariate Analysis of Variance (PERMANOVA) (Anderson, 2001) and Analysis of Similarity (Clarke, 1993). Similarity percentages analysis (SIMPER) (Warwick et al., 1990) was used to identify significant taxa driving the differences among treatments. The BEST (Bio-Env + STepwise) procedure (Clarke et al., 2008) was used to determine correlations between community and soil chemical data. Alpha diversity indices, Margalef's richness, Pielou's evenness and Shannon diversity, were computed for each sample in PRIMER-6. Normality and homogeneity of variance were checked by plotting the residuals on a quantile-quantile plot (qqPlot function) and using leveneTest functions in R's car package, respectively. Alpha diversity indices, transformed by aligned ranks (Wobbrock et al., 2011) were subjected to four-way ANOVA performed using R version 3.3.2 in RStudio (version 1.0.136). Transformations were carried out using the art function in R's ARTools package. Tukey's multiple comparisons were computed using the lsmeans function and cld function in R's lsmeans and multcompView packages, respectively, for all significant differences. All differences were considered significant at a P-value < 0.05.

2.2.5 Molecular Ecological Network Analysis (MENA)

Co-occurrence molecular ecological networks were constructed and analyzed using the Molecular Ecological Network Analysis Pipeline (http://ieg2.ou.edu/MENA) (Deng et al., 2012). Molecular Ecological Network Analysis (MENA) was implemented with random matrix theory (RMT)-based methods to automatically identify a similarity threshold for network construction (Deng et al., 2012; Luo et al., 2006) that was subsequently visualized with Cytoscape (Shannon et al., 2003). Topological indices were calculated including indexes of individual nodes, modules and interactions (Deng et al., 2012). In network analysis, a group of nodes highly connected among nodes of the group but much less connected to nodes outside the group is defined as a module (Newman, 2006; Olesen et al., 2007). The leading eigenvector of the community matrix method was used for module separation and modularity calculations with a modularity threshold of 0.4 to define modular structures in the network (Newman, 2006; Shi et al., 2016). Network modules were grouped by modularity (module #) with the size of the node corresponding to the node degree (connectivity). Node connectivity within module (Z_i) and among modules (P_i) was used to classify nodes as module hubs ($Z_i > 2.5$, $P_i \leq 0.62$), network hubs ($Z_i > 2.5$, $P_i > 0.62$), connectors ($Z_i \leq 2.5$, $P_i > 0.62$) or peripherals ($Z_i \leq 2.5$, $P_i \leq 0.62$) (Deng et al., 2012; Olesen et al., 2007). Correlations of soil chemical data (moisture content, Ca, Na, K, Mg, C, N and pH) to modules within the network was carried out with Module-EigenGene analyses, modules with less than 5 members were excluded. Sequences were deposited in the NCBI short read archive (https://www.ncbi.nlm.nih.gov/sra) under accession SRP098931.

2.3 Results

2.3.1 Effect of soil, cropping system and sampling time on the soil microbial community

A total of 67,785,019 high quality reads were obtained after paired-end assembly. After chimera filtering and the removal of 4,911 OTU singletons and doubletons, 16,867 OTUs (6,443,815 sequences) remained for analyses. In both soils, *Acidobacteria*, *Proteobacteria*, *Actinobacteria* and *Planctomycetes* were the predominant phyla, constituting ~70% and ~60% of the total sequences in the Oxisol and Mollisol, respectively (Figure A2, Figure A3).

Measures of richness, evenness, and Shannon diversity exhibited trends that varied principally according to soil and crop type (Table A3). The individual effects of soil, crop type, and time were significant across all diversity measures (ART-ANOVA: Table A3). The interactive effects of soil type*time and crop*time were significant though soil type*crop interactions were not. Overall, Oxisol bacterial communities consistently exhibited significantly lower evenness, diversity and richness, compared to the Mollisol (Table 2.1, Table A3). Overall, pre-harvest samples exhibited higher richness ($F=126.1$, $p<0.001$), evenness ($F=112.2$, $p<0.001$), and diversity ($F=144.8$, $p<0.001$) than the pre-plant samples.

Table 2.1. Diversity indices according to soil type, cropping system and biochar treatment

Soil Type	Treat	Margalef's Richness (d)		Pielou's Evenness (J')		Shannon Diversity (H')	
		Pre-Plant	Pre-harvest	Pre-Plant	Pre-harvest	Pre-Plant	Pre-harvest
Oxisol	Nap-BC	235.4±3.95^{a}	360.7±9.63^{defg}	0.9623±0.0005^{a}	0.9703±0.0004^{fghij}	6.906±0.019^{a}	7.426±0.030^{efghijk}
	Nap-NBC	266.3±6.50^{ab}	345.4±8.73^{de}	0.9630±0.0008^{ab}	0.9686±0.0006^{efg}	7.036±0.032^{ab}	7.356±0.034^{efg}
	Corn-BC	300.2±8.57^{bc}	325.6±7.80^{cd}	0.9642±0.0007^{abc}	0.9688±0.0005^{efgh}	7.168±0.035^{bcd}	7.300±0.029^{defg}
	Corn-NBC	321.0±6.39^{cd}	326.2±6.22^{cd}	0.9657±0.0005^{cd}	0.9661±0.0006^{cde}	7.257±0.026^{def}	7.278±0.024^{def}
	Bare-BC	212.8±10.55^{a}	353.8±13.47^{cdefg}	0.9593±0.0008^{a}	0.9708±0.0005^{fghij}	6.778±0.047^{a}	7.409±0.045^{efghijk}
	Bare-NBC	253.1±13.32^{ab}	339.0±8.72^{cdef}	0.9665±0.0008^{bcdefg}	0.9673±0.0007^{cdefg}	7.013±0.048^{abc}	7.334±0.033^{defghi}

	Nap-BC	303.0±8.48^{bc}	391.3±13.57^{fg}	0.9679±0.0005^{defg}	0.9728±0.0006^{ij}	7.213±0.034^{cde}	7.520±0.051^{hijk}
	Nap-NBC	316.6±7.17^{cd}	412.5±6.65^{g}	0.9682±0.0004^{defg}	0.9736±0.0004^{j}	7.266±0.028^{def}	7.598±0.019^{k}
Mollisol	Corn-BC	394.2±9.11^{fg}	369.0±4.98^{efg}	0.9716±0.0007^{hij}	0.9699±0.0005^{fghi}	7.524±0.034^{ijk}	7.447±0.018^{ghijk}
	Corn-NBC	388.1±6.23^{fg}	356.1±11.23^{def}	0.9716±0.0003^{hij}	0.9699±0.0008^{fghi}	7.513±0.020^{hijk}	7.402±0.037^{fghij}
	Bare-BC	317.8±15.69^{b} ^{cde}	424.7±13.45^{g}	0.9694±0.0004^{defghij}	0.9747±0.0007^{j}	7.280±0.061^{cdefgh}	7.639±0.038^{jk}
	Bare-NBC	293.2±17.10^{a} ^{bcd}	332.3±52.97^{bcdefg}	0.9660±0.0015^{abcdef}	0.9738±0.0003^{ghij}	7.160±0.075^{bcdef}	7.347±0.178^{bcdefghijk}

[1]Superscript letters indicate significant ANOVA (P<0.05) with Tukey's multiple.

A clear difference was observed in bacterial community composition between the Oxisol and Mollisol (Figure A4) (pseudo-F=107.08, p=0.001) and was best explained by soil Mg content (BEST: rho=0.704; RELATE: P=0.704, p=0.001). Differences in community membership between soil types, derived from SIMPER analyses, were driven primarily by *Acidobacteria*. Broadly, microbial community composition also varied significantly between cropping systems, regardless of soil type (pseudo-F=7.769, p=0.001). *Acidobacteria* again contributed most to community dissimilarity, contributing 43% of the SIMPER-derived differences. The Oxisol-biochar soils contained the most unique OTUs while the Oxisol control soils contained no unique OTUs (Figure A5).

2.3.2 Effect of biochar on the soil microbial community in low and high fertility soils

Overall, while biochar amendment as a single factor did not significantly impact alpha diversity indices, biochar*soil type interactions were significant for richness (F=6.91, p<0.01) and Shannon diversity (F=7.40, p<0.01), but not evenness (F=0.74, p=0.39) (Table 2.1; Table A3). While biochar*time interactions were significant across all alpha diversity indices, biochar*crop interactions were significant for richness

(F=16.41, p<0.001) and Shannon diversity (F=16.65, p<0.001), but not evenness. Initial biochar amendment (pre-plant) resulted in a decrease in richness, diversity, and evenness for both soils, with the exception of the bare soil in the Mollisol where biochar amendment increased alpha-diversity. In addition, biochar amendment approximately 1yr post-amendment (pre-harvest) generally resulted in higher alpha diversity compared to samples taken at the initial biochar amendment (pre-plant).

In the Oxisol, biochar amendment under napiergrass significantly shifted bacterial community composition (pseudo-F=7.15 P=0.001), with distinct clustering in both pre-plant (pseudo-F=4.46 P=0.001) and pre-harvest samples (pseudo-F=1.86 P=0.006) (Figure 2.1A). Smaller replicate dispersion with biochar amendment was also evident across all samples (Table A4). Biochar amendment in the pre-plant samples in the Oxisol-napiergrass soil increased the relative abundance of *Proteobacteria* with a decrease in *Acidobacteria* and *Actinobacteria*, though *Acidobacteria* recovered in abundance at pre-harvest. A combination of soil Na (RELATE: P=0.509, p=0.001), Mg (RELATE: P=0.445, p=0.001), K (RELATE: P=0.214, p=0.001), and moisture content (RELATE: P=0.520, p=0.01), were most correlated to bacterial community composition (BEST: rho=0.592).

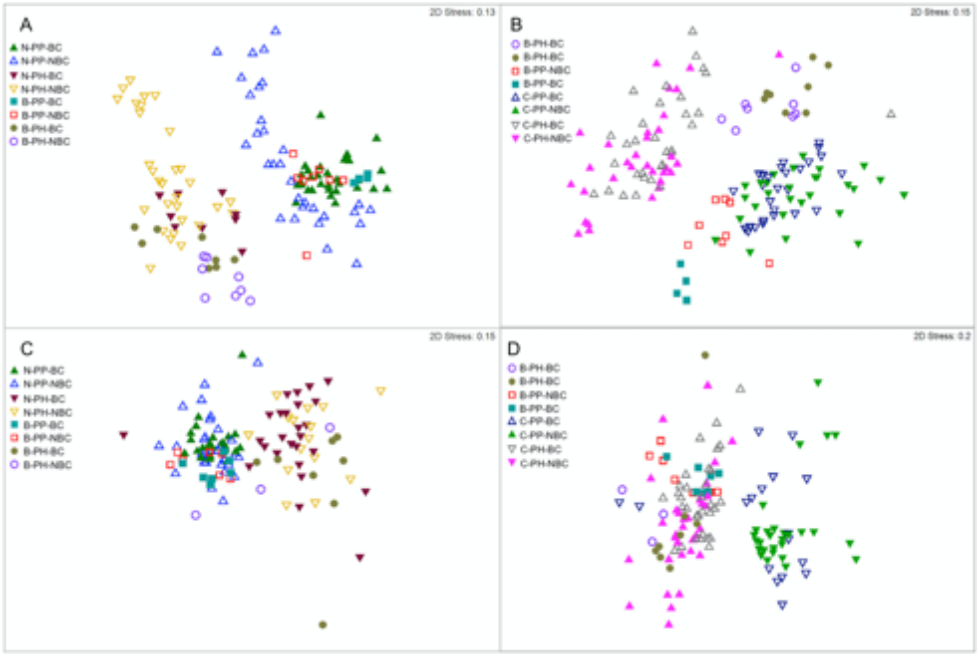


Figure 2.1. Non-metric multi-dimensional scaling (nMDS) plot depicting differences in bacterial community composition. Biochar-amended soils are indicated by closed symbols and soils without biochar are shown as open symbols. Squares and circles indicate the bare plots from pre-plant and pre-harvest sampling times. A: Oxisol under napiergrass. B: Oxisol under corn C. Mollisol under napiergrass D. Mollisol Corn. Legend names indicate cropping system (B: bare; N: napiergrass, C: corn), sampling time (PP: pre-plant, PH: pre-harvest) and treatment (NBC: no biochar, BC: biochar).

In the Oxisol, biochar amendment under corn also significantly impacted soil bacterial community composition (Pseudo-F=1.50, p=0.038), with a less pronounced impact on the pre-plant samples (Pseudo-F=1.43, p=0.026) than the pre-harvest samples (pseudo-F=1.92, p=0.001) (Figure 2.1B). The combination of soil Mg (RELATE: P=0.560, p=0.001) and moisture (RELATE: P=0.630, p=0.001) was correlated with community composition (BEST: rho=0.637). Significant changes in community composition with biochar amendment were driven primarily by a decrease in relative abundance of *Acidobacteria* and *Actinobacteria* and an increase in *Proteobacteria*, with contributions of 32%, 20% and 20% to the total Bray-Curtis dissimilarity, respectively.

Compared to the Oxisol, the overall biochar effect on bacterial community composition was less pronounced in the Mollisol. The effect of biochar amendment on alpha diversity in the Mollisol varied according to cropping system. For example, biochar amendment decreased alpha diversity under napiergrass and increase alpha diversity under corn and in bare plots, although not always significantly, in both pre-plant and pre-harvest samples. A significant effect on community composition under napiergrass (pseudo-F=1.44, p=0.031), driven by an increase in *Acidobacteria* was identified. Biochar addition decreased replicate dispersion under napiergrass in the pre-plant samples only (Table A4). A significant sampling time effect on bacterial community composition was found (pseudo-F=14.03, p=0.001) while replicate dispersion also increased (Figure 2.1C). Differences between sampling times were driven by a lower pre-harvest relative abundance of *Proteobacteria*. Microbial community composition was most explained by a combination of Mg (RELATE: P=0.528, p=0.001) and Ca (RELATE: P=0.351, p=0.001), (BEST: rho=0.520).

In the Mollisol-corn samples, significant differences in microbial composition with treatment (pseudo-F=1.81, p=0.007) and sampling time (pseudo-F=10.89, p=0.001) were identified (Figure 2.1D). In pre-plant samples biochar significantly increased replicate dispersion (Table A4). Increases in the relative abundance of *Acidobacteria* and *Crenarchaeota* and decreased relative abundance of *Proteobacteria* contributed to 26%, 15% and 34% of the Bray-Curtis dissimilarity with biochar addition, respectively. SIMPER analysis also showed that a decrease in *Acidobacteria* and increases in *Proteobacteria* and *Crenarchaeota* contributed 26%, 34% and 15% to dissimilarity with sampling time, respectively. Similar to the other soil type/crop type groups, microbial

community composition was most correlated to a combination of soil Na (RELATE: P=0.412, p=0.001), Mg (RELATE: P=0.470, p=0.001) and K (RELATE: P=0.465, p=0.001), (BEST: rho =0.517).

2.3.4 Biochar effects on microbial networks in the Oxisol

Molecular ecological network analysis, based on 16,867 OTUs, was employed to decipher microbial community co-occurrence patterns. The networks in the control and biochar-amended Oxisol contained 21.5% and 27.1% of the sequences, and the networks in the control and biochar-amended Mollisol contained 31.3% and 34.0% of the sequences from their respective OTU tables employed for co-occurrence analysis. Value of R^2 of power law ranged from 0.82 to 0.94, indicating scale-free network characteristics (Table 2.2). Overall, biochar-amended soil assemblages were larger, consisted of a greater number of nodes, and were more connected and complex. To determine potential topological roles of specific nodes within the network, nodes were classified according to their *Zi* (within module connectivity) versus *Pi* (among module connectivity) coefficients (Figure 2.2). Two network hubs and 19 module hubs were identified (Table A5). Constructed network properties were significantly different to those from randomized networks (Table A6).

Table 2.2. Topological properties of molecular ecological networks of bacterial communities under biochar amendment.

Soil	Oxisol		Mollisol	
Treatment	Control	Biochar	Control	Biochar
Similarity Threshold	0.730	0.660	0.600	0.610
Modularity	0.569	0.474	0.602	0.652
Total nodes	133	191	249	266
Total links	272	430	403	431
R^2 of power-law	0.94	0.874	0.906	0.815
Average degree (avgK)	4.09	4.503	3.237	3.241
Average clustering coefficient (avgCC)	0.116	0.105	0.147	0.097
Harmonic geodesic distance (HD)	4.359	3.887	5.146	5.104
Average path distance (GD)	3.64	3.344	3.2	4.288
Geodesic efficiency (E)	0.229	0.257	0.194	0.196
Harmonic geodesic distance (HD)	4.359	3.887	5.146	5.104
Maximal degree	28	32	46	36
Nodes with max degree	Acidobacteria OTU2714250	Bacteroidetes OTU848824	Acidobacteria OTU717396	Proteobacteria OTU614944
Centralization of degree (CD)	0.184	0.146	0.174	0.125
Maximal betweenness	3423.298	3333.394	8658.943	8920.543
Nodes with max betweenness	AcidobacteriaOTU2714250	Acidobacteria OTU4442148	Proteobacteria OTU614944	Proteobacteria OTU614944
Centralization of betweenness (CB)	0.377	0.173	0.274	0.243
Maximal stress centrality	42860	49129	37967	64334
Nodes with max stress centrality	AcidobacteriaOTU2714250	Acidobacteria OTU4442148	Proteobacteria OTU614944	Proteobacteria OTU614944
Centralization of stress centrality (CS)	4.639	2.557	1.187	1.751
Maximal eigenvector centrality	0.359	0.349	0.508	0.353
Nodes with max eigenvector centrality	AcidobacteriaOTU209467	Bacteroidetes OTU848824	Acidobacteria OTU717396	Acidobacteria OOTU728640
Centralization of eigenvector centrality (CE)	0.308	0.309	0.481	0.324
Density (D)	0.031	0.024	0.013	0.012
Reciprocity	1	1	1	1
Transitivity (Trans)	0.073	0.058	0.113	0.061
Connectedness (Con)	0.789	0.849	0.72	0.821
Efficiency	0.97	0.978	0.987	0.989
Hierarchy	0	0	0	0
Lubeness	1	1	1	1

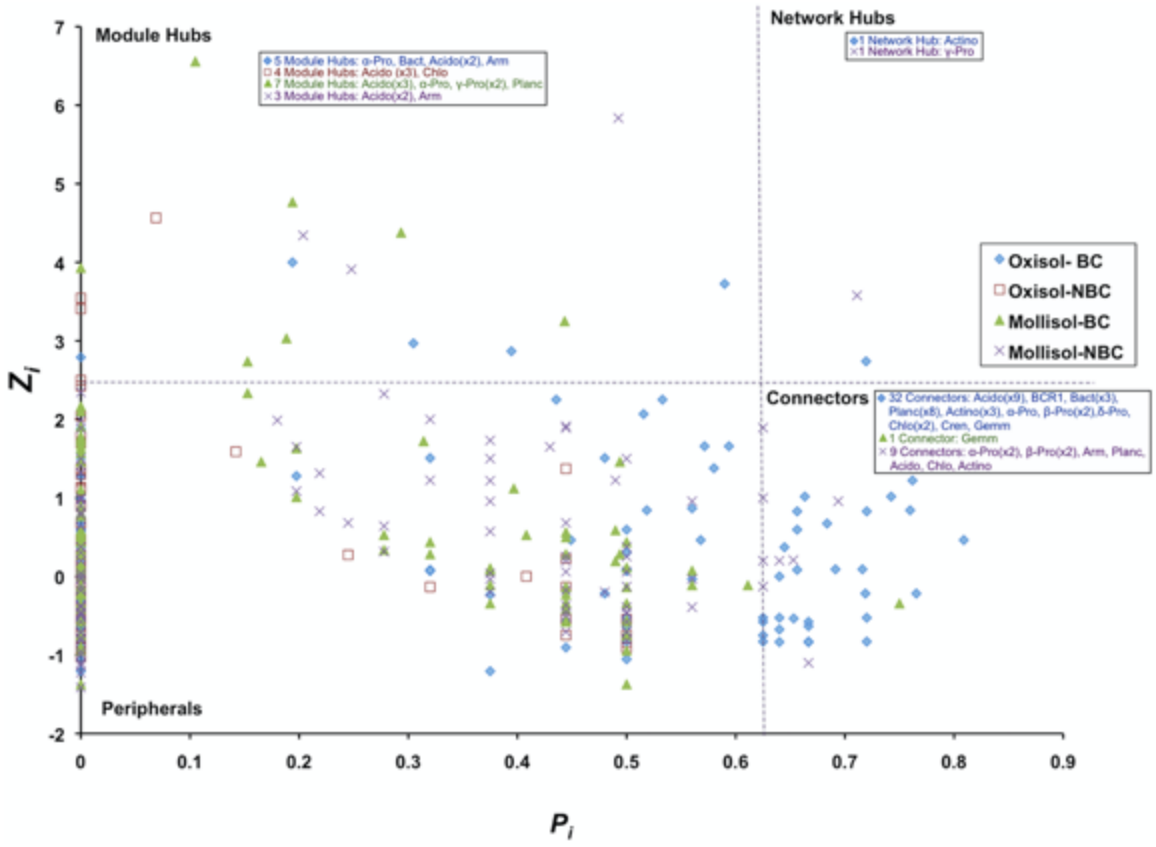


Figure 2.2. Topological roles of OTUs based on distribution of nodes on *Zi* (within module) vs. *Pi* (among module) connectivity scatter plot. Each symbol represents an OTU from the four networks. Phylogenetic affiliation of hubs and connectors are listed with the following abbreviations: Acido, *Acidobacteria*; Actino, *Actinobacteria*; Arm, *Armatimonadetes*; Pro, *Proteobacteria*; Bact, *Bacteroidetes*; Chlo, *Chloroflexi*; Cren, *Crenarchaeota*; Gemm, *Gemmatimonadetes*; Planc, *Planctomycetes*.

Biochar addition to the Oxisol soils resulted in a more complex and connected network. Nodes in the control network grouped to 5 modules (Figure 2.3A), each consisting of at least 5 nodes per module, while the biochar network grouped to 8 modules (Figure 2.3B). Connectivity and links increased with biochar as did average degree (i.e. average links per node) (Table 2.2). Interactions in the control network were evenly split between positive (49.6%) and negative (50.4%), while biochar addition resulted in an increase in negative interactions (62.8%). In the biochar-network, the most

dominant taxa in modules 9 and 17 were *Acidobacteria* composing 44.4% and 38.9% of the modules followed by *Planctomycetes* (22.2% and 16.7%). Module 11 was positively correlated to moisture, negatively correlated to soil C and was primarily composed of *Acidobacteria* (72.2%) while module 19 was composed of *Proteobacteria* (36.4%), *Planctomycetes* (27.3%) and *Actinobacteria* (18.2%). All nodes of module 1 belonged to *Proteobacteria* while the majority of nodes in module 10 were *Proteobacteria* (38.5%) followed by *Bacteroidetes* (13.5%) and *Acidobacteria* (11.5%). Module 18 was composed of *Bacteroidetes* (33.3%), *Proteobacteria* (28.6%) and *Actinobacteria* (14.3%). Module 13 appeared unique, with nodes representative of *Planctomycetes* (37.5%) and *Gemmatimonadetes* (25.0%).

In the Oxisol-control network the two largest modules, 7 and 8, contained 31.6% (42 nodes) and 39.1% (52 nodes) of the total number of nodes, respectively and were strongly positively correlated with one another (Figure 2.3A). In addition, both modules exhibited a significant negative correlation to soil pH and cations and a significant positive correlation to C and N. Oxisol biochar network modules were more highly correlated with each other than the control and could broadly be placed into two groups (Figure 2.3B). Modules 9, 17, 11 and 19 formed one putative assemblage (group 1). All modules in group 1 were positively correlated to Mg and K and negatively correlated to N and Ca. Group 2 contained modules 1, 10, and 18 that were positively correlated to water content, pH and, with the exception of module 10, positively correlated to N. Groups 1 and 2 were negatively correlated to each other, with the exception of module 10 that exhibited a weak positive correlation to group 1. *Acidobacteria* dominated these modules, comprising 31.0% and 32.7% of modules 7 and 8, respectively. *Crenarchaeota*

was only identified in module 7, comprising 19.1% of the total nodes while modules 9 and 10 contained 10.5% (14 nodes) and 5.3% (7 nodes) of the total number of network nodes. Module 9 was significantly negatively correlated with soil moisture and Na; taxa within this module were primarily *Proteobacteria* (50% of nodes) and *Acidobacteria* (21.4%). Module 10 was dominated by *Acidobacteria* (57.1% of nodes) and was significantly positively correlated with soil pH, Mg and K and significantly negatively correlated with soil C and N.

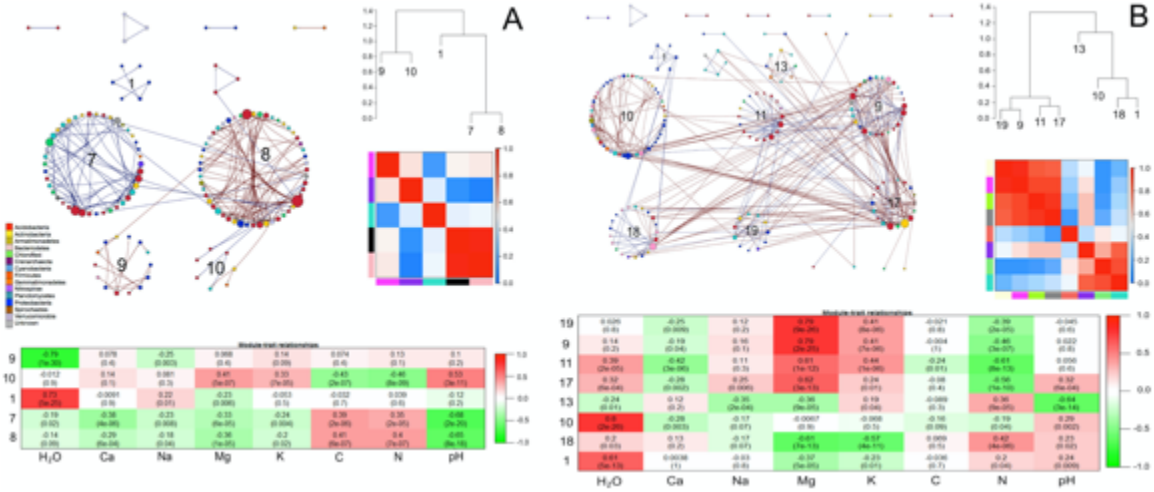


Figure 2.3. Molecular ecological network analysis of the Oxisol. (A) Oxisol-Control Network (B) Oxisol-Biochar Network. Dots represent nodes whose size indicates connectivity, node color represents taxonomy at the phyla level. Lines indicate co-occurrence between nodes colored either blue for positive or red for negative. Each circular grouping is a module. Numbers within modules correspond to numbers indicated in the hierarchical clustering. Top Right: Hierarchical clustering based on Pearson correlations among module-eigengenes and a heatmap of module eigengenes of the corresponding network. Bottom: Correlations of module-eigengenes and environmental factors for the corresponding network.

2.3.5 Effect of biochar amendment on microbial network analysis in the Mollisol

The effects of biochar treatment on microbial networks in the Mollisol were less pronounced than in the Oxisol (Figure 2.4). Overall, the number of links and nodes were more abundant, though a smaller average degree, connectivity and larger harmonic geodesic distance indicated that the Mollisol networks were less complex than the Oxisol (Table 2.2) with fewer strong correlations among modules and soil chemical properties. Interactions in the control network were more positive (54.6%) than negative (45.4%) while biochar addition resulted a moderate increase in negative interactions (56.6%). The majority of nodes in both the Mollisol-biochar and -control networks grouped to 8 modules containing 80.7% and 88.0% of the total nodes in the Mollisol-control and Mollisol-biochar networks, respectively.

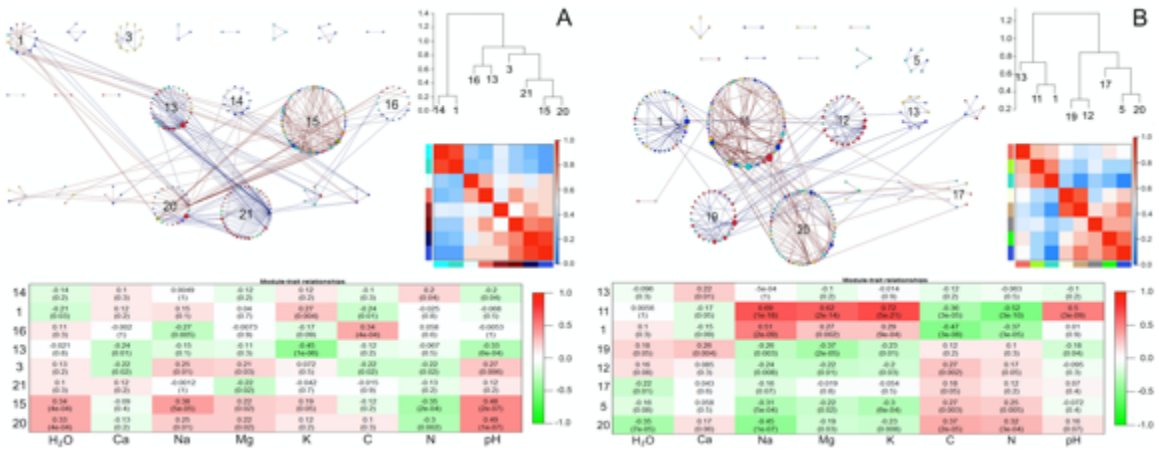


Figure 2.4. Molecular ecological network analysis of the Mollisol. (A) Mollisol-Control network; (B) Mollisol-Biochar network. Dots represent nodes whose size indicates connectivity, node color represents taxonomy at the phyla level. Lines indicate co-occurrence between nodes colored either blue for positive or red for negative. Each circular grouping is a module. Numbers within modules correspond to numbers indicated in the hierarchical clustering. Top Right: Hierarchical clustering based on Pearson correlations among module-eigengenes and a heatmap of module eigengenes of the corresponding network. Bottom: Correlations of module-eigengenes and environmental factors for the corresponding network.

Mollisol-control network modules grouped to three minor assemblages (Figure 2.4A). Modules 1 and 14 were highly correlated and formed one assemblage (group 1), composed of 53.9% and 81.8% *Proteobacteria*, respectively (Figure 2.4A). The second group was formed from weakly correlating modules 13 and 16 while the third group contained modules 15, 20 and 21 (Figure 2.4B). Overall, module 15 was the largest in the network, accounting for 31.8% of the total nodes. Modules 15 and 20 had a significant positive correlation with soil moisture, Na, Mg and pH, while negatively correlated with N. Module 3 was not strongly correlated with other modules in the network and was composed entirely of *Actinobacteria* with positive correlations to soil pH, Na and Mg and negative correlations to soil C and N. The predominant phyla in module 13 were the *Acidobacteria* (46.2%) followed by *Planctomycetes* (15.4%) and *Chloroflexi* (15.4%) while module 16 was composed of *Proteobacteria* (31.3%), *Acidobacteria* (25%) and *Planctomycetes* (25%). The third group was formed from module 15, 20, and 21 (Figure 2.9a). Module 15 was largest in the network, accounting for 31.8% of the total network nodes and dominated by *Proteobacteria* (28.1%), *Planctomycetes* (21.9%) and *Acidobacteria* (10.9%). In contrast, module 20 was composed of *Acidobacteria* (23.8%), *Planctomycetes* (19.1%) and *Proteobacteria* (14.3%). Module 21 was primarily *Acidobacteria* (59.0%) and had a significant negative correlation with soil Mg. Module 3 was not strongly correlated with other modules in the network and was composed entirely of *Actinobacteria* with positive correlations to soil pH, Na and Mg and negative correlations to soil C and N.

The addition of biochar to the Mollisol resulted in modules grouping to 3 assemblages (Figure 2.4B). Group 1 contained modules 1, 11 and 13. Module 13 was a

small module with a weak positive correlation to soil Ca and contained *Crenarchaeota* (50%), *Actinobacteria* (40%) and *Proteobacteria* (10%). *Proteobacteria* were dominant (~40%) in modules 1 and 11. Module 11 was the largest module in the network (32.1% of all nodes) with strong positive correlations to soil Na, Mg, K and pH and negative correlations with soil Ca, N and C (Figure 2.4B). Similarly, module 1 was positively correlated with soil Na, Mg and K and was negatively correlated with soil C and N. Group 2 in the network was formed by modules 19 and 13. Modules 13 and 19 were primarily *Acidobacteria*, (73.9% and 72%, respectively). The third group was formed from module 5, 17 and 20. Module 5 was composed of *Proteobacteria* (50.0%) and *Planctomycetes* (50.0%) while module 20 was composed of *Planctomycetes* (32.1%), *Proteobacteria* (18.9%), *Acidobacteria* (13.2%) and *Chloroflexi* (11.3%). *Cyanobacteria Chlorobi*, *Armatimonadetes*, *Bacteriodetes* and *Planctomycetes* were evenly distributed (14.3% per phylum) in module 17 with the exception of *Acidobacteria*, which made up 28.6% of the module.

2.4 Discussion and Conclusion

2.4.1 Biochar has the greatest effect on the microbial community of the Oxisol

Soil type was the strongest determinant of microbial community composition from the onset of the study, followed by cropping system particularly over time as the crops established and progressed through multiple harvest rotations. Napiergrass and corn further shaped the microbial community after one planting season, compared to a small disturbance effect initially detected in the bare, unplanted plots. The influence of biochar amendment was significant in both soils, but the magnitude of the impact on the microbial community was strongest in the low fertility Oxisol in both the pre-plant and

pre-harvest for both cropping systems. Module-Eigengene analyses enabled us to correlate specific modules with environmental properties and identify relationships among modules. Acidobacteria was highly abundant in modules 7 and 8 in the Oxisol-control network with the modules strongly negatively correlated with soil pH and positively correlated with soil C and N. Indeed, previous work has shown that the abundance of Acidobacteria is negatively correlated with soil pH (Jones et al., 2009; Männistö et al., 2007; Naether et al., 2012) though these results contradict a previous negative correlation with C availability (Fierer et al., 2007). In the more responsive Oxisol with biochar amendment, correlations among modules were stronger with two antagonistic module groups, perhaps indicating two distinct ecological niches due to differing resource allocation strategies.

Changes in community assemblages were mirrored by alterations in microbial community composition. Previously, soil type was shown to be a strong determinant of soil microbial community composition (Docherty et al., 2015; Girvan et al., 2003), as have altering land management practices (Zhao et al., 2016) which, in our case was reflected by tillage in the corn versus no-tillage management in the napiergrass. However, soil type is a proxy for differences in soil structure, clay and organic matter content and particle size that influence nutrient content and availability. While the majority of changes in soil chemical properties due to biochar addition were non-significant, shifts in pH (Docherty et al., 2015; Fierer and Jackson, 2006), moisture (Gordon et al., 2008) and cation concentrations (Lehmann et al., 2011) are common factors that influence microbial community composition, which were reflected in their correlations to specific modules in our study.

Biochar not only influenced the composition of the bacterial community, as illustrated by ordination, but also initially decreased the diversity, richness, and evenness, although generally not significantly. These decreases were observed in other short-term biochar amendment studies that coincided with increases in the relative abundance of *Actinobacteria* with biochar (Hu et al., 2014; Khodadad et al., 2011). With the exception of the corn plot in the Mollisol, alpha-diversity markedly increased over time with regards to cropping system in both soils. In the Oxisol, alpha-diversity tended to be higher in biochar amended soils indicating a combinatorial influence of both temporal variability (Lauber et al., 2013) and plant cover on the microbial community. Coinciding with this increase over time, alpha-diversity values also converged among the crops by pre-harvest. This was not expected, as napiergrass is a perennial tropical grass possessing a higher root density than annual corn, which can potentially support significantly higher SOC, microbial diversity and biomass than annual crops (Culman et al., 2010; Liang et al., 2011). However, a previous study that examined the influence of cropping system on the soil microbial community structure found that the effects of cropping system on alpha-diversity were only detected during peak aboveground biomass and that the rhizosphere of perennial and annual plants does not uniquely shape the soil microbial community (Hargreaves et al., 2015). The plant physiological traits during peak aboveground biomass in conjunction with biochar-amendment may in part explain the increase in diversity at pre-harvest and the convergence of alpha-diversity in the perennial and annual cropping systems. Furthermore, we found that conventionally tilled plots (i.e. corn) typically had higher alpha-diversity than no-till plots (i.e. napiergrass), particularly during pre-plant. The effects of tillage on the microbial community are

highly varied as previous studies have shown that conventional tillage led to lower abundance and diversity of soil bacteria and fungi due to disturbances that reduce soil aggregates and alter soil aeration, temperature and water content (Lienhard et al., 2013; Mathew et al., 2012). There is also evidence that tillage does not have a significant effect on diversity compared to no-till fields but significantly affects the bacterial community composition, the effect of tillage had a strong indirect effect on microbial community composition by directly affecting soil edaphic factors and nutrients (Smith et al., 2016). However, since tillage regime is nested within the cropping system further experimentation is needed to elucidate the influence of tillage on biochar-amended soils and the combined effects on the soil microbial community.

As a whole, biochar amendment in the Oxisol decreased the relative abundance of Acidobacteria Gp-6*,* the most abundant taxa in both soil types, and increased the abundance of Actinobacteria*.* This is consistent with previous work that showed an increased abundance of Actinobacteria in biochar-amended soil, supporting the notion that members of that phylum are well adapted to recalcitrant C-rich environments (Hu et al., 2014; Khodadad et al., 2011; O'Neill et al., 2009). In the Mollisol, biochar had a small but significant effect with increases in the relative abundance of N-cycling organisms such as *Nitrosospheraceae* and members of *Alphaproteobacteria* with cultured representatives known for N fixation, suggesting that biochar may increase N availability, though this is not supported by our soil chemical data. Our findings are consistent with a recent study which found that biochar shifted the microbial community with increases in *Alphaproteobacteria* and decreases in *Acidobacteria,* and that sampling time and soil effects had a greater influence than that of biochar treatment (Jenkins et al., 2017).

2.4.2 Biochar increases resistance of the microbial community and may enhance N cycling

Network modules derive from either synergistic or antagonistic microbial interactions or niche partitioning that results in the covariation of nodes in response to environmental factors (Shi et al., 2016). Soil properties, such as moisture and pH have been shown to alter ecological network properties (Barberán et al., 2012; Tylianakis et al., 2007) and changes in soil physiochemical properties induced by biochar addition may also alter the resilience of the microbial community to perturbations (Orwin et al., 2006). Results from the present study showed that biochar addition increased network complexity, linkages, and size, perhaps due to increased bacterial interactions and niches. With biochar, the larger numbers of links were also increasingly negative in direction, suggesting antagonistic or competitive interactions, such as for substrate acquisition. Thus, we interpret the higher complexity under biochar treatment as an increase in niche partitioning and interactions that supplant the bulk soil's previously more disconnected microhabitats (Fierer and Lennon, 2011; Torsvik et al., 2002). This may be due to a direct biochar effect by increasing niche availability for colonization due to the large biochar surface area and abundant potential microhabitats, especially when added to the more weathered Oxisol. Conversely, this may be a direct effect of C addition in the form of biochar as free air CO_2 enrichment (FACE) has been shown to increase network complexity in grassland soils, likely due to increased C inputs (Zhou et al., 2011, 2010). This suggests that the increase in negative interactions (competitive or antagonistic) may result from competition for new biochar C or nutrient inputs. This has important implications for improving soil C sequestration as the preferential mineralization of

biochar over native SOM can slow mineralization of the native SOC through negative priming (Lehmann et al., 2015; Rittl et al., 2015).

Previous work has shown that hubs (nodes that are highly connected within a module or the network) and connectors (those linking modules) may serve as keystone taxa, as they have important roles in maintaining network integrity (Faust and Raes, 2012; Olesen et al., 2007). The removal of these 'keystone' nodes may result in the disassembly of modules and networks as a whole (Paine, 1995; Power et al., 1996) thus reducing the stability of the microbial community (Lu et al., 2013; Olesen et al., 2007) to environmental perturbation. Within the Oxisol network, biochar amendment increased the number of putative keystone taxa derived from the connectors and network hubs, indicating that this assemblage was less sensitive to change. Notably, four connectors were identified to be associated with ammonia oxidizing and N-fixing lineages such as the *Crenarchaeota*, *Burkholderiales* and *Rhizobiales* (Hallam et al., 2006). In addition, abundant nodes of *Sphingomonadaceae* in the control were replaced by nodes classified to *Bradyrhizobiaceae* that include symbiotic N-fixing, denitrifying, and oligotrophic non-symbiotic bacteria (King, 2007) that may also participate in nitrification (Starkenburg et al., 2006), and are known to catabolize lignin aromatics (Kelly et al., 2000). Interestingly, modules associated with biochar amendment containing high abundances of these N cycling bacteria were also negatively correlated with soil N. This may indicate that N-fixing bacteria make an important contribution to increasing network complexity in the Oxisol under biochar amendment and may be more important than nitrifying or denitrifying bacteria, considering the negative module correlation with soil N. This is supported by previous studies that found biochar amendment increased potential N

fixation (Harter et al., 2014) and greater abundances of *Proteobacteria* involved in N cycling (Anderson et al., 2011; Orr and Ralebitso-Senior, 2014).

In contrast, biochar decreased the number of connectors and removed the network hub in the Mollisol. The putative keystone species connectors identified in the Mollisol network were again affiliated with *Rhizobiales* and *Burkholderiales.* Members of *Burkholderiales* have been previously shown to respond to changes in land use (Salles et al., 2004) and correlated with mineral weathering in soils (Lepleux et al., 2012). In this context, biochar may exert an opposite effect within the Mollisol soil. By removing the same types of functional putative keystone taxa that serve as important hubs in the Oxisol-biochar network, there is a potential for reduced N cycling within the Mollisol. Interestingly, the network hub was affiliated with the order *Xanthomaonadales*, a group that harbors many major phytopathogens (Naushad and Gupta, 2013). The disappearance of this hub after biochar addition coincides with the use of biochar to reduce plant disease (Atkinson et al., 2010).

2.4.3 Conclusion

Soil type was the greatest determinant of the microbial community composition. With respect to soil type, the effect of biochar on microbial community composition and assemblage patterns was lower than that of cropping system and sampling time. There was a greater impact of biochar on microbial community composition in the low fertility Oxisol than the high fertility Mollisol, though significant effects also were observed in that soil. Soil microbial community assemblages were more complex with biochar incorporation, especially in the Oxisol, with a higher connectivity driven by module and network hubs comprised of putative N cycling bacteria. Overall, the combined network

indices suggest that microbial assemblages under biochar exhibit a higher resistance to environmental perturbation, perhaps increasing the sustainability of soil function, though this remains experimentally unresolved.

CHAPTER 3

COMPARATIVE METAGENOMICS REVEALS ENHANCED NUTRIENT CYCLING POTENTIAL AFTER TWO YEARS OF BIOHAR AMENDMENT IN A TROPICAL OXISOL

Published in: Applied and Environmental Microbiology

2019. Comparative Metagenomics Reveals Enhanced Nutrient Cycling Potential After Two Years of Biochar Amendment in a Tropical Oxisol. *Applied and Environmental Microbiology,* 85: e02957-18.

Coauthors have acknowledged the use of this manuscript in my dissertation

Authors: Julian Yu, Lauren Deem, Susan E. Crow, Jonathan L. Deenik, and C. Ryan Penton

3.1 Introduction

Burgeoning global population and accelerated urbanization of developing countries is increasing competition for land, water, and energy resources and amplifying the imperative for agricultural intensification without comprising the environment for future generations (United Nations, 2017). To feed this growing and urbanized population, global food production must increase by ~70% (Alexandratos and Bruinsma, 2012), putting additional pressure on existing natural resources already under unsustainable management practices. Past increases in global food production was accomplished by intensification facilitated by massive inputs of synthetic nitrogen (N) fertilizers that ultimately conferred high environmental costs. A significant amount of applied nitrogen is lost from agricultural fields, which can cause eutrophication of aquatic ecosystems, loss of diversity, and increase nitrate leaching as well as increase nitrogen

oxide (NO_x) production (Arizpe et al., 2011; Tilman et al., 2002; Vitousek et al., 1997), leading to increased greenhouse gas (GHG) flux to the atmosphere.

Integrative solutions are required to re-structure productive systems into 'climate smart agriculture' and models of 'sustainable intensification' in order to increase food production from existing farmland in ways that reduce environmental impacts, such as a reduction in GHG emissions and through enhancing carbon (C) sequestration(Campbell et al., 2014; Garnett et al., 2013; Griscom et al., 2017). In this context, incorporation of biochar into soil is a promising management strategy for sustainable agriculture owing to its potential to sequester C and improve soil fertility (Jha et al., 2010; Lehmann et al., 2006). Biochar is a C-rich product of biomass pyrolysis and contains large portions of aromatic compounds that influence its stability and C sequestration potential in soil (Keiluweit et al., 2010; Wiedemeier et al., 2015). Documented beneficial effects of adding biochar to soil include increases in moisture retention, pH and cation exchange capacity (CEC) (Laghari et al., 2016; Lehmann et al., 2006), decreases in N_2O and CH_4 emissions (Aguilar-Chávez et al., 2012; Feng et al., 2012; Jeffery et al., 2016; Wang et al., 2012; H.-J. Xu et al., 2014), and decreases in N leaching from soil (Clough and Condron, 2010; Ding et al., 2010).

As part of a sustainable management practice, biochar addition induces changes in the soil physical and chemical properties and shifts in the soil microbiome. However, the microbial response to biochar addition depends strongly on soil type and cropping system, as well as the properties of the biochar being added (Anders et al., 2013; Docherty et al., 2015; Girvan et al., 2003; Jenkins et al., 2017; Lehmann et al., 2011; Steinbeiss et al., 2009; J. Yu et al., 2018). The observed effects of biochar on microbial

processes are variable. Some studies have observed an increase in soil respiration (Luo et al., 2011; Smith et al., 2010; Wang et al., 2012), although decreases or no changes have also been observed (Dempster et al., 2012; Noyce et al., 2015; Steinbeiss et al., 2009). The effects of biochar on microbial community composition has also been reported with some contradictory findings. Several studies have observed increases in *Actinobacteria, Proteobacteria*, *Bacteroidetes*, and *Gemmatimonadetes* (Anderson et al., 2011; Hu et al., 2014; Khodadad et al., 2011; Kolton et al., 2011) and decreases in *Acidobacteria* in biochar-amended soils (Jenkins et al., 2017; J. Yu et al., 2018), while others have reported decreases in *Proteobacteria and Bacteroidetes* (Ding et al., 2013; Hu et al., 2014; Kolton et al., 2011). A number of studies have attempted to assess the influence of biochar pyrolysis temperature (Budai et al., 2016; Dai et al., 2017), feedstock (Z. Yu et al., 2018), soil type, cropping system (H.-J. Xu et al., 2014; J. Yu et al., 2018), and addition with N-fertilizer (Bi et al., 2017; Tan et al., 2018) on the soil microbiome. Shifts in the microbiome composition and function influenced by biochar addition have the potential to impact GHG emissions, alter nutrient mineralization, and influence plant growth promotion. However, the dynamics and mechanisms of biochar impacts on microbial community composition as well as function remain poorly understood.

Many studies on the effect of biochar amendment on the soil microbiome have been based on analysis of the *16S rRNA* gene which revealed important shifts in community composition. However, there remains a lack of information concerning functional gene content and diversity which limits our understanding of the impacts of biochar on potential microbial function. The potential of the soil microbiome to control the fate of C and N in soils may be investigated using a shotgun metagenomic approach

in order to better elucidate the functional significance of a shift in community composition in response to biochar amendment than amplicon sequencing alone. To date, only one study has used a shotgun metagenomic approach to investigate the microbial community of aged biochar and the adjacent soils collected from a northern forest (Noyce et al., 2016). Our work represents the first study that applied shotgun metagenomics to agricultural biochar-amended soils.

In this study, we report on the shotgun metagenomic analysis of the soil microbial community of tropical Oxisol soils that experienced two years of biochar amendment under napiergrass cultivation. Our previous analyses of samples collected from the same soils in the first year of biochar amendment using targeted amplicon sequencing coupled with molecular ecological networks revealed that biochar amendment induced significant shifts in the microbial community, increased diversity and network complexity. However, whether the observed changes in the community composition reflects a shift in the functional gene diversity, whether the response to biochar amendment are attributed to a few taxa as opposed to being global, and what the functional adaptations underlining the response remain unknown in our previous study (J. Yu et al., 2018). The objective of the present study was to provide a high-resolution description of the community complexity, the genes and taxa responding to biochar amendment, and their potential effects on the soil C and N cycling. We expect the functional gene content of the biochar-amended metagenomes to reflect the shift in the community composition observed in the previous study and functional potential to reflect the results of the network analysis from our previous study, particularly with regard to enhanced potential for N-cycling and competition for resources associated with biochar.

3.2 Materials and Methods

3.2.1 Sample collection

A field experiment was established in November 2013 on the island of Oahu, Hawaii, United States at the Poamoho agricultural experimental research station managed by the College of Tropical Agriculture and Human Resources, University of Hawaii Manoa (21°32'30"N; 158°05'15"W). Detailed information on the experimental setup of the field experiment, biochar, and application rates were described in a previous study (J. Yu et al., 2018). Briefly, the soil at Poamoho is an acidic Oxisol with 44% clay rich in kaolinite and iron oxides with low CEC (NRCS Web Soil Survey). Napiergrass yield was determined as the total dry weight normalized by the number of plants before calculating the total dry weight per hectare of land because the number of plants in each plot varied slightly.

Our previous analysis of samples collected from the same field study during the first year and using *16S rRNA* amplicon sequencing, revealed that biochar had a significant effect on the soil community of the Oxisol compared to a Mollisol and the effect of biochar was consistently more pronounced under napiergrass (*Pennisetum perpereum* var. green bana, a C4 tropical, perennial, grass cultivated as a potential biofuel feedstock) cultivation compared to the annual cropping system (J. Yu et al., 2018). Therefore, for this study we selected a critical subset and analyzed the Oxisol under napiergrass, which is managed as a zero-tillage (i.e., ratoon harvested) system that retains the belowground environment and live root mass during harvest, approximately two years after the initial biochar amendment. Soils were collected in November 2015 from four replicate plots for biochar-amended and control soils (collecting and compositing eight

samples from randomly selected locations within each plot) prior to harvest and transported on dry ice to the laboratory. Soil chemical properties were determined as previously described in Chapter 3 (J. Yu et al., 2018) and are summarized in Table 4.1. Soils samples were frozen at -80°C without the addition of any protective agent until ready for further processing.

3.2.2 Experimental setup

Biochar-amended and control samples were collected in November 2015. Previously frozen field-moist soils were thawed, composited, and then sieved using a 2mm sieve. Six soil microcosms were set up in by adding 10g of soil to a 150mL serum bottles, three bottles containing biochar-amended soil and three with control soil. Microcosms were pre-incubated at 4°C open to the ambient atmosphere for 7 days to allow the soils to equilibrate then closed with bromobutyl rubber septums before incubation at 23°C. For the determination of cumulative CO_2, 200µL of headspace from each microcosm was sampled in triplicate using a gas-tight syringe (VICI Precision Sampling, Baton Rouge, LA). Soil microcosms were not continuously aerated. The CO_2 concentration in the bottles were measured using a gas chromatograph equipped with a flame-ionization detector (SRI instruments, Torrance, CA). The headspace was measured after microcosm setup (day 0) and after 2, 4, 6, 8, 10, 12, and 14 days of incubation. A standard curve was generated prior to measurement for each time point, each standard curve contained four points ranging from 50 ppm to 5,000 ppm CO_2 for 0-day and 2-day measurements and later from 5,000 ppm to 50,000 ppm CO_2 for the remaining gas measurements. In order to determine the rate of CO_2 production the concentration of CO_2 was adjusted to account for the ambient CO_2 concentration in the headspace. A linear

model was then used to determine soil CO_2 production rate between biochar-amended and control microcosms. The rate of CO_2 production was calculated from the best-fit line. After 14 days of incubation, soils were stored at -80°C until DNA extraction.

3.2.3 DNA extraction, sequencing, and pre-processing

Genomic DNA was extracted from 4g of soil using the DNeasy PowerMax Soil kit (Qiagen Company, Hilden, Germany) as described previously (J. Yu et al., 2018) and final DNA concentrations were quantified by Qubit dsDNA high-sensitivity kit (ThermoFisher Scientific, Waltham, MA, USA) using the Qubit 3.0 (ThermoFisher Scientific, Waltham, MA, USA). From each sample, 1μg of genomic DNA was used for library preparation. Briefly, DNA was first fragmented using the Covaris system (Covaris, Woburn, MA, USA), and ligated with Illumina TruSeq paired-end adaptors. Sequencing was carried out using the 2 x 150 high output platform on the Illumina NextSeq 500 instrument. The resulting sequencing reads were quality filtered and trimmed to remove the Illumina adaptors using Trimmomatic version 0.36 (Bolger et al., 2014), paired end reads were interleaved using the interleave-reads.py script from khmer version 2.1.1(Crusoe et al., 2015) before assembly.

3.2.4 Metagenome assembly and gene annotation

The assembly of metagenomes was carried out using MEGAHIT v1.1.2 (Li et al., 2016, 2015) and the quality of the assemblies was assessed with QUAST version 3.0 (Gurevich et al., 2013). Assembled reads were used as input into the MG-RAST pipeline (Meyer et al., 2008) for downstream processing and annotation. After quality filtering and removal of artificial duplicate reads, protein-coding genes and rRNA genes included in the assembled contigs were identified using FragGeneScan (Rho et al., 2010) and

SortMeRNA (Kopylova et al., 2012), respectively, through the MG-RAST pipeline. Annotation of amino acid sequences from the predicted protein-coding genes were searched against the SEED database (Overbeek et al., 2005) using BLAT (Kent, 2002) with default settings. The best match for each read using a cutoff E-value of <1E-7, an alignment length of 25 amino acids, and an amino acid identity of >60% against the SEED (Overbeek et al., 2005) genes was recorded and the number of best-hit reads was taken as a proxy for the abundance of SEED genes and subsystems in each sample. The relative abundances of domains in the metagenomes were estimated based on the best match of amino acid sequences against the RefSeq database (O'Leary et al., 2016) using MG-RAST. Raw sequences were deposited in GenBank under PRJNA497915 and the assembled reads were deposited in MG-RAST under project ID mgp83293.

3.2.5 Estimating community complexity and determination of differentially present pathways

The relative abundances of different phyla/classes in each sample were quantified by the number of reads assigned to a taxon using the same cutoffs as described above and normalized by sample size. To examine differences in the abundances of bacteria as a result of biochar amendment, the average abundances from three replicates (biochar-amended and control soils) of phyla that made up less than 1% of the whole community were analyzed separately from those which comprised at least 1% of the whole community. Data sets were subject to Hellinger transformation for Bray-Curtis dissimilarity matrices and significant differences in the microbial community between treatments were tested with Permutational Multivariate Analysis of Variance (PERMANOVA)(Anderson and Walsh, 2013) using the ADONIS function in R's vegan

package (Oksanen et al., 2018). Phyla that were significantly differentially present were identified using the paired t-test. Differences were considered significant at a P-value of < 0.05. Estimates of average coverage and sequence diversity for each metagenomic dataset were carried out with Nonpareil 3 using default settings (Rodriguez-R et al., 2018; Rodriguez-R and Konstantinidis, 2014). Metagenomic coverage was calculated and visualization of the nonpareil curves was carried out using the nonpareil package in R studio. Shannon diversity, Margalef's richness, and Pielou's evenness indices were calculated for each sample using the *16s rRNA* gene-based OTU count tables from MG-RAST at the genus level. Shannon diversity was calculated using the diversity function in the vegan package in R studio, Pielou's evenness was defined as the Shannon index H' divided by the log of the species number, and Margalef's richness was defined as the number of species minus 1 divided by the natural logarithm of the total number of individuals. Paired student's t-tests were carried out to determine whether or not the control and biochar-amended samples differed significantly from each other in alpha diversity.

To identify pathways that were significantly differentially present between the control and biochar-amended samples, the DESeq2 package (Anders and Huber, 2010) was employed in RStudio (version 1.0.136). A count table of the functional annotation was generated with the SEED level-3 subsystem which is similar to a Kyoto Encyclopedia of Genes and Genomes (KEGG) pathway. Each column represented a sample and each element was the number of reads from the sampled assigned to the SEED subsystem. DESeq2 was then used, with the default settings, to estimate the effective library size and variance. The size factor of the metagenomes was then used to

normalize the counts prior to detection of differences between biochar-amended and control samples for each SEED subsystem.

3.3 Results

3.3.1 Soil chemical characteristics and respiration

We focused our study on soils collected two years after the initial addition of biochar to an Oxisol under napiergrass cultivation. Eight samples from the control and biochar-amended soils were used to determine the soil chemical characteristics. These soils, collected pre-harvest, had few measurable differences in elemental concentration, nutrient status, and associated crop yield (Table 4.1). As expected, mean C concentration (C%) of the biochar-amended soils was significantly higher than soil control soils. Otherwise, biochar-amended soils contained slightly higher soil N%, but the differences were not statistically significant. Soil pH was close to neutral in both biochar-amended and control soils. No statistical differences were observed in soil moisture or base cations (calcium – Ca^{2+}, sodium – Na^{2-}, magnesium – Mg^{2+}, and potassium – K^{+}), although soil base cations were generally higher in biochar-amended samples, with the exception of Ca (Table 4.1). The napiergrass crop yield, harvested approximately one month after the soil core collection, was higher in biochar-amended plots than compared to control plots, (Figure B1), but the difference also was not statistically significant ($p = 0.233$, paired t-test).

Table 3.1. Soil characteristics of the Oxisol used in the microcosms. Bolded values indicate significantly different ($p < 0.05$) levels between biochar-amended and control soils.

Soil Chemical	**Mean ± Standard Error**		**p-value**
Ca (mg kg^{-1} soil)	1554.14 ± 106.00		0.828
Na (mg kg^{-1} soil)	35.85 ± 1.83		0.608
Mg (mg kg^{-1} soil)	235.10 ± 12.40		0.254
K (mg kg^{-1} soil)	861.98 ± 56.05		0.199
pH	6.70 ± 0.123		0.709
Moisture %	35.51 ± 0.88		0.152
Carbon %	1.73 ± 0.11		**0.001**
	Control	**Biochar**	
	1.37 ± 0.02	2.08 ± 0.13	
Nitrogen %	0.170 ± 0.003		0.162

Soil respiration, or cumulative CO_2 production from the soil, was measured as a proxy for microbial activity for each of the microcosms over a 14-day period. Overall, the concentration of CO_2 in the headspace from the control soil was significantly higher than to the biochar-amended soil at all times point measured (Figure 3.1). The mean CO_2 production rate in the biochar-amended microcosm was slightly lower (0.011 μg C-CO_2 g^{-1} soil day^{-1}) compared to the control (0.014 μg C-CO_2 g^{-1} soil day^{-1}), although the difference in respiration rate was not significant (p-value = 0.14, two sampled T-test)

(Figure 3.1). However, when substrate quality was taken into account, the biochar-amended microcosm respiration rate was significantly lower (0.005 µg C-CO_2 g^{-1} soil-C day^{-1}) compared to the control (0.010 µg C-CO_2 g^{-1} soil-C day^{-1}) (p-value < 0.001, two sample T-test)(Figure 3.1).

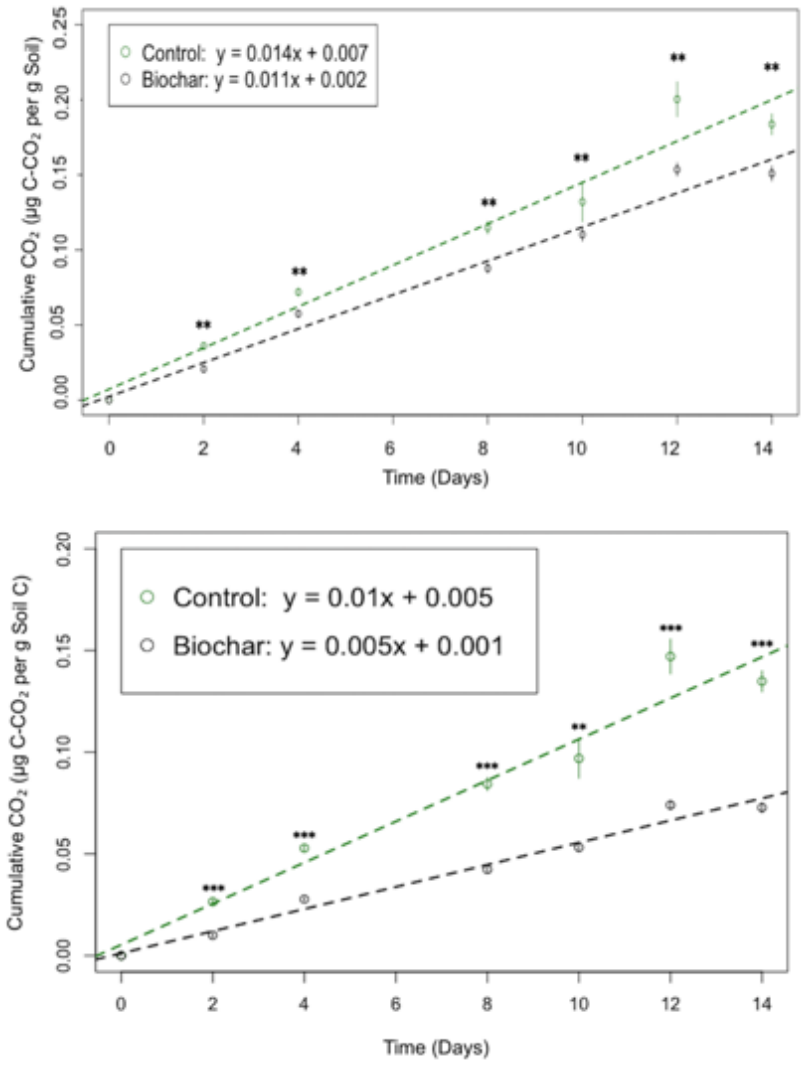


Figure 3.1. Cumulative CO_2 production over a 14-day incubation period. Top: CO_2 production per gram of soil. Bottom: CO_2 production per gram of soil carbon. Equation for best-fit lines are given next to figure legends. Points represent the average microcosm CO_2 concentration and error bars represent the standard error of the mean (n = 6); green circle: control soil microcosms, black circles indicate biochar-amended soil microcosms; ***, P < 0.001; **, P < 0.01, *, P < 0.05.

3.3.2 Statistics of metagenomes and community complexity

Sequencing from three replicate samples representing the biochar-amended soils (BC1 to BC3) and three samples representing the non-biochar control soil (NBC1 to NBC3) yielded approximately 10 to 40 gigabytes of paired-end sequence data per sample. Four metagenomes (NBC1, NBC2, NBC3, and BC3) each had between 11 to 15Mbp of sequences while two metagenomes (BC1 and BC2) had a range of 45 to 50Mbp of sequences (Table B1). The estimated coverage based on the read redundancy value calculated using Nonpareil revealed an average coverage of about 0.15 and 0.28 for the metagenomes obtained from control and biochar-amended Oxisol samples, respectively. Application of Nonpareil estimates revealed that large sequencing efforts were required for these soil samples, where up to 1Tb of sequence data were expected to be necessary to achieve nearly complete (99%) abundance-weighted average coverage (Figure 3.2). Sequence diversity values, a measure of alpha diversity derived from Nonpareil curves, showed no differences between biochar-amended (average = 28.29) and control (average = 28.22) soils. The assembly of the metagenomes recovered ~280 000 and ~1.5 million contigs of at least 1kbp in length from the control and biochar-amended samples, respectively. The N_{50} values averaged from biochar-amended soil metagenomes were slightly higher than the controls (1 133 vs. 915bp), reflecting the lower sequence coverage determined by Nonpareil for the control metagenomes (Table

B1, Figure 3.2). Assemblies were processed through the MG-RAST pipeline where approximately 11% of the total sequences failed to pass the quality control pipeline across all metagenomes (Table B2). The number of *rRNA* genes were approximately 2,000 and 6,000 sequences for control samples including BC3 and two biochar-amended samples, respectively (Table B2). In biochar-amended and control metagenomes an average of 3.6 million and 1.1 million sequences (72% of total sequences) contained predicted genes of known function, and 1.36 million and 778,000 sequences (28% of total sequences) contained predicted genes with unknown function, respectively (Table B2).

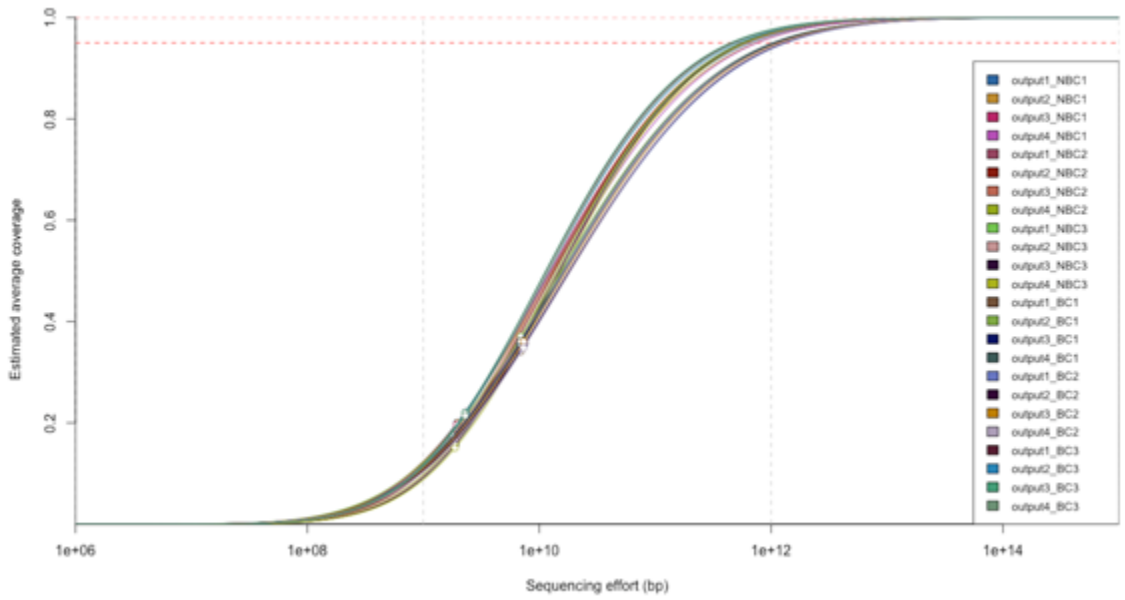


Figure 3.2. Average metagenomic coverage. Estimated from the portion of non-unique reads as a function of the size of subsamples randomly drawn from the metagenomes of biochar-amended and control soils. The solid line indicates the fitted model based on subsampling, the empty circles mark the actual size and estimated coverage of the metagenome data set, the red and pink horizontal dashed line indicates the 95% and 100% average coverage level, respectively. Abbreviations: BC: biochar-amended samples and NBC: non-biochar control samples, number following abbreviation indicates the sequencing technical replicate.

3.3.3 Microbial community structure and diversity

Prokaryote sequences represented the majority of each microcosm community sampled, with over 99% of the total number of genes recovered with best matches against bacterial and archaeal genomes in MG-RAST (Table B1). Bacterial sequences predominated the prokaryotic sequences, averaging ~99% of sequences in all samples. Archaeal sequences comprised approximately 0.43% and 0.63% and eukaryotes represented approximately 0.41% and 0.45% of the total sequences in the control and biochar-amended samples, respectively. Domain-level differences in abundance were significant for archaea and viruses ($p<0.05$, two-tailed paired t-test), archaeal abundance was higher in controls and viruses were greater in biochar-amended samples (Table B1). *Euryarchaeota* and *Crenarchaeota* were the most abundant phyla within the archaea, representing 74.4% and 80.9% and 13.7% and 13.3% in the control and biochar-amended samples, respectively (data not shown). The next most abundant phyla in archaea were the *Thaumarchaeota* which represented 10.8% and 4.6% of the total archaeal sequences in control and biochar-amended samples. Significant differences in archaeal relative abundance was observed for *Euryarchaeota* and *Thaumarchaeota* ($p<0.05$, paired t-test). Within eukaryotes, no significant differences were observed for fungal abundance. *Ascomycota* and *Basidiomycota* were the two most abundant fungal phyla, which accounted for approximately 89% and 11% of the total fungal sequences, respectively.

The *Ascomycota* were enriched in the biochar-amended samples and *Basidiomycota* were enriched in the control samples, although the differences in relative abundance were not significantly different. Bacterial phyla that comprised at least 1% of the community included *Proteobacteria*, *Actinobacteria*, *Bacteroidetes*, *Firmicutes*, *Acidobacteria*, *Chloroflexi*, *Cyanobacteria*, *Planctomycetes*, *Verrucomicrobia*, and *Gemmatimonadetes*. *Proteobacteria* and *Bacteroidetes* were 31% (54.6% in biochar-amended and 41.7% in controls) and 104% (4.5% in biochar-amended vs. 2.2% in controls) higher in the biochar-amended samples, respectively. *Actinobacteria* were 33% higher in controls (38.3% in controls vs. 25.6% in biochar-amended), *Firmicutes* (5.0% in controls vs. 3.8% in biochar-amended) and *Chloroflexi* (2.2% in controls vs. 1.4% in biochar-amended) both were approximately 25% higher in controls, and *Cyanobacteria* were approximately 12% higher in controls samples than compared to biochar-amended samples (1.6% in controls and 1.2% in biochar-amended). The relative abundances of *Acidobacteria, Gemmatimonadetes*, *Planctomycetes,* and *Verrucomicrobia* were not significantly different between treatments. Alpha-diversity indices (i.e. Margalef's richness, Pielou's evenness, and Shannon diversity), based on *rRNA* gene-containing reads recovered in the metagenomes, exhibited no significant differences between control and biochar-amended samples (Table B3).

Within bacteria, several significant differences were observed at the phyla level (Figure 3.3A). In biochar-amended samples the relative abundances of *Proteobacteria* and *Bacteroidetes* were significantly higher than the controls. In the controls the relative abundances of *Actinobacteria*, *Firmicutes*, *Chloroflexi*, and *Cyanobacteria* were significantly higher than the biochar-amended samples.

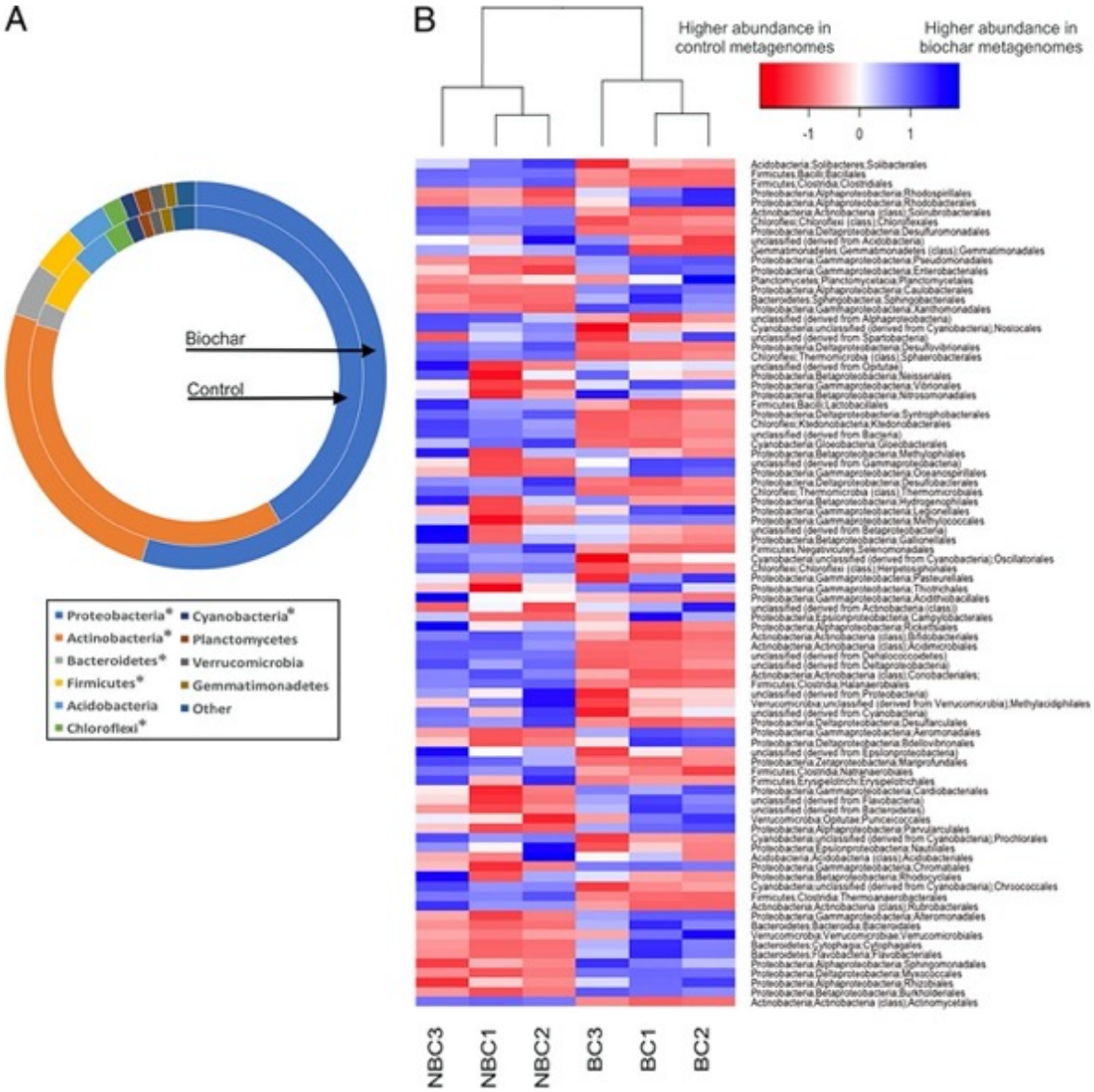


Figure 3.3. Shifts in taxon abundance as effects of biochar amendment. (A) Rings represent the average abundances of phyla that make up at least 1% of the whole community. Phyla that are significantly different in abundance between biochar-amended and control samples are marked by an asterik ($P<0.05$, two-tailed paired t-test). (B) Heatmap of the normalized abundance at the class level for bacteria in the six microcosm metagenomes. Color code based on higher relative abundance in control (red) or in biochar-amended (blue) (see scale on the top right).

A heatmap of the relative abundances at the class level confirmed that the samples from the two different treatments clustered separately (Figure 3.3B), although the differences between biochar-amended and control samples were not significant ($p = 0.1$, PERMANOVA). Biochar-amended metagenomes had higher relative abundances of *Proteobacteria* belonging to *Alphaproteobacteria*, *Betaproteobacteria*, *Gammaproteobacteria*, and *Deltaproteobacteria*, and *Bacteroidetes* belonging to the classes, *Bacteroidia*, *Cytophagia*, *Flavobacteria*, and *Sphingobacteria*. Phyla that comprised less than 1% of the community were generally higher in the controls compared to biochar-amended samples with the exception of the *Spirochaetes*, *Fibrobacteres*, and *Tenericutes*.

3.3.4 Relative abundances of metabolic pathways in biochar-amended versus control metagenomes

Of the total pathways at the SEED subsystem level-3, 380 of 1,035 were significantly differentially abundant (p-value <0.05). The majority of the significant differences in pathway abundances between biochar-amended and control samples were small, typically a $\log_2$-fold change <1 (Table B4). Nonetheless, several significant changes were noted and these changes were consistent among the replicates. For example, clustering of samples and replicates based on level-1 subsystems showed that the biochar-amended versus the control samples clustered together (Figure B2). A large portion of pathways involved in carbohydrate metabolism showed significant changes in relative abundance (Figure 3.4). In particular, several pathways that are involved in central carbohydrate metabolism were enriched in controls including some pathways involved in methane metabolism, (Figure 3.4). Significant changes in methane

metabolism related pathways included the ethylmalonyl-CoA pathway (LFC = 0.577), soluble methane monooxygenase (LFC = 0.741), and dehydrogenase complexes (LFC = 1.28). Other pathways in the carbohydrate subsystem enriched in control samples were within fermentation including butanol biosynthesis (LFC = 0.374), lactate fermentation (LFC = 0.227), one-carbon metabolism (LFC = 0.323), and sugar alcohol utilization including inositol catabolism (LFC = 0.251) and mannitol utilization (LFC =0.342). Pathways involved in CO_2 fixation, such as CO_2 uptake and genes that encoded for carboxysomes (e.g. carbonic anhydrase) and labile carbon source metabolism were enriched in biochar-amended samples. Pathways involved in labile C source metabolism that were higher in biochar-amended samples included utilization of a number of monosaccharides, disaccharide utilization, such as meliboise utilization (LFC = 4.64) and sucrose utilization (LFC = 2.33), organic acid utilization, such as malonate decarboxylase (LFC = 1.78) and methylcitrate cycle (LFC = 1.32), and polysaccharide degradation including glycogen metabolism (LFC = 2.77) and cellulosomal enzymes (LFC = 0.692) (Figure 3.4, Table B4).

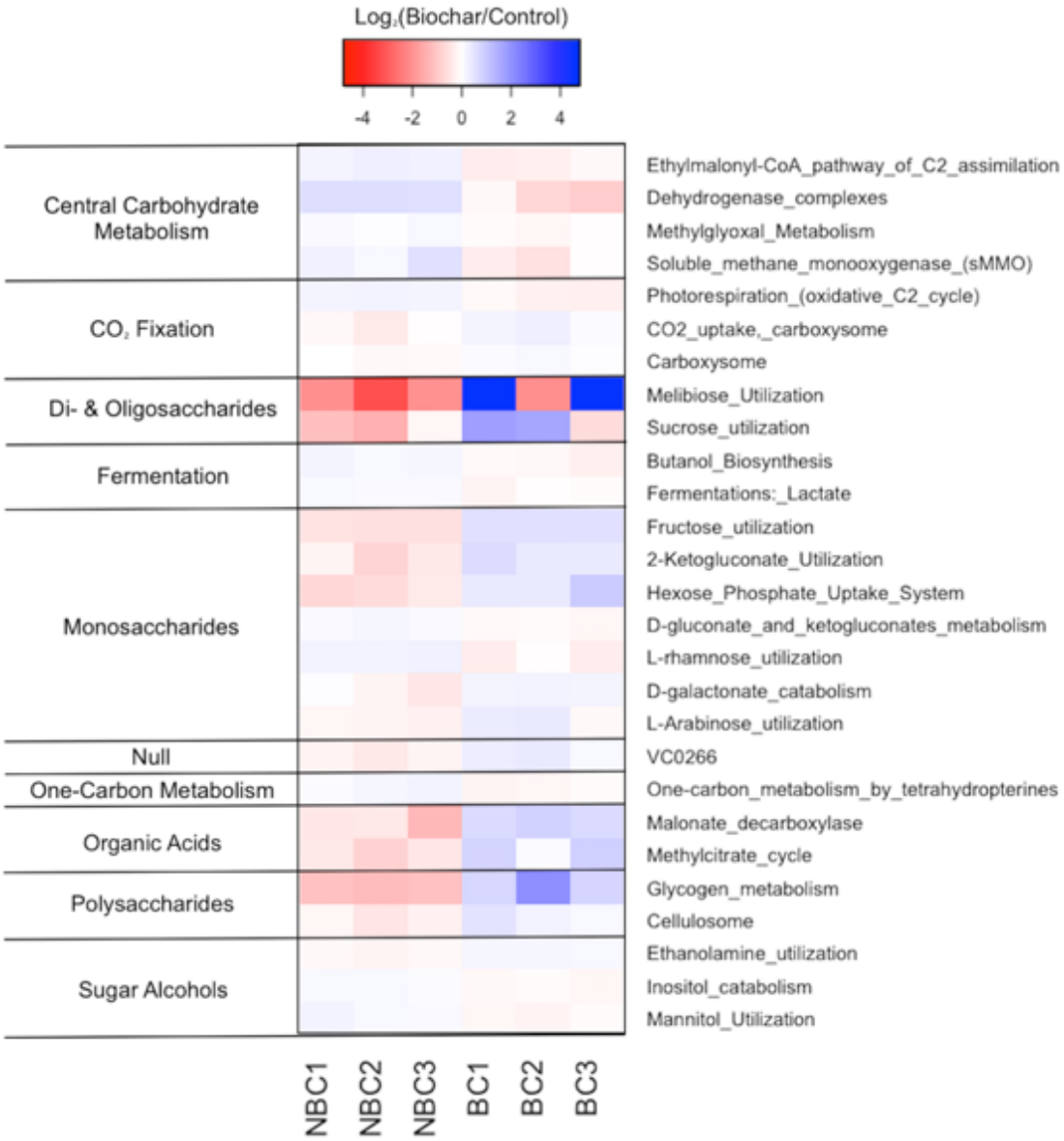


Figure 3.4. Significant changes in abundance of carbohydrates pathways as an effect of biochar addtion. Row labels on the left indicate the level-2 subsystem classification and labels on the right indicate the level-3 subsystem classification for each microcosm metagenome (columns). Color code is based on the magnitude of change, scale values indicate the $\log_2$-fold change (see scale on the top).

In the respiration subsystem, control samples were enriched in pathways involved in carbon monoxide dehydrogenases, succinate dehydrogenase and respiratory complex 1 (e.g. NADH ubiquinone oxidoreductase). Biochar-amended samples were enriched in pathways involved in NiFe-hydrogenase maturation, respiratory dehydrogenase-1, which included several dehydrogenases involved in amino acid, sugar and alcohol dehydrogenation, and several cytochrome oxidases (Figure 3.5A). The majority of pathways in the metabolism of aromatic compounds subsystem was enriched in biochar-amended samples (Figure 3.5B). Additionally, the benzoate degradation and carbazol degradation clusters were also enriched in biochar-amended samples. Conversely, pathways in the secondary metabolism subsystem were enriched in the controls (Figure 3.5B), including cinnamic acid degradation and genes for 4-coumarate--CoA ligase-1. The pathways involved in metabolism of aromatic compounds subsystem enriched in biochar-amended samples included metabolism of central aromatic intermediates including salicylate and gentisate catabolism (LFC = 1.50), catechol degradation (LFC = 1.78), and peripheral pathways for catabolism of aromatic compounds such as chlorobenzoate (LFC = 0.584), quinate (LFC =0.845), and naphthalene and antracene (LFC = 0.369) degradation.

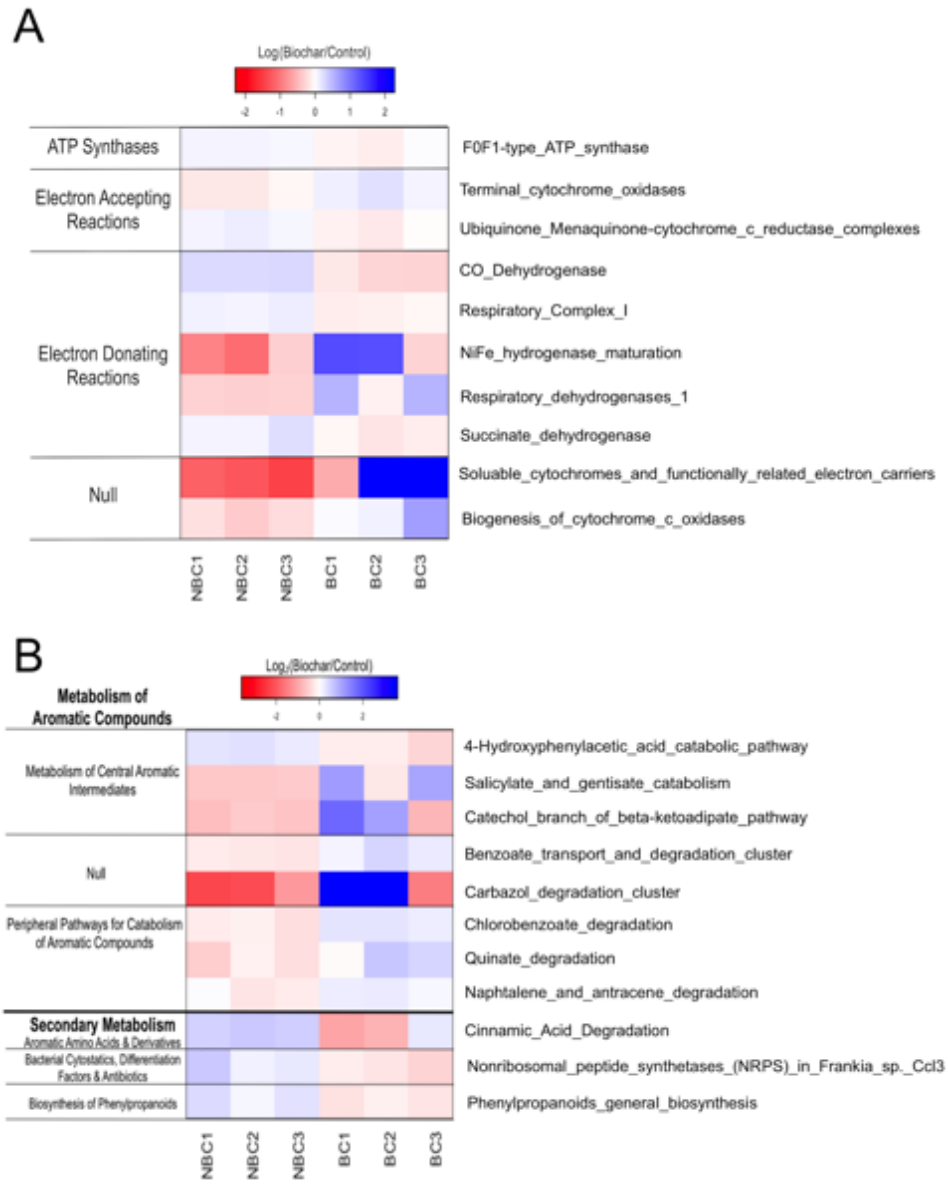


Figure 3.5. Significant changes in abundance of different pathways in respiration, metabolism of aromatic compounds, and secondary metabolism as an effect of biochar addtion. Row labels on the left indicate the level-2 subsystem classification and labels on the right indicate the level-3 subsystem classification for each microcosm metagenome (columns). Color code is based on the magnitude of change, scale values indicate the $\log_2$-fold change (see scale on the top of each heatmap). (A) Heatmap repesenting pathways in the respiration subsystem. Labels on the left indicate the level-2 subsystem classification and labels on the right indicate the level-3 subsystem classification. (B) Heatmap representing pathways in secondary metabolism and metabolism of aromatic compounds. Bolded labels indicate the level-1 subsystems classification.

With respect to the nitrogen metabolism subsystem, pathways involved in denitrification, which included genes for nitrous and nitric oxide reductases, their maturation and activation proteins as well as genes for the copper-containing nitrite reductase accessory protein, and allantoin utilization were enriched in biochar-amended samples (Figure 3.6A, Figure B3). Control samples were enriched in pathways involved in ammonia assimilation, specifically genes for ammonia transporters and glutamine synthetases (Table B4). Pathways involved in N-fixation, specifically nitrogenase transcriptional regulators were higher in controls (Figure 3.6A, Figure B3). Control samples were significantly enriched for dissimilatory nitrite reductase; however, it is important to note that the genes belonging to this subsystem were involved in c-type cytochrome and heme d_1 biosynthesis rather than genes encoding the nitrite reductase enzymes (Figure 3.6A, Figure B3). Additionally, the majority of significantly differentially present pathways involved in amino acid degradation/utilization and their derivatives were enriched in the controls (Figure 3.6A). Significantly differentially present pathways involved in amino acid degradation or utilization and their derivatives included the putrescine utilization pathway (LFC = 0.726), arginine deaminase (LFC = 0.378), branched-chain amino acid biosynthesis (LFC = 0.731), histidine degradation (LFC = 0.266), threonine and homoserine biosynthesis (LFC = 0.263), and creatine and creatinine degradation (LFC = 0.249). Biochar-amended samples were enriched in pathways involved in leucine degradation (LFC = 1.43) and valine degradation (LFC =1.92).

The majority of genes related to the cycling of other nutrients, such as phosphorus (P), potassium (K), and iron (Fe) metabolism were enriched in biochar-amended samples

(Figure 3.6B). Control samples were enriched in pathways involved in P uptake in cyanobacteria and hemin uptake in gram-positive bacteria. Finally, the pathways in the sulfur metabolism subsystem were enriched in biochar-amended samples (Figure 3.6B). Organic sulfur assimilation was enriched in controls, this included pathways such as alkanesulfonate assimilation and utilization of glutathione, which included ABC-type nitrate/sulfonate/bicarbonate transport systems and putative glutathione transporters, respectively. The majority of genes related to the cycling of other nutrients enriched in biochar-amended samples included phosphate-binding DING proteins (LFC = 1.59) and phosphate metabolism (LFC = 1.05), potassium homeostasis (LFC = 0.349), Hemin transport system (LFC = 3.05), transport of iron (LFC = 0.815), vibrioferrin synthesis (LFC = 1.45), and biosynthesis of siderophore pyoverdine (LFC = 0.412), galactosylceramide and sulfatide metabolism (LFC = 5.73), thioredoxin-difulfide reductase (LFC = 0.433) and taurine utilization (LFC = 1.29).

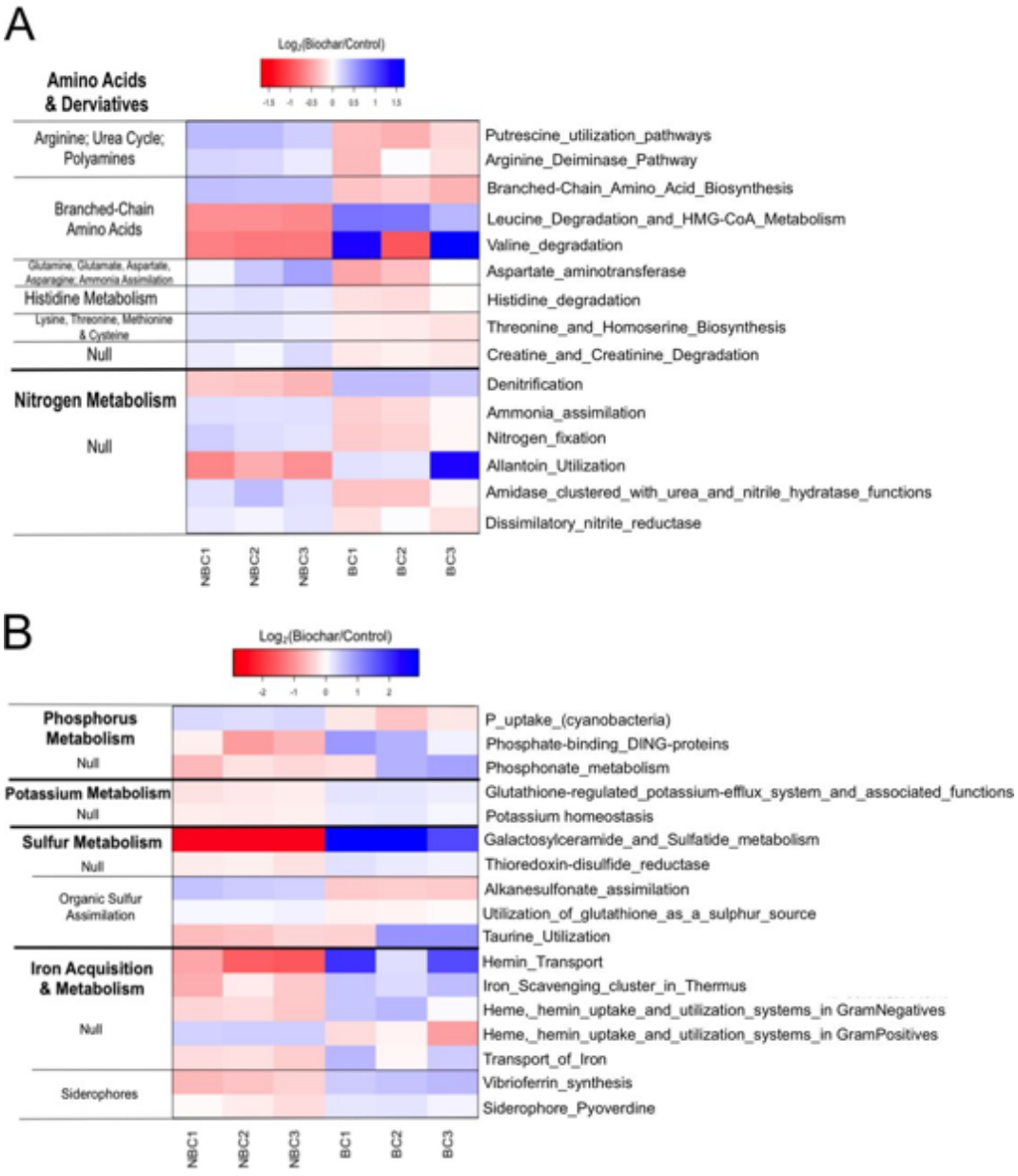


Figure 3.6. Significant changes in abundance of different pathways for nutrient acquistition and metabolism. Row labels on the left indicate the level-2 subsystem classification and labels on the right indicate the level-3 subsystem classification for each microcosm metagenome (columns). Color code is based on the magnitude of change and scale values indicate the log_2-fold change (see scale on the top of each heatmap), bolded labels indicate the level-1 subsystems classification. (A) Heatmap repesenting pathways in the amino acids degradation and biosynthesis, and N metabolism. (B)) Heatmap repesenting pathways in the phosphorus, potassium, sulfur metabolism, and iron metabolism.

3.4 Discussion and Conclusion

3.4.1 Composition and stability of microbial community responding to biochar

The use of metagenomics to probe putative functional changes in the microbiome within microcosms containing Oxisol soils under napiergrass cultivation two years after the initial addition of biochar revealed a deep level of insight into microbiome responses to this amendment. Shifts in the microbial community composition were much less pronounced compared to our previous study (J. Yu et al., 2018) where the overall changes in the composition of the microbiome were small though significant. This may reflect the effects of homogenization of the soils by sieving since there is evidence that different soil fractions support distinct microbial communities (Fox et al., 2018). Communities may differ between the <2 mm fraction and the large soil aggregates (>2mm). Conversely, the majority of functional genes/pathways did not exhibit significant differences in abundance between control and biochar-amended metagenomes. It is important to note that the metagenomic snapshots reported here might have missed short-term changes to microbial community composition or functional gene abundances due to biochar amendment. Additionally, the number of rRNA gene sequences identified in the metagenomic data was low compared to the number of gene-encoding sequences. Nonetheless, the taxa shifts within our metagenomic dataset reflected the shifts observed in our previous analysis (J. Yu et al., 2018).

Consistent with previous studies based on *16S rRNA* gene amplicons, we showed that *Proteobacteria* and *Bacteroidetes* relative abundances significantly increased in biochar-amended samples and that the relative abundance of *Acidobacteria* decreased (Jenkins et al., 2017; Kolton et al., 2011; Li et al., 2018; J. Yu et al., 2018). Overall, all

classes of *Proteobacteria* were more abundant in the biochar-amended samples, consistent with our previous study (J. Yu et al., 2018) in which we observed that biochar increased *Proteobacteria* abundance in the Oxisol as early as one month and up to one year after the initial amendment. Notably, the orders *Rhizobiales* and *Burkholderiales* were most abundant and higher in biochar-amended samples, and have been characterized as N-fixers; more broadly as N-cycling generalists, carrying genes for the majority of the assimilatory and dissimilatory N pathways (Nelson et al., 2015). Furthermore, some members of both bacterial orders have the ability to degrade recalcitrant compounds including some naturally occurring aromatic compounds and organic contaminants such as those used as pesticides, herbicides, or fungicides. For example members of *Burkholderiales* have been shown to degrade pentachlorophenols (Tong et al., 2015) and members of *Rhizobiales* can degrade compounds such as 4-fluorocatechol and catechols (Carvalho et al., 2006). In this study, biochar-amended samples nearly doubled the relative abundance of *Bacteroidetes*. *Bacteroidetes* in agricultural soils are less well-characterized compared to their characterization in aquatic ecosystems with higher abundances suggested as an indicator of good soil quality (Wolińska et al., 2017). *Flavobacteria* seem to be an important class of *Bacteroidetes* in soils, their abundance has been observed to be influenced by electric conductivity, pH, soil Na, Zn, Mg and Ca (Wolińska et al., 2017). The slight increase in soil base cations and pH in biochar-amended samples appears to support the increase of *Flavobacteria* in biochar-amended soils. Additionally, members of this class participate in organic matter turnover and the degradation of various aromatic compounds (Bernardet and Nakagawa, 2006; Wolińska et al., 2017).

As a number of families belonging to *Actinobacteria* have been characterized as a group that plays an important role in the decomposition of plant cell wall polymers and recalcitrant organic matter (Lewin et al., 2016), we expected the increased soil C% associated with the biochar and napiergrass root exudates would favor the *Actinobacteria*. Unexpectedly, we observed a decrease in the *Actinomycetales* relative abundance in biochar-amended samples, which was contrary to the findings of previous studies (Anderson et al., 2011; Dai et al., 2017; Khodadad et al., 2011; Kolton et al., 2011; Lanza et al., 2016). However, previous reports on biochar functionality related to shifts in microbial community composition were often carried out in short-term studies (e.g. less than one year) (Anderson et al., 2011; Dai et al., 2017; Khodadad et al., 2011; Kolton et al., 2011; Lanza et al., 2016). In contrast, studies have reported decreases in their relative abundance at least two years after initial addition of biochar (Li et al., 2018; Zheng et al., 2016). Thus, the observed changes in *Actinobacterial* abundance are likely related to temporal shifts or driven by changes in organic carbon quality originating from plant litter and/or biochar (Lauber et al., 2013). The decreased abundance of *Actinobacteria* may suggest a lower C degradation rate that may, in part, explain the lower CO_2 production in the biochar-amended microcosms two years after amendment.

3.4.2 Biochar decreases the abundance of assimilatory N pathways but increases denitrification

Although the observed difference in soil N concentration was not statistically significant, pathways involved in N assimilation were significantly higher in the controls. Conversely, biochar-amended samples contained significantly higher abundances within the denitrification pathway. These findings indicate that the addition of biochar to an

Oxisol potentially resulted in better retention of N, as soil N% increased over the two years since the initial addition of the soil amendment. Compared to our previous study, soil N% measured two years after the initial addition of biochar was higher in both controls and biochar-amended soils compared to soil N% after one year of biochar addition. The increase in soil N% may reflect the higher abundance of N-fixation genes and assimilatory N pathways in our control soils. Furthermore, the relative abundance of N-cycling generalist and denitrifying *Proteobacteria*, such as the *Rhizobiales, Pseudomonadales* and *Burkholderiales*, were higher in the biochar-amended samples, consistent with our previous findings (J. Yu et al., 2018). In addition, the archaeal phyla *Thaumarchaeota* were lower in biochar-amended samples. These belong to a population of ammonia-oxidizers that are likely major drivers of nitrification and are influenced by soil organic carbon and pH (Lu et al., 2017; Pester et al., 2011). Although, ammonia-oxidizing archaea are not capable of nitrification-denitrification and thus do not contribute to N_2O, their contribution to global N_2O may occur indirectly through the oxidation of nitrogenous compounds that are converted into substrate for denitrifying organisms (Stieglmeier et al., 2014). The decrease in abundance of ammonia oxidation and nitrification pathways, and increase in denitrifying *Proteobacteria* and denitrification related genes in biochar-amended samples may increase the potential to mitigate N_2O emissions and reduce N losses from soil (Heylen et al., 2006; Hink et al., 2018; Philippot, 2002; Stieglmeier et al., 2014; Zhu et al., 2013).

These observations suggest that the addition of biochar to an Oxisol resulted in better retention of inorganic N, as reflected in increased soil N% over the two years since biochar addition, as well as increased N availability and the potential to mitigate N_2O

emissions, in agreement with studies that have shown increased N bioavailability with biochar amendment (Zheng et al., 2013) and studies which showed that biochar amendment decreased N_2O emissions (Harter et al., 2016, 2014; He et al., 2017; Wang et al., 2012). The increased potential for denitrification is also consistent with the observations of the higher abundances of genes encoding soluble cytochromes, specifically cytochrome c, and respiratory dehydrogenases in biochar-amended samples (Chen and Strous, 2013).

3.4.3 Enhanced potential for acquisition for nutrients associated with biochar and other compounds

The significantly enriched pathways in biochar amended soils within the carbohydrate subsystem exhibited conspicuous responses to plant growth activity, such as the utilization of a number of labile carbon sources, mainly plant-derived sugars (Gunina and Kuzyakov, 2015). This may be linked with the slightly increased, though non-significant, napiergrass yield from the biochar-amended plots. Though the increase in yield was non-significant, there may be increases in root exudates that increase labile carbon input into the soil that were not measured in this study (Gunina and Kuzyakov, 2015; Sekiya et al., 2013). Additionally, pathways involved in the metabolism of aromatic compounds were significantly higher in biochar-amended samples, including pathways for the degradation of some naturally occurring aromatics from plants and polycyclic aromatic hydrocarbons (PAH), likely associated with the biochar (Buss et al., 2015). This finding contrasts to previous studies that observed decreased degradation of PAHs in biochar-amended soils due to limited bioavailability such as PAH adsorption onto the biochar surface (Dutta et al., 2017; Quilliam et al., 2013). Interestingly, control

samples were enriched in the pathways involved in degradation of lignin precursors, (i.e. cinnamic acid) (Pometto and Crawford, 1981) and several ring-cleaving enzymes within the 4-hydroxyphenylacetic acid catabolism pathway (Barbour and Bayly, 1981).

In the respiration subsystem, biochar-amended samples were generally enriched in genes for cytochromes, while the pathways or genes enriched in controls were primarily dehydrogenases. The increased abundance of genes encoding cytochromes may be related to the increased abundance of denitrification and metabolism of other nutrients in the biochar-amended samples. Abundant respiration genes in the controls included some associated with methylotrophy, carbon monoxide dehydrogenases, NADH dehydrogenase (quinone) and ATP synthase. With respect to the cycling of P, K, S, and Fe, overall pathways involved in the metabolism of these nutrients were significantly higher in biochar-amended samples, except for organic S assimilation. This may link to the slightly increased concentration of soil base cations in the biochar-amended soil, suggesting that they are bioavailable. The function-level descriptions of these pathways could be broadly categorized as uptake and transport systems and generally included ATP transporter and permeases. Additionally, Fe metabolism in biochar-amended samples showed an increased abundance of genes involved in siderophore synthesis and uptake, which may be a result of increased soil pH since iron is insoluble at higher pH values (Colombo et al., 2014). Although there are few studies that have focused on the effects of biochar on Fe and S metabolism, there is evidence to suggest that the redox state of Fe can enhance P, N, and S availability in biochar-amended soils (Joseph et al., 2015; Li et al., 2012). The increased abundance of these genes could also coincide with the synthesis of the cytochromes, hemes and other electron transport proteins as well as Fe-S cluster

enzymes including some of the dehydrogenases and hydrogenases, as Fe-S clusters proteins are involved in many fundamental processes including respiration and denitrification (Brzóska et al., 2006).

While previous studies have used a single phylogenetic marker to investigate biochar effects on the soil microbial community (Anderson et al., 2011; Hu et al., 2014; Jenkins et al., 2017; Kolton et al., 2011; H.-J. Xu et al., 2014), to date only one has utilized shotgun metagenomics to examine the biochar effects on the microbial community (Noyce et al., 2016). Our results from the biochar-amended soil metagenomes showed some similarities to this previous study of biochar metagenomes (Noyce et al., 2016). The average abundance of genes in our metagenomes at the level 1 subsystem group of carbohydrates, clustering-based subsystems, and amino acids and derivatives accounted for the majority of functional genes across all our metagenomes. Additionally, genes related to iron acquisition and metabolism were more abundant in metagenomes associated with biochar compared to controls. However, our main findings contrast to the results of Noyce et al., (2016). Here, we observed significant differences in functional gene abundances for genes related to N, P, and S cycling. In addition, the biochar-amended soil metagenomes in our study showed increases in abundance for genes related to the metabolism of aromatic intermediates, and genes related to amino acids and derivatives were less abundant compared to the control soil metagenomes, in contrast to the previous study (Noyce et al., 2016). It is important to note that the previous study analyzed the microbial community of aged biochar particles and the adjacent soil, whereas our analyses examined the bulk soil with and without biochar in soil

microcosms. Additionally, they examined forest soils, which typically have higher microbial diversity than agricultural soils (L. F. Roesch et al., 2007).

3.4.4 Conclusions

These data reveal that the soil microbial community response to biochar is not transient over two years and that the shifts observed previously underlie functional adaptations to changes in nutrient availability induced by biochar. Our data showed that biochar increased soil C% and the abundance of genes involved in substrate acquisition and utilization. In agreement with our previous study, biochar enhanced the potential for denitrification, specifically genes for nitric oxide and nitrous oxide reductases, and decreased the abundance of ammonia oxidizers which may have large implications for decreasing the emissions of a potent GHG such as N_2O. Biochar increased the abundance of genes involved in utilization of labile C and aromatic compounds and the fitted respiration rate between the control and biochar-amended microcosms exhibited a significant difference. Additionally, the cumulative CO_2 emissions from the control soil microcosms were significantly elevated in all time points compared to the biochar-amended soil microcosms. This may suggest that the microbial community utilizes the plant- or biochar-associated carbon more efficiently for the production of microbial products and incorporation into microbial biomass (Sinsabaugh et al., 2013). However, the effects of biochar on the microbial carbon use efficiency remains experimentally unresolved and outside of the scope of this study. Disentangling the direct and indirect effects of biochar on the soil microbial community remains a challenge. Additional samples across time should be examined and coupled with flux data and measures of C

use efficiency before robust conclusions can emerge with respect to biochar effects on C and N cycling by the soil microbiome.

CHAPTER 4

DNA-STABLE ISOTOPE PROBING SHOTGUN METAGENOMES REVEALS RESILIENCE OF ACTIVE SOIL MICROBIAL COMMUNITIES TO BIOCHAR AMENDMENT IN AN OXISOL SOIL

4.1 Introduction

Modern agriculture faces multiple challenges: it must produce more food and fiber to feed a growing global population, adopt more efficient and sustainable management strategies for production, and adapt to climate change (FAO, 2017). These challenges require action by restructuring agroecosystems in order to increase food production from existing farm land while concomitantly achieving major reductions in environmental impacts (Campbell et al., 2014; Garnett et al., 2013). In this regard, incorporation of biochar into soils is a promising management strategy to address the reduction of greenhouse gas (GHG) emissions by enhancing carbon (C) sequestration in agricultural soils, while concurrently improving soil fertility (Jha et al., 2010; Lehmann et al., 2011; Paustian et al., 2016). Biochar is a C-rich product of biomass pyrolysis, which contains large portions of aromatic compounds that influence its stability and the spatial organization of C within soil particles (Hernandez-Soriano et al., 2016; Wiedemeier et al., 2015). Concomitant with carbon sequestration, biochar is intended to improve soil properties relevant to crop productivity (Jeffery et al., 2011). The hypothesized mechanisms for potential improvements to soil fertility include increased cation exchange capacity (CEC) and soil pH, as well as enhanced water and nutrient retention (Laghari et al., 2016; Lehmann et al., 2011). Biochar addition has been reported to influence the soil microbial community through direct and indirect changes in soil physical and chemical

properties (Anderson et al., 2011; Jenkins et al., 2017; O'Neill et al., 2009). Soil microbial communities are complex and play key roles in sustaining soil function due to their significant role in regulating global nutrient and carbon cycling via fundamental ecological processes such as mineralization and decomposition. It is crucially important to understand the effects of biochar on soil microbial communities in order to predict the potential for C sequestration and nutrient cycling under large-scale agricultural production.

Despite the widespread interest in the application of biochar as a sustainable management practice, the effects of biochar on the soil microbiome still remain relatively underexplored due to the vast metabolic and phylogenetic diversity of the microorganisms present in soils. Several studies have reported changes in the soil microbial community after biochar amendment, with increasing or decreasing microbial biomass, while others have found no significant effects (Anders et al., 2013; Chen et al., 2016; Elzobair et al., 2016; Li et al., 2018). Similarly, previous studies have indicated that biochar significantly altered microbial community composition, however, biochar effects have been reported with some contradictory findings on the significant changes in the relative abundance of bacterial groups. Several studies have observed increased relative abundance of *Actinobacteria, Bacteroidetes, Planctomycetes, Proteobacteria* and *Gemmatimonadetes* (Anderson et al., 2011; Khodadad et al., 2011; Kolton et al., 2011; Sheng and Zhu, 2018) and decreased relative abundance of *Acidobacteria* and *Chloroflexi* (Jenkins et al., 2017; H.-J. Xu et al., 2014). Others have reported decreased or no change in *Proteobacteria*, *Bacteroidetes,* and *Actinobacteria* (H.-J. Xu et al., 2014; Zheng et al., 2016). Overall, various changes in the microbial community have been

reported after biochar application though these effects are not uniform and depend strongly on soil type, biochar feedstock, application rate and cropping system (Gomez et al., 2014; Khodadad et al., 2011; Lehmann et al., 2011; Steinbeiss et al., 2009; Thies et al., 2015; J. Yu et al., 2018; Zhang et al., 2019).

The ecology of soil microbial communities and changes in these communities due to biochar addition has principally been investigated using molecular techniques. These studies have primarily focused on the composition and diversity of the total community derived from soil genomic DNA, which may or may not be active. Examination of active microbial populations can reveal how communities respond to changing environmental conditions and contribute to nutrient cycling, C stabilization and storage. In order to predict the impact of the microbiome on soil ecosystem function, it is critical to specifically target members of the active soil microbial community. To this end, DNA stable isotope probing (SIP) is a cultivation-independent method that can be used to elucidate links between microbial activity and identity within environmental samples (Chen and Murrell, 2010; Coyotzi et al., 2016; Lee et al., 2011; Verastegui et al., 2014). It relies on the incorporation of stable isotope labels into microbial DNA during growth on ta labeled substrate, thus acting as a filter to enrich the DNA of active populations. DNA-SIP has been coupled with shotgun metagenomic sequencing to identify new functional and adaptive traits of microbial taxa and to directly link microbial populations with ecological processes (Eyice et al., 2015; Ziels et al., 2018). Metagenomic approaches have been applied to examine these highly diverse ecosystems, providing descriptions of the taxonomic and genetic potential of natural microbial communities. Further, assembling and binning of contigs from metagenomes has allowed for the

recovery of genome sequences of abundant and rare populations (metagenomic assembled genomes or MAGs) from various environments. However, there have been no previously reported studies coupling DNA-SIP with shotgun metagenomics to recover population MAGs from biochar-amended soils.

In the present study, we performed DNA-SIP coupled with shotgun metagenomics to investigate the active fresh-organic matter degrading populations of the soil microbiome of a tropical Oxisol that experienced two years of biochar amendment under napiergrass cultivation. The objectives of this study were: (1) to identify and explore the effects of biochar amendment on active degrading soil microbial populations, and (2) to gain insight into the functional aspects of the active community. Targeting the active community allowed for the recovery of higher quality MAGs, which enabled the characterization of gene content to test the conclusions concerning individual capabilities and metabolisms. We hypothesized that the impact of biochar on the soil microbial communities would still be apparent after two years following a single application of biochar. Furthermore, we hypothesized that soil microbial communities would exhibit a significant change, due to biochar addition, in the composition and abundance of the metabolically active populations and their functional responses in terms of both their nutrient cycling potential and their use of biochar-derived recalcitrant (e.g. aromatic) carbon substrates in these Oxisol soils under Napiergrass cultivation. We expected that, based on the previous metagenomic analyses (Yu et al., 2019), that biochar amendment would increase the relative abundances of two bacterial phyla in the active population, *Bacteroidetes* and *Proteobacteria*. We also expected that the active population of biochar-amended soils would exhibit an increased genetic potential for denitrification.

4.2 Methods and Materials

4.2.1 Overview of Sites and Sample Collection

Soil samples were collected from a field experiment on the island of Oahu, HI, USA at the Poamoho agricultural research station managed by the College of Tropical Agriculture and Human Resources, University of Hawaii Manoa (21º32'30"N, 158º01'15"W). The soil at Poahomo is an acidic Oxisol with 44% clay rich in kaolinite and iron oxides with low CEC (NRCS Web Soil Survey). Detailed descriptions of the field experiment, biochar type and biochar application rate were described in a previous study(J. Yu et al., 2018). Samples were collected from plots under napiergrass (*Pennisetum perpereum* var. green bana) cultivation, which is a zero-tillage (i.e. ratoon harvested) system that retains the below-ground environment, approximately 2 years after a single addition of biochar. Soils were collected on November 2015 from four replicate plots from biochar-amended and control soils prior to harvest. Each plot was split in half and three half-plot 0 – 10cm depth cores were taken randomly and mixed to create a composite. Four composite samples were taken per half plot for a total of 8 replicates per plot. Samples transported on dry ice to the laboratory and were frozen at -80ºC without addition of any protective agent until ready for further processing. Soil chemical properties were determined as previously described (J. Yu et al., 2018; Yu et al., 2019), and are summarized in Table C1.

4.2.2 Preparation of Stable Isotope Probing Soil Microcosms

Biochar-amended and control soils, previously frozen field-moist, were thawed and sieved through a 2mm sieve, sample replicates were composited based on the respective plot from which the soils were collected. Microcosms were prepared by adding

10g of soil in 150ml serum bottles and pre-incubated at 4ºC open to the ambient atmosphere in the dark for 7 days to allow the soils to equilibrate. Uniformly labeled (>97 atom % ^{13}C) ^{13}C-perennial ryegrass (*Lolium perenne* – aboveground biomass) (IsoLife, Wageningen, Netherlands) was powdered using a mortar and pestle, 0.5% (w/w) was added to soils before bottles were sealed and capped with butyl rubber septa. Each microcosm with ^{13}C-labeled perennial ryegrass was paired with an identical '^{12}C-control' microcosm amended with the corresponding unlabeled ^{12}C-perennial ryegrass (~1.1% atom ^{13}C). ^{12}C-control microcosms were used to control for background presence of GC-rich DNA in higher density CsCl gradient fractions (Youngblut and Buckley, 2014). All microcosms were maintained at 23ºC for 14 days in the dark. Soil respiration as a proxy for activity was measured in parallel microcosms prepared using 5g of soil and 0.05% (w/w) ^{13}C-perennial ryegrass, soil microcosms were not continuously aerated. For determination of cumulative CO_2 and N_2O, 200µl of headspace from each microcosm was sampled in triplicate using a gas-tight syringe (VICI Precision Sampling, Baton Rouge, LA). Headspace CO_2 and N_2O content was measured on a GC-ECD-FID (SRI 8610C) after microcosms were set up (day 0) and after 1, 3, 5, 7, 10 and 14 days of incubation. A standard curve was generated prior to measurement for each time point, each standard curve contained four points ranging from 250ppm to 5000ppm CO_2 for day 0 and day 1 measurements and later from 2500ppm to 25,000ppm CO_2 for remaining gas measurements. Similarly, a four-point standard curve for was generated to determine N_2O concentration ranging from 0.5ppm to 25ppm for all time points. Cumulative gas concentrations were calculated for each microcosm by summing the aggregate gas production over the 14-day incubation.

4.2.3 DNA Extraction and Density-Gradient Centrifugation

Soil samples were collected for DNA extraction from ^{13}C-ryegrass fed microcosms after 14 days of incubation. Soil DNA was extracted from 5g of soil using the DNeasy PowerMax Soil kit (Qiagen Company, Hilden, Germany) as described previously (J. Yu et al., 2018). An initial extraction, followed by a second successive extraction, was conducted on each sample to improve DNA extract yield. A successive extraction involved adding new aliquots of bead solution, 0.5M Tris buffer (pH 9), 0.2M phosphate buffer (pH 8) were and solution C1 to the soil pellet after initial lysis, centrifugation, and removal of supernatant containing crude DNA extract. Lysis and centrifugation steps were then repeated. The DNA extracts from the initial and successive extraction was pooled and concentrated using a DNA120 SpeedVac (Thermo Savant) and was quantified using the Qubit dsDNA high-sensitivity kit (ThermoFisher Scientific, Waltham, MA, USA) using the Qubit 3.0 (ThermoFisher Scientific, Waltham, MA, USA).

DNA extracts (3μg DNA) were subjected to density-gradient centrifugation and fractionation (Dunford and Neufeld, 2010). Briefly, DNA extracts were mixed with gradient buffer (0.1M Tris-HCl, 0.1M KCl, and 1mM EDTA) and 7.163M CsCl solution and loaded into 4.8ml polypropylene Quick-Seal tubes (Beckman Coulter, Brea, CA). Density gradient centrifugation was performed with a VTi 65.2 rotor at 55,000 rpm at 20ºC for 60 hours in an OptimaMax ultracentrifuge (Beckman Coulter, Brea, CA) with the vacuum on, maximum acceleration, and no brake on deceleration. Gradients were displaced with mineral oil (Johnson Johnson) pumped into the top of the Optiseal tube using a syringe pump (KD Scientific), and approximately 250μl fractions were collected

dropwise from a needle in the bottom of the tube. The temperature corrected refractive index (nD-TC 20ºC) of each gradient fraction was immediately measured using an AR200 digital refractormeter (Reichart, Ithaca, NY), and buoyant density was calculated from the refractive index using the equation $\rho = a\eta - b$, where ρ is the density of the CsCl (g ml^{-1}), η is the measured refractive index, and *a* and *b* are coefficient values of 10.9276 and 13.593, respectively, for CsCl at 20°C(Birnie, 1978). DNA was precipitated from each fraction as described by Dunford and Neufeld (2010). The pellet was suspended in sterile TE buffer and the final concentration of DNA in each fraction was measured using the Qubit dsDNA high-sensitivity kit (ThermoFisher Scientific, Waltham, MA, USA) using the Qubit 3.0 (ThermoFisher Scientific, Waltham, MA, USA).

4.2.4 Quantitative PCR

To further detect differences in buoyant density values between the ^{12}C- and ^{13}C-incubated microcosms, quantitative PCR was conducted on DNA from gradient fractions with buoyant densities ranging from 1.682 to 1.719 g ml^{-1}. The qPCR targeted the 16S rRNA gene fragment using the 341F/797R primer pair(Nadkarni et al., 2002). qPCR was performed using the QuantStudio3(Applied Biosystems). Each 20µl reaction mix contained 1µl DNA template, 500nM of each forward and reverse primers, 7µl PCR-grade water, 10µl PowerUp SYBR green Master Mix (2X, Applied Biosystems). The amplification procedure for all qPCR assays consisted of an initial denaturation at 95ºC for 3min, followed by 40 cycles of denaturation at 95ºC for 45s, annealing at 60ºC for 45s, and extension at 72ºC for 1min, and a final extension at 72ºC for 7min. All samples were analyzed in duplicate, no-template controls were included on each qPCR run.

Plasmid standards for qPCR were prepared by cloning the 16S rRNA PCR amplicon fragment from *E. coli* K-12 into a pCR4-TOPO plasmid using the TA TOPO cloning kit (Invitrogen, Carlsbad, CA). Plasmids containing the target PCR amplicon sequence were quantified by Qubit. Gene copy numbers were calculated from the measured DNA concentration and the molecular weight of the ligated plasmid containing the PCR amplicon insert. Calibration standards included 10^8, 10^7, 10^6, 10^5, 10^4, 10^3, 10^2 gene copies per reaction and included in triplicate in each qPCR run. The average slope of the calibration curve was -3.4051 (97.45% PCR efficiency) and the R^2 value was 0.988.

4.2.5 Metagenomic Sequencing, Assembly and Binning

Pooled volumetric fractions from heavy DNA (Figure S1) from density-gradient centrifugation were used to generate an Illumina sequence library with an average insert size of 400bp that was sequenced on an Illumina NextSeq 500 with paired-end 150bp reads at the DNASU Core Facility at Arizona State University. The metagenomic sequencing produced an average of 49.4M reads for biochar-amended samples and 40.9M reads for control samples. Estimates of average coverage and sequence diversity for each metagenomic data set were carried out with Nonpareil 3 using default settings (Rodriguez-R et al., 2018; Rodriguez-R and Konstantinidis, 2014). The raw sequencing reads were quality filtered and trimmed to remove Illumina adaptors using Trimmomatic version 0.36 (Bolger et al., 2014), paired-end reads were interleaved using the interleave-reads.py script from khmer version 2.1.1 (Crusoe et al., 2015) before assembly. The assembly of metagenomes was carried out using SPAdes version 3.11.1 (Bankevich et al., 2012) with default parameters and the kmer list: 27, 37, 47, 57, 67, 77, 87. The assembled contigs were quality checked by mapping the raw reads to contigs using Bowtie2 version

2.2.5 (Langmead et al., 2009; Langmead and Salzberg, 2012). SAMtools version 1.8 (Li et al., 2009) was used to sort and index the mapping files and extract contig coverage information. Coverage of the assembled contigs was calculated using BEDTools2 version 2.24.0 (Quinlan and Hall, 2010), assembled contigs quality filtered to remove contigs with <90% coverage. The quality of the filtered assemblies was assessed with QUAST version 3.0 (Gurevich et al., 2013).

The mapping data and coverage information were used to bin contigs into population genome bins separately for each ^{13}C-metagenome with MetaBat version 2.12.1 (Kang et al., 2015) using a minimum contig length of 2000bp. CheckM version 1.0.11 (Parks et al., 2015) was used to evaluate the level of bin completeness and contamination based on domain-level single-copy genes. Genome bins (i.e. MAGs) with over 50% completion according to CheckM were imported in to Anvio version 6.1 (Eren et al., 2015) to be manually curated, which typically improved bin quality by reduction of contamination level. The quality of refined MAGs was assessed by running CheckM and MAGs with >50% completeness and <10% contamination were used for downstream analysis.

4.2.6 Metagenomic Annotation and 16S rRNA Gene Analysis

Taxonomic classification for each MAG was carried out using GTDB-Tk(Chaumeil et al., 2019) against the Genome Taxonomy Database (GTDB) (Parks et al., 2019, 2018). MAG abundance was calculated using the "bin_coverage_individualassembly.pl" script (http://github.com/seanmcallister/bin_coverage_tools.git). For the assessment of taxonomic composition of each metagenome, 16S rRNA gene fragments were first

recovered from metagenomes using Barrnap version 0.9 (https:github.com/tseemann/barrnap). To assess community structure, Barrnap output sequences were parsed to remove 23S and 5S gene fragments then input in the RDP classifier (Wang et al., 2007) with confidence cutoff of 80%. The resulting output was used to generate a Bray-Curtis distance matrix in Rstudio v. 3.3.2 using the phyloseq package (McMurdie and Holmes, 2013). Protein-coding genes within the MAGs were identified using Prodigal version 2.6.3 (Hyatt et al., 2010) and functional annotation was carried out using GHOSTKOALA (Kanehisa et al., 2016). We specifically focused on the effect of each treatment on the presence or absence of genes for the catabolic processes of various C-complexes with different decomposability, ranging from the highly recalcitrant aromatic compounds to the more labile monosaccharides, sugar acids and sugar alcohols, more attention was also given to the genes for N metabolism. Statistics were performed using Rstudio v. 3.3.2 with general dependency on the following packages: ggplot2 (Wickham, 2009), dplyr (Wickham et al., 2019), cowplot (Wilke, 2017) and reshape2 (Wickham, 2007). The vegan R-package (Oksanen et al., 2018) provided tools to calculate non-metric multi-dimensional scaling on Bray-Curtis distance matrix (vegdist) and significant differences in the functional and taxonomic communities between treatments were tested with permutational analysis of variance (PERMANOVA) (Anderson and Walsh, 2013) and analysis of similarity (ANOSIM) (Clarke et al., 2008). To identify genes that were differentially present between active community of control and biochar-amended samples, DESeq2 package was employed (Anders and Huber, 2010). A count table of functional annotations was generated using the Kyoto Encyclopedia of Genes and Genomes (KEGG) orthology (KO) terms. Each column

represented a metagenome and each element was the count of reads from the metagenome assigned to the KO term. DESeq2 was used with default settings to estimate the effective size library and variance to normalize the counts prior to the detection of difference between biochar-amended and control metagenomes for each KO term.

Accession numbers. Raw sequences and assembled MAGs were deposited in GenBank under PRJNA622594.

4.3 Results

4.3.1 Enrichment of ^{13}C-DNA and statistics of metagenomes

Our study focused on soils collected 2 years after the initial addition of biochar to an Oxisol soil under napiergrass cultivation (J. Yu et al., 2018). Eight samples from the biochar-amended and control plots, collected prior to harvest, were used to determine soil chemical characteristics. Between plots, few exhibited significant differences in elemental concentration and nutrient status (Table S1). Mean C concentration (C%) of biochar-amended soils was previously shown to be significantly higher than compared to soils from control plots (Yu et al., 2019). Between plots, soil moisture was also significantly different for one biochar-amended plot (Table S1). However, in our previous study we did not find significant difference in moisture between biochar-amended and control plots, which may have resulted from comparison of technical replicates compared to biological replicates (Yu et al., 2019). Similar to our previous findings, no statistical differences between soil plots were observed in soil base cations (calcium [Ca^{2+}], sodium [Na^{-}], magnesium [Mg^{2+}], and potassium [K^{+}]), pH or total nitrogen concentration. Comparison of the active community between biochar-amended and control soil microcosms was based on the respiration, or cumulative gas production.

The rate of CO_2 production was significantly higher in microcosms amended with ryegrass however no significant differences were observed between biochar-amended and control soil microcosms (Figure C1). After 14 days of incubation, CO_2 concentration comprised approximately 15% of the headspace. In our previous comparative metagenomic study, we found significantly higher copies of genes involved in denitrification (Yu et al., 2019), therefore in the current experiment we measured N_2O gas to further explore this. However, no significant difference was found between N_2O production rates in the biochar-amended and control microcosms.

Total DNA concentrations were measured in 23 density gradient fractions to detect buoyant density shifts after the consumption of ^{12}C- or ^{13}C-labeled perennial ryegrass after 14 days. The heavy density fractions with buoyant density from 1.70 to 1.717g ml^{-1} contained between 58-times to 2.9-times and between 166.8-times to 16.4-times more DNA in the control and biochar-amended microcosms, respectively (Figure 4.1A, 4.1B). To further confirm the enrichment of ^{13}C-labeled DNA, the 16S rRNA gene was quantified in density fractions between 1.683 and 1.718 g ml^{-1}. The heavy density-gradient factions with buoyant density ranging from 1.701 to 1.711g ml^{-1} contained over 100-times more 16S rRNA gene copies in ^{13}C-incubated samples than in the ^{12}C-controls for both biochar-amended and control microcosms (Figure 4.1C, 4.1D). Heavy gradient fractions from biochar-amended and control microcosms containing at least 100-times higher levels of ^{13}C incorporation were thereafter pooled for each microcosm for subsequent shotgun metagenomic sequencing.

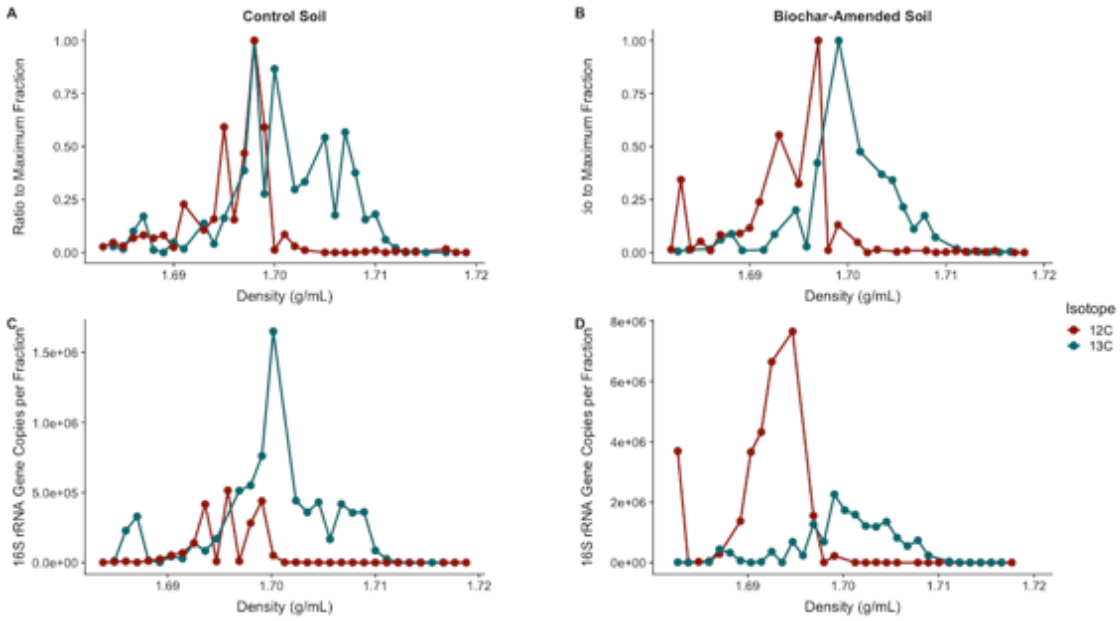


Figure 4.1. Isopycnic separation of DNA from density-gradient fractionation. Normalized DNA concentration in each fraction recovered after isopycnic separation of DNA from the ^{13}C-incubated microcosms and ^{12}C-controls for control soil microcosms (A) and biochar-amended (B). DNA was measured with Qubit for each density gradient fraction, and divided by the maximum fraction value. Each point represents an average of four replicates. Gradient fractions from ^{13}C-incubated microcosms were subsequently pooled for metagenomic sequencing. Total copies of 16S rRNA genes measured by qPCR for each density-gradient fraction recovered from isopycnic separation of DNA from ^{13}C-incubated microcosms and ^{12}C-controls for control soil microcosms (C) and biochar-amended microcosms (D). Density gradient fractions >1.70g/ml pooled for subsequent metagenomic sequencing. Each point represents an average of four biological replicates.

^{13}C-labeled DNA was sequenced from four replicate samples representing the biochar-amended soils (Plots 1, 3, 4, 8) and four samples representing the control soils (Plots 2, 5, 6, 7), yielding approximately 24 to 53 megabytes of short paired-end sequence data per sample. The estimated coverage based on the read redundancy value calculated by the Nonpareil algorithm revealed an average coverage of approximately 0.65 and 0.54 for metagenomes obtained from biochar-amended and control Oxisol samples, respectively (Figure C2). On average, the coverage of the DNA-SIP

metagenomes (0.60, this study) was much higher compared to our previous study using whole community metagenomes (0.32, Yu et al., 2019) of the same soils. The sequence diversity values, a measure of alpha-diversity derived from Nonpareil curves, exhibited no differences between the biochar-amended (average, 21.23) and control soils (average, 21.04). Metagenomes from ^{13}C-labeled biochar-amended and control soil were assembled and quality checked to produce contigs for binning. The quality assembled contigs in biochar-amended and control metagenomes amounted to 361,137bp and 258,035bp within contigs longer than 1.5kb, respectively. The N_{50} values averaged 580bp and 592bp from biochar-amended and control metagenomes. Sequence statistics for each treatment plot were summarized in Table 5.1.

Table 5.1. Metagenomic sequence and assembly summary.

				Nonpareil		SPADES Assembly		
Samples	Treatment	No. Reads	Trimmed Reads	Coverage (%)	Diversity	No. Contigs	N50	Longest Contig
Plot 1	Biochar-amended	48,939,158	43,886,293	62.02	21.59	1,685,259	731	214,999
Plot 3	Biochar-amended	53,550,803	49,275,476	70.64	20.78	2,573,173	604	116,946
Plot 4	Biochar-amended	45,680,993	41,882,029	63.85	21.15	2,601,521	505	127,320
Plot 8	Biochar-amended	49,575,137	45,710,094	64.48	21.40	2,841,923	480	290,581
Plot 2	Control	49,463,602	45,320,132	70.67	20.88	2,302,470	503	651,253
Plot 5	Control	48,647,720	44,555,996	69.83	20.64	2,381,807	491	137,757
Plot 6	Control	24,655,227	22,260,113	9.22	21.20	1,528,627	453	179,238
Plot 7	Control	41,014,445	37,866,468	65.91	21.44	1,002,610	922	102,465

5.3.2 Active Community Taxonomic Composition and Functional Diversity.

The taxonomic affiliations of recovered 16S rRNA gene fragments (metagenome derived) showed little to no differences between the biochar-amended and control metagenomes (Figure 4.2). The active bacterial community in biochar-amended and

control metagenomes were mostly represented by the phyla *Actinobacteria* at 44.9% and 53.5%, followed by *Proteobacteria* at 41.2% and 30.8%, respectively (Figure 2A). In both biochar-amended and control metagenomes, the next most abundant phyla were the *Bacteroidetes* and *Gemmatimonadetes* which represented about 4.4% and 3.6% of their respective communities, followed by Acidobacteria and Firmicutes which represented about 2.3% and 1.3% of their communities (Figure 2A). The remaining bacterial phyla represented less than 1% of the community. Biochar had no significant effect the relative abundance of most bacterial phyla, though *Proteobacteria* were significantly enriched in the biochar-amended metagenomes (two-tailed t-test, $P < 0.05$)(Figure2B).

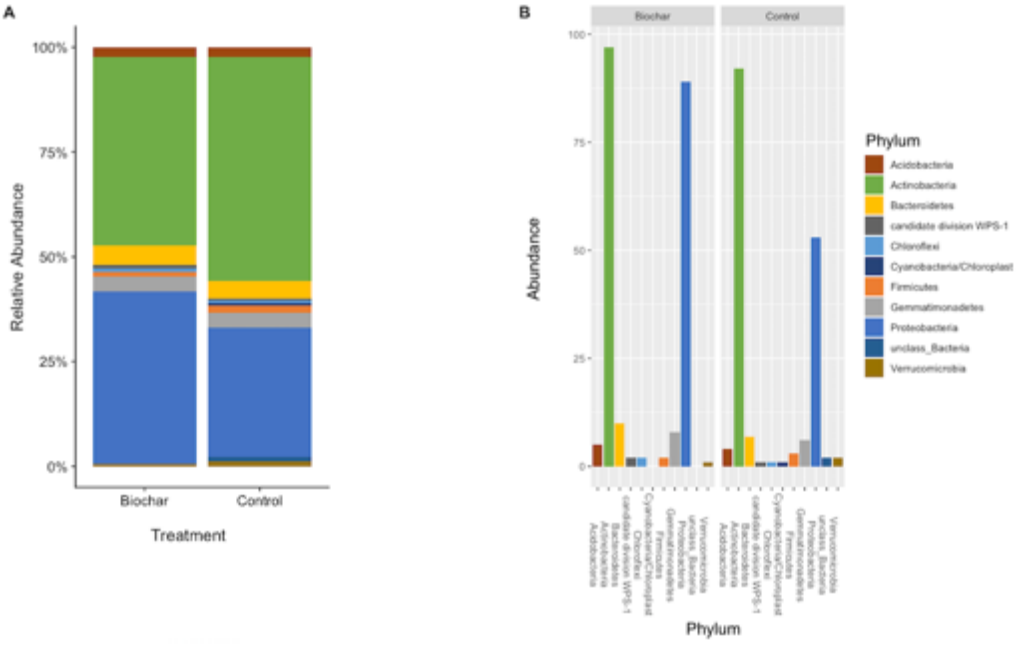


Figure 4.2. Taxonomic affiliation of recovered 16S rRNA gene fragments. (A) relative proportion and (B) abundance of bacterial phyla for biochar-amended and control treatments. Underlying data is based on 16S rRNA gene-encoding fragments recovered from metagenomic datasets.

Biochar also did not cause a significant shift in taxonomic β-diversity, based on Bray-Curtis distances of phylum-level active community composition (ANOSIM, P =

0.66)(Figure 4.3A). In addition, biochar amendment generally did not significantly shift the functional gene content of the active community, summarized as KO terms (ANOSIM, P = 0.16)(Figure 4.3B). However, of the 6097 KO terms with abundances adequate for P value assignment in DESeq2, three KO terms differed significantly (adjusted P <0.05) and another eight differed nearly significantly (adjusted P < 0.1) between control and biochar-amended metagenomes. DESeq2 analysis revealed a statistically significant decrease in nitrate reductase abundance (KO00370 *narG*; *narZ*; *nxrA*) in biochar-amended metagenomes and a significant enrichment of genes involved in bacterial motility-pilus systems and type VI secretion systems (Table C2).

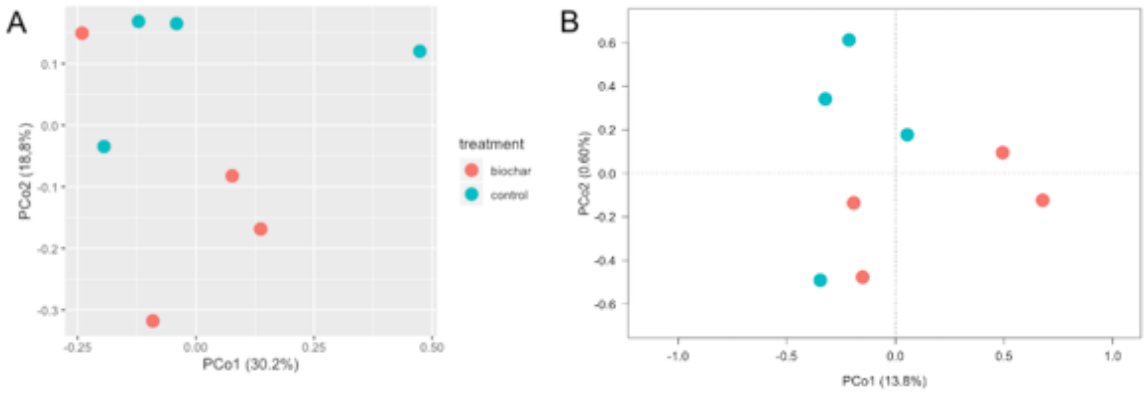


Figure 4.3. Taxonomic and functional shifts as an effect of biochar amendment. (A) PCoA plot of taxonomic community composition. (B) Principle coordinate analysis (PCoA) Plot of KO term annotations. Underlying data are based on Bray-Curtis distance matrix derived from a KO term count matrix. Underlying data are a Bray-Curtis distance matrix of 16S rRNA gene-encoding fragments recovered with Barrnap and processed in the RDP classifier.

5.3.3 Recovery of MAGs and diversity of MAGs involved in C and N cycling.

To precisely identify and quantify individual populations in the active community, we performed genome binning analysis of the individually assembled metagenomic data sets. Between 20 and 48 bins were recovered through binning for each individual metagenome. Due to low completeness of some MAGs, a threshold of 50% completeness and less than 10% contamination, based on the presence of 71 single-copy bacterial genes, was established for further analysis. These medium- to high-quality MAGs collectively recruited about 4.11% and 4.81% of the short reads, on average, for the both^{13}C-biochar-amended and ^{13}C-control, respectively. After refining genomic bins, 84 population MAGs (49 and 35 MAGs from ^{13}C-biochar-amended and ^{13}C-control) remained, these represented ~25% of the total MAGs obtained. Assigned taxonomies at the family-level and genomic characteristics of genome bins used in this study are summarized in Table 2 (Table C3). Genome size ranged from 1.84Mbp to 11.9Mbp, and G+C% content varied from 58.3% to 73.1% (Table C3). Inferred taxonomy revealed that most MAGs recovered from the active community represented members of *Acidobacteria*, *Actinobacteria*, *Gemmatimonadetes*, and *Proteobacteria (Alphaproteobacteria, Betaproteobacteria* and *Gammaproteobacteria)* in both soil metagenomes, whereas *Myxococcota* (D*eltaproteobacteria*) were characteristic of biochar-amended soils (Figure C3).

Estimates of MAG abundance within a metagenome was calculated by normalizing average bin coverage by the contig lengths. The majority of recovered MAGs in both the ^{13}C-biochar-amended and ^{13}C-control metagenomes belonged to

phylum *Actinobacteria* (Figure 4.4), represented by *Actinomycetales* (avg. coverage of metagenome: 5% biochar-amended, 11.6% control), *Mycobacteriales* (avg. coverage of metagenome: 13.3% biochar-amended, 13.7% control), *Propionibacteriales* (avg. coverage of metagenome: 1.7% biochar-amended, 1.4% control), *Streptosporangiales* (avg. coverage of metagenome: 7% biochar-amended, 10.1% control), 20CM-4-69-9 (avg. coverage of metagenome: 0.8% biochar-amended, 0.8% control), and *Streptomycetales* (avg. coverage of metagenome: 43.6% biochar-amended, 48.1% control)(Figure 4.4). Approximately 20% (10/49) of MAGs recovered from ^{13}C-biochar-amended and ^{13}C-control soils were taxonomically assigned at the order-level to *Streptomycetales*. The next most abundant MAGs recovered were assigned to phylum *Gemmatimonadetes* which represented an average coverage of 11.9% (7 MAGs) and 10% (5 MAGs) of ^{13}C-biochar-amended and ^{13}C-control metagenomes, respectively (Figure 4.4A). MAGs assigned to phylum *Proteobacteria*, represented by order *Burkholderiales* (avg. coverage of metagenome: 0.8% biochar-amended, 1.3% control) and *Sphingomonadales* (avg. coverage of metagenome: 1.8% biochar-amended, 2.2% control), were recovered from both ^{13}C-biochar-amended and ^{13}C-control metagenomes. Proteobacterial orders *Rhizobiales* and *Xanthomonadales* MAGs were only recovered from the biochar-amended metagenomes and comprised on average 2.9% and 0.8% coverage of the ^{13}C-biochar-amended metagenomes, respectively. Additionally, the *Myxococcota* were only recovered from one ^{13}C-biochar-amended metagenomes, further classified as *Haliangiales* and *Polyangiales* with 1.9% and 2.4% of coverage of the Plot 8 metagenome, respectively (Figure 4.4B). *Acidobacteria* MAGs recovered from ^{13}C-biochar-amended and ^{13}C-control metagenomes were assigned to order

Vicinamibacterales and *Acidobacteriales*, respectively, and represented 0.9% of the coverage their respective metagenome (Figure 4.4).

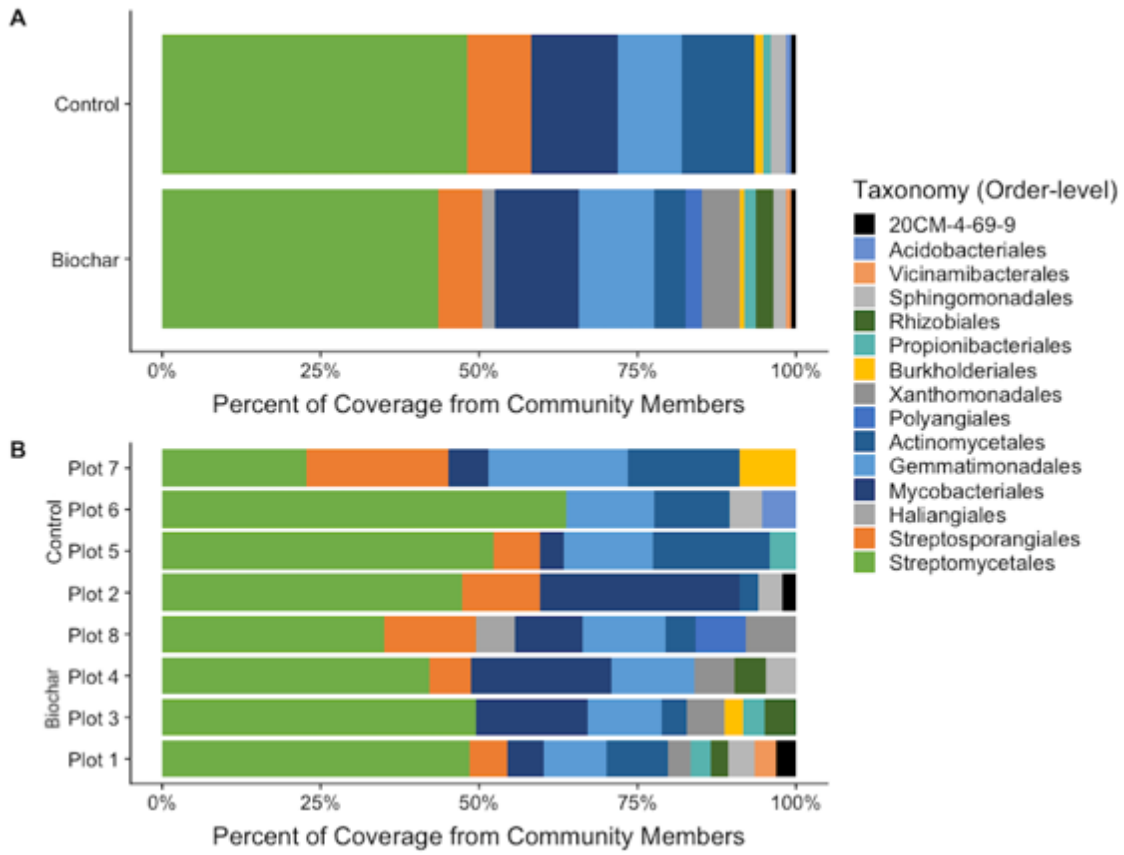


Figure 4.4. Proportion of abundance of recovered populations from metagenomes. (A) proportion of MAG abundance from biochar-amended and control metagenomes. (B) Proportion of MAG coverage from each plot. Abundance was calculated as bin coverage normalized by contig lengths. Taxonomic classification is based on GTDB-Tk database.

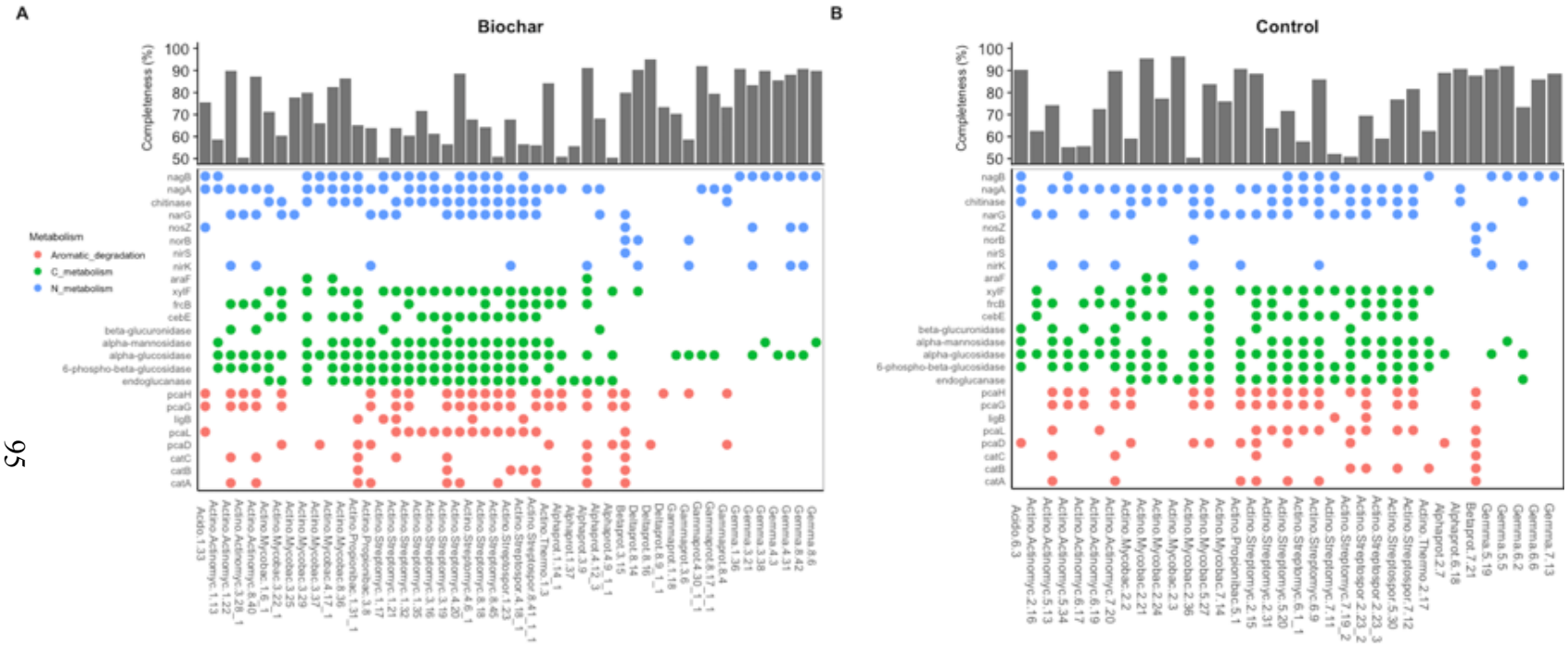


Figure 4.5. Metabolic features of medium- and high-quality MAGs recovered from biochar-amended and control metagenomes. (A) Presence/absence of gene in MAGs recovered from biochar-amended metagenomes and completeness of biochar MAGs and taxonomic classification at phylum-level. (B) Presence/absence of gene in MAGs recovered from control metagenomes and completeness of control MAGs and taxonomic classification at phylum-level.

The examination of key N cycling genes showed that 46 MAGs, representing different bacterial phyla, possessed at least one gene involved in denitrification. Genes involved in nitrification and nitrogen fixation were not observed in the recovered MAGs. Among MAGs that possessed denitrification genes, 25 and 21 MAGs were recovered from ^{13}C-biochar-amended and ^{13}C-control metagenomes, respectively. MAGs obtained from both soils contained a gene involved in single steps of the denitrification pathway. Those that contained genes involved in denitrification generally belonged to the phyla *Actinobacteria* and *Proteobacteria*. Of the 34 *Actinobacteria* MAGs that possessed denitrification genes, four MAGs recovered from biochar-amended soils and six MAGs recovered from control soils contained at least one copy of *nirK* and *narG* genes (Figure 4.5A, 4.5B). Nearly all MAGs assigned to *Streptomycetales* and *Streptosporangiales* had at least one copy of *narG*. Two *Alphaproteobacteria* MAGs recovered biochar-amended soil contained one copy of either *nirK* or *narG* genes, however, *Alphaproteobacteria* MAGs recovered from the control soil did not possess denitrification genes. Both *Burkholderiales* MAGs possessed all necessary genes to perform complete denitrification (i.e., reduction of NO_3^- or NO_2^- to N_2) (Figure 4.5). At least one copy of *nirK* and *norB* genes were found in a *Gammaproteobacteria* (Bin3.6) and *Deltaproteobacteria* (Bin8.14) MAG recovered from biochar-amended soil. Nearly half of *Gemmatimonadetes* MAGs contained a copy of *nirK,* of these four MAGs, all recovered from biochar-amended metagenomes, also contained a copy of *nosZ*. In addition, the *Acidobacteria* MAG recovered from the biochar-amended soil (Bin 1.33) possessed the *nosZ* gene, while nosZ was not observed in the Acidobacteria MAG recovered from the control metagenomes.

Other N-cycling genes observed in recovered MAGs included a gene for a cytochrome c nitrite reductase (*nrfA*) associated with dissimilatory nitrate reduction to ammonium (DNRA), which was found in two MAGs recovered from biochar-amended metagenomes (Bin1.21 and Bin8.9_1_1). All recovered *Gemmatimonadetes* MAGs also possessed *nagB* (ammonia from amino sugars) (Figure 4.5A, 4.5B).

In addition to N-cycling, we sought to identify genes in the recovered MAGs that encode for enzymes directly involved in the decomposition of plant organic carbon via hydrolysis of glycosidic bonds that target cellulose (e.g. endoglucanases), hemi-cellulose (e.g., xylanases), cellobiose (e.g. beta-glucosidase), and ring-opening enzymes involved in degradation of aromatic compounds prevalent in soils. Most *Gemmatimonadetes* MAGs contained genes involved in degradation of labile carbohydrates such as endoglucanase, alpha-glucosidase and alpha-mannosidase but did not have genes for aromatic degradation (Figure 4.5A, 4.5B). On the other hand, both Betaproteobacteria (i.e. *Burkholderiales*) MAGs possessed key genes in the beta-ketoadipate pathway including genes for catechol ortho-cleavage to 3-oxoadipate (i.e., *catABC* and *pcaDL*) and the ring-opening step of protocatechuate degradation (i.e., *pcaGH*). However, genes for the degradation of more labile compounds were not observed in these MAGs. *Alphaproteobacteria* and *Gammaproteobacteria* MAGs possessed genes involved in a single step of the beta-ketoadipate pathway and genes associated with degradation of labile carbohydrates and sugar transport systems. Overall, Actinobacteria MAGs possessed multiple copies of gene associated with the degradation of plant biomass C, such as cellulose, hemi-cellulose and cellobiose (i.e., endoglucanases, beta-glucosidases,

alpha-glucosidases, alpha-mannosidase), binding proteins involved in sugar transport, ring-opening enzymes or a partial beta-ketoadipate pathway (Figure 4.5A, 4.5B).

5.4 Discussion and Conclusions

5.4.1 Biochar had negligible effects on the active soil community.

In this study, we examined the active community of a tropical Oxisol two years after the initial addition of biochar under napiergrass cultivation. We investigated the impact of biochar amendment on the genomic diversity and functional potential of active soil bacterial community using DNA-SIP shotgun metagenomics and MAGs (see below). Here, we did not observe a significant shift in the composition of the active ryegrass-degrading community in response to biochar. This finding contrasts with our previous study, based on 16S rRNA amplicon analysis, which found significant changes in the community composition and alpha diversity in response to a month and a year after biochar addition (J. Yu et al., 2018). Although this is consistent with our previous comparative metagenomic study, which showed that biochar did not have a significant shift the community two years after biochar addition (Yu et al., 2019). Altogether, this may indicate that the community is resilient as we were unable to detect compositional changes in the whole and active community as time from disturbance increased. Certainly, the strength of the disturbance and the frequency it is applied can have an effect on the resilience of the microbial composition (Allison and Martiny, 2009). Here and our previous studies, biochar was only added at the beginning of the experiment. In addition, the microbial community was initially sensitive to perturbations related to the addition of biochar but the strongest determinant of the community composition was soil

type, as well as the degree of biochar-related changes in composition determined by soil type (J. Yu et al., 2018). Although examination of 16S rRNA gene fragments extracted from each individual metagenome did show a significant increase in *Proteobacteria* abundance in the biochar metagenomes, it is important to note that the number of recovered 16S rRNA genes per metagenome was extremely low compared to the number of gene-encoding sequences. This may reflect difficulties presented by the massive data volume of metagenomes, high sequence similarity of 16S rRNA genes and skewed species abundance which make rRNA recovery from metagenomic datasets difficult (Yuan et al., 2015). In addition, the similarity of the active communities between biochar-amended and control soils may reflect the conditions of the experimental set up. For instance, sieved soils resulting in different size fractions have been shown to support distinct microbial communities (Bach et al., 2018; Fox et al., 2018) and the input of fresh organic matter has been shown to stimulate a select group of bacteria (Pascault et al., 2013). Previous studies using ^{13}C-DNA-SIP showed that the C assimilating bacterial phyla found in heavy-fraction soil DNA enriched with maize and wheat residue were primarily distributed among phyla *Actinobacteria, Proteobacteria and Firmicutes*, and the quality of plant material has a strong influence on the composition of the degrading communities (Bernard et al., 2007; Fan et al., 2014; Pascault et al., 2013; Su et al., 2017). Here, the major bacterial phyla recovered from the active community were primarily distributed among known plant biomass degrading *Actinobacteria* suborders, such as *Actinomyectales, Streptomycetales, Propionibacteriales, Mycobacteriales*, with genomes

known to be particularly enriched in carbohydrate-active enzyme genes (Lewin et al., 2016).

Previous studies have examined how short- and longer-term biochar application affects soil communities (Anders et al., 2013; Jenkins et al., 2017; Noyce et al., 2015; Zhang et al., 2019). They principally revealed that biochar amendment is accompanied by significant shifts in soil chemistry and the soil microbial community. Other studies have observed negligible biochar effects on soil community structure, GHG production, and plant productivity or that biochar effects were transient and showed no long-term effects (1-3 years) on microbial growth rates in agricultural soils (Azeem et al., 2020; Meschewski et al., 2019; Rousk et al., 2013). Our results concur with the latter in that biochar amendment did not significantly shift the active taxonomic or functional communities, at least over a period of two years. These findings contradict the results of our previous study on the same soils (Yu et al., 2019), which observed significantly higher relative abundances of *Proteobacteria* and *Bacteroidetes* and an enrichment of genes involved in pathways, such as denitrification, respiration and metabolism of aromatic compounds with biochar amendment. We also failed to find support of our initial hypothesis, based on our earlier findings, that biochar would have a significant positive effect on genes involved in denitrification in the active microbial community. The results of our current study showed that the *narG* gene, encoding nitrate reductase, was significantly higher in the control soil metagenomes, while no significant differences were observed for other denitrification genes, such as *nirK*/*nirS*, *norB*, and *nosZ*. This was not expected since previous studies focused on biochar effects on denitrification

found that biochar increased the abundance of nitrite reductase genes (*nirK*/*nirS*) (Ducey et al., 2013; Liu et al., 2018), and nitrous oxide reductase genes (*nosZ*) (Harter et al., 2016; H. J. Xu et al., 2014) in soil. Overall, our results showed that biochar addition did not affect the active denitrifying community, which may suggest that long-term effects of biochar application do not affect the potential for microbially-mediated N loss from these agricultural soils.

We also observed a significant increase in genes for an outer membrane usher protein (*fimD*) and type VI secretion system protein (*impL*) associated with biochar, which may indicate bacterial movement and communication (Gallique et al., 2017; Yang and Dirk van Elsas, 2018). However, whether this is impacted by biochar or reflect indirect effects of the microcosm experiment remain unresolved and outside the scope of this study. Based on these results we conclude that even if the agricultural application of biochar impacts the soil microbial community in the short-term the effects are not lasting in the active community. These findings may suggest that the active soil microbial community is functionally resilient to biochar application, and biochar effects may be overwritten by the other factors, such as land management or cropping system (Azeem et al., 2020; Hardy et al., 2019).

5.4.2 Recovery of populations of the active community.

By coupling SIP with shotgun metagenomics we targeted the active community and improved resolution within the high diversity environment of the soil and demonstrated the ability to assemble several high quality MAGs. By assembling MAGs, we have gained a new depth of insight into the putative nutrient cycling and life strategies

of some Oxisol agricultural soil microorganisms that was not possible with only metagenomics. We recovered 12 *Gemmatimonadetes* MAGs from ^{13}C-DNA with an average coverage of about 11%, which composed a higher proportion of the active community than expected. *Gemmatimonadetes* were better represented in the recovered MAGs than compared to our previous studies based on 16S rRNA amplicon and rRNA gene fragments (metagenome-derived), which composed approximately 1-2% of the Oxisol soil communities (J. Yu et al., 2018; Yu et al., 2019). This contrast with other SIP studies, which have generally recovered *Gemmatimonadetes* sequences from the unlabeled light fraction suggesting this group may be oligotrophic and likely correspond to K-strategist (Bernard et al., 2007; Pascault et al., 2013).

Our finding highlights that low abundant soil bacteria can be metabolically versatile and fast-growing (i.e., sufficient growth within 14 days). For instance, *Gemmatimonadetes* MAGs encoded the genes involved in labile C (e.g., starch) metabolism and organic N cycling (e.g. N-acetyl glucosaminidase). In addition, four of the *Gemmatimonadetes* MAGs encoded enzymes necessary for the reduction of NO_2 and N_2O (i.e., *nirK* and *nosZ*), which is consistent with studies that have reported *Gemmatimonadetes* as *nirK* denitrifiers and have N_2O reduction ability (Helen et al., 2016; Park et al., 2017). Interestingly, this finding contrasts somewhat with earlier studies that have previously shown that the co-occurrence of *nirS* and *nosZ* is the predominant pattern of denitrification genes (Graf et al., 2014). This may suggest that less abundant microorganisms may play an important role in increasing functional redundancy, which can enhance the ability of soil communities to counteract environmental disturbances.

The functional importance of low-abundant microbes may be due to effects that are disproportionately large given their abundance (i.e. keystone species) or as a provision of insurance effect, that rare species offer a pool of genetic resources that may be activated under the appropriate conditions (Jousset et al., 2017). Shade et al. (2014). estimated that conditionally rare taxa, those which are rare in most conditions but become dominant occasionally, made up 1.5% to 28% of all microbes.

In both the biochar-amended and control metagenomes, MAGs that contain a nitrite reductase gene predominantly harbored *nirK*, which encodes the copper-containing nitrite reductase. The cytochrome cd_1 nitrite reductase encoded by the *nirS* gene was only found in the *Burkholderiales* MAGs, which also were the only MAGs that encoded all enzymes required to perform complete denitrification. Variable abundance ratios of *nirK* and *nirS* genes have previously been reported, with a trend of *nirK* abundances to be more sensitive to nutrient changes and higher in bulk soil, and *nirS* abundance to be higher in the rhizosphere (Bárta et al., 2010; Henry et al., 2004; Kandeler et al., 2006). This would be consistent with our soil collection (i.e. bulk soil) although we did not observe significant difference in soil chemicals. These findings are consistent with previous studies that have proposed a modular assembly for denitrification pathways in soils and suggested shared regulatory mechanisms that may constrain the loss of *nor* and *nos* in *nirS*-type denitrifiers (Graf et al., 2014; Orellana et al., 2014). In addition, nine MAGs related to several actinobacterial suborders had *nirK* and *narG* genes, though whether there are co-occurrence patterns between *nirK* and *narG* remain unclear. In fact, majority of *Actinobacteria* MAGs from both metagenomic datasets contained at least one

copy of *narG* gene. Earlier studies of *narG* diversity in soil environments had previously identified sequences related to those from *Actinobacteria* (Palmer and Horn, 2012; Philippot et al., 2002), which may highlight the importance of *Actinobacteria* in the nitrate reducing community of Oxisol soils. Altogether, these findings suggest that a reduction of oxidized N species to N_2 would require the concerted participation of different N-reducing bacteria and highlight the importance of accounting for the different organisms and their interactions to better understand denitrification processes in soils ecosystems.

We explored the impact of active microbial populations in the potential breakdown and recycling of plant biomass in soils, by surveying genes associated with biomass and aromatic degradation in the recovered MAGs. Overall, the *Actinobacteria* MAGs encoded the greatest number and variety of enzymes involved in the degradation of plant biomass, which was expected since this taxonomic group has many representatives that have been characterized for their ability to degrade a variety of labile and recalcitrant organic compounds. For example, *Actinomycetes* can compete with fungi for lignin degradation (De Boer et al., 2005), Mycobacteria can degrade polycyclic aromatic hydrocarbons under oligotrophic conditions (Uyttebroek et al., 2006), and aerobic cellulose degradation has been demonstrated by a number of *Actinobacteria* species (Anderson et al., 2012). In the biochar-amended soil metagenomes we recovered more diverse *Proteobacteria* MAGs, which was not surprising due to the higher amount of total C% in the biochar-amended soils. The *Rhizobiales* MAGs contained the genetic potential to degrade a variety plant organic C and complete or partial β-ketoadipate

pathway, similar to many related *Rhizobiales* (MacLean et al., 2006). The β-ketoadipate pathway is present in many members of the *Rhizobiaceae* family, emphasizing the importance of aromatic acid catabolism in this family(Parke and Ornston, 1986). In addition to the denitrification pathway, *Burkholderiales* MAGs also had the complete set of genes in the β-ketoadipate pathway but did not have gene for degradation or transport of labile plant C compounds. This finding was not surprising as the representative of the *Burkholderiales* order (genus *Cupriavidus*) have been reported to degrade recalcitrant C and aromatic compounds including lignin (Shi et al., 2013) and phenoxy herbicides (Cuadrado et al., 2010). From a functional point of view, the active population was composed of a small diversity of species that harbored different degradation capabilities, which may suggest the different trophic behaviors with copiotrophic *Actinobacteria* (Ho et al., 2017) and *Rhizobiales* (Bastida et al., 2015) and oligotrophic *Acidobacteria* (Fierer et al., 2007; Ho et al., 2017) and *Burkholderiales* (Nicolitch et al., 2019) with the genetic potential to degrade labile (e.g., cellulose and hemicellulose) or more refractory compounds like aromatics, respectively.

5.4.3 Conclusion

The combination of metagenome and MAG analysis allowed for an increased understanding of the potential biological functions of the active soil microbial community as altered by biochar addition. Potential carbon cycling pathways in both datasets appeared to not be significantly altered by biochar, especially related to complex carbon sources. In addition, we observed no difference in genes involved in the denitrification pathway. However *narG* was significantly higher in the control metagenomes of the

active communities. In summary, this study demonstrated the application of DNA-SIP combined with shotgun metagenomics and genomic binning to identify active populations in a tropical Oxisol soil under biochar amendment. The results indicated that the taxonomic and functional composition of the active community was not significantly affected by biochar amendment. Finally, we were able to recover high quality MAGs of low-abundance populations using DNA-SIP to target the active community. These results may suggest that application of biochar may influence the microbial communities and their function soon after application, however, the effects on the microbial community are not lasting. Although biochar did not have lasting effects on the active soil community, it may still be a promising strategy for the intended purpose of biochar in agricultural soil. For example, biochar addition can result in long-term sequestration of C without a significant long-term influence on the soil microbial community which may lead to unexpected nutrient losses from the soil through biotic processes, such as denitrification.

CHAPTER 5

CONCLUSION

The demand for food security is increasing as the world population continues to grow. The increasing competition for land and resources poses challenges in addition to climate change towards achieving global food security. To meet these challenges requires action throughout the food systems towards more sustainable practices. Biochar amendment is a promising strategy for sustainable agriculture because of its ability to increase C sequestration in the soil and improve soil fertility. However, biochar effects on the soil are variable due to the variety of feedstocks and pyrolysis temperatures that produce different biochars. In addition, biochar addition can change the soil environment and affect soil microbial communities. The soil microbiome governs biogeochemical cycling that is vital to life on this planet and is associated with soil quality. Understanding and predicting the impacts of biochar on the soil microbial structure and function have not been fully explored due to the complexity of the soil microbiome. This dissertation investigated the effects of biochar amendment on the soil microbiome of tropical agricultural soils to provide a comprehensive understanding of the effects of biochar on (i) short-term effects on the bacterial community composition and assembly, (ii) whether biochar addition continued to affect the microbial community composition and functional difference in the longer-term (2 years), and (iii) whether biochar affected the compositional and functional community of the active community in biochar-amended soils.

In Chapter 3, we determined the effects of biochar amendment on bacterial community composition and assemblage in two contrasting soil types under two cropping systems. Analysis of the 16S rRNA amplicon sequences showed that soil type was the main driver of the soil community composition, followed by the cropping system and sampling time. Our results showed that biochar had a greater effect in the low fertility Oxisol soil compared the fertile Mollisol. Biochar resulted in distinct clustering of the community in the Oxisol soils under napiergrass, which was less pronounced under corn cultivation. These shifts in the community were primarily driven by increased relative abundance of *Proteobacteria* and decreased relative abundance of *Actinobacteria* and *Acidobacteria*. Analysis of microbial assemblage showed consistent results as the analysis of in community composition. Finally, our results revealed that biochar amendment in the Oxisol resulted in a more complex network and increased the number of negative interactions.

Based on the findings in Chapter 3, we further examined the Oxisol soil under napiergrass cultivation, approximately two years after the initial addition of biochar. In Chapter 4, we utilized shotgun metagenomics to investigate changes in the taxonomic composition and functional community in soil microcosms, which contained soils from biochar-amended and control plots. Our analysis showed that the relative abundance of *Proteobacteria* and *Bacteroidetes* was significantly higher in biochar-amended soils, although the overall community was not significantly different between biochar-amended and control soils. Our results also showed that biochar-amended soils were significantly enriched in key metabolic pathways related to C turnover, such as utilization of plant-

derived carbohydrates and aromatic degradation, as well as denitrification. These community shifts were in part associated with the increase in soil C represented by biochar.

In Chapter 5 we studied the active community of the same subset of soils used in Chapter 4 by coupling DNA-SIP with shotgun metagenomics to target the microbial populations actively degrading ^{13}C-labeled perennial ryegrass. In this study, we showed that the active community was composed of high-abundant and low-abundant populations belonging to *Actinobacteria*, *Proteobacteria*, *Gemmatimonadetes*, and *Acidobacteria*. Our results revealed that the biochar did not have a significant effect on the active taxonomic and functional communities. In addition, we found that the narG gene, which encodes a nitrate reductase, was significantly higher in the control soils. These findings contrast the findings in Chapter 4, which found that biochar enriched for genes in the denitrification pathway. In addition, examination of recovered of metagenomic assembled genomes showered that putative denitrifying genomes generally contained one gene or a partial denitrification pathway.

Overall, this dissertation contributes to the growing field of biochar research as a practical sustainable management strategy in large scale agriculture. There is urgent need to move towards sustainable agriculture to meet food security goals without exacerbating soil degradation and climate change through the release of GHG from agricultural soils. Gaining a better understanding of the practical benefits of biochar application and the repercussions of biochar addition on key biogeochemical processes carried out by the soil microbial community can help make better sustainable management strategies. Here, we

showed that soil communities are initially sensitive to changes in the soil environment related to biochar addition. Although the whole and active soil microbial communities appear to be resilient to biochar addition, total soil C was significantly higher in biochar-amended soils compared to that adjacent Oxisol soil. Collectively, these findings support the use of biochar for the purpose of enhancing C sequestration in agricultural soils.

REFERENCES

Aguilar-Chávez, Á., Díaz-Rojas, M., Del, M., Cárdenas-Aquino, R., Dendooven, L., Luna-Guido, M., 2012. Greenhouse gas emissions from a wastewater sludge-amended soil cultivated with wheat (Triticum spp. L.) as affected by different application rates of charcoal. Soil Biology and Biochemistry 52, 90–95. doi:10.1016/j.soilbio.2012.04.022

Alexandratos, N., Bruinsma, J., 2012. World agriculture towards 2030/2050: the 2012 revision, ESA Working paper. Rome. doi:10.1016/S0264-8377(03)00047-4

Allison, S.D., Martiny, J.B.H., 2009. Resistance, resilience, and redundancy in microbial communities. In the Light of Evolution 2, 149–166. doi:10.17226/12501

Anders, E., Watzinger, A., Rempt, F., Kitzler, B., Wimmer, B., Zehetner, F., Stahr, K., Zechmeister-Boltenstern, S., Soja, G., 2013. Biochar affects the structure rather than the total biomass of microbial communities in temperate soils. Agricultural and Food Science 22, 404–423.

Anders, S., Huber, W., 2010. Differential expression analysis for sequence count data. Genome Biology 11. doi:10.1186/gb-2010-11-10-r106

Anderson, C.R., Condron, L.M., Clough, T.J., Fiers, M., Stewart, A., Hill, R.A., Sherlock, R.R., 2011. Biochar induced soil microbial community change: Implications for biogeochemical cycling of carbon, nitrogen and phosphorus. Pedobiologia 54, 309–320. doi:10.1016/j.pedobi.2011.07.005

Anderson, I., Abt, B., Lykidis, A., Klenk, H.P., Kyrpides, N., Ivanova, N., 2012. Genomics of aerobic cellulose utilization systems in actinobacteria. PLoS ONE 7. doi:10.1371/journal.pone.0039331

Anderson, M.J., 2001. A new method for non-parametric multivariate analysis of variance. Austral Ecology 26, 32–46. doi:10.1111/j.1442-9993.2001.01070.pp.x

Anderson, M.J., Walsh, D.C.I., 2013. PERMANOVA , ANOSIM , and the Mantel test in the face of heterogeneous dispersions : What null hypothesis are you testing? Ecological Monographs 83, 557–574. doi:10.1890/12-2010.1

Arizpe, N., Giampietro, M., Ramos-Martin, J., 2011. Food security and fossil energy dependence: An international comparison of the use of fossil energy in agriculture (1991-2003). Critical Reviews in Plant Sciences 30, 45–63. doi:10.1080/07352689.2011.554352

Atkinson, C.J., Fitzgerald, J.D., Hipps, N.A., 2010. Potential mechanisms for achieving

agricultural benefits from biochar application to temperate soils: A review. Plant and Soil. doi:10.1007/s11104-010-0464-5

Azeem, M., Sun, D., Crowley, D., Hayat, R., Hussain, Q., Ali, A., Tahir, M.I., Jeyasundar, P.G.S.A., Rinklebe, J., Zhang, Z., 2020. Crop types have stronger effects on soil microbial communities and functionalities than biochar or fertilizer during two cycles of legume-cereal rotations of dry land. Science of the Total Environment 715, 136958. doi:10.1016/j.scitotenv.2020.136958

Bach, E.M., Williams, R.J., Hargreaves, S.K., Yang, F., Hofmockel, K.S., 2018. Greatest soil microbial diversity found in micro-habitats. Soil Biology and Biochemistry 118, 217–226. doi:10.1016/j.soilbio.2017.12.018

Bankevich, A., Nurk, S., Antipov, D., Gurevich, A.A., Dvorkin, M., Kulikov, A.S., Lesin, V.M., Nikolenko, S.I., Pham, S., Prjibelski, A.D., Pyshkin, A. V., Sirotkin, A. V., Vyahhi, N., Tesler, G., Alekseyev, M.A., Pevzner, P.A., 2012. SPAdes: A new genome assembly algorithm and its applications to single-cell sequencing. Journal of Computational Biology 19, 455–477. doi:10.1089/cmb.2012.0021

Barberán, A., Bates, S.T., Casamayor, E.O., Fierer, N., 2012. Using network analysis to explore co-occurrence patterns in soil microbial communities. The ISME Journal 6, 343–351. doi:10.1038/ismej.2011.119

Barbour, M.G., Bayly, R.C., 1981. Control of meta-Cleavage Degradation of 4-Hydroxyphenylacetate in Pseudomonas putida. Journal of Bacteriology 147, 844–850.

Barrow, C.J., 2012. Biochar: Potential for countering land degradation and for improving agriculture. Applied Geography 34, 21–28. doi:10.1016/j.apgeog.2011.09.008

Bárta, J., Melichová, T., Vaněk, D., Picek, T., Šantrůčková, H., 2010. Effect of pH and dissolved organic matter on the abundance of nirK and nirS denitrifiers in spruce forest soil. Biogeochemistry 101, 123–132. doi:10.1007/s10533-010-9430-9

Bastida, F., Selevsek, N., Torres, I.F., Hernández, T., García, C., 2015. Soil restoration with organic amendments: Linking cellular functionality and ecosystem processes. Scientific Reports 5, 1–12. doi:10.1038/srep15550

Bernard, L., Mougel, C., Maron, P.A., Nowak, V., Lévêque, J., Henault, C., Haichar, F.E.Z., Berge, O., Marol, C., Balesdent, J., Gibiat, F., Lemanceau, P., Ranjard, L., 2007. Dynamics and identification of soil microbial populations actively assimilating carbon from 13C-labelled wheat residue as estimated by DNA- and RNA-SIP techniques. Environmental Microbiology 9, 752–764. doi:10.1111/j.1462-2920.2006.01197.x

Bernardet, J.-F., Nakagawa, Y., 2006. An Introduction to the Family Flavobacteriaceae, The Prokaryotes. doi:10.1007/0-387-30747-8

Bi, Q., Chen, Q., Yang, X., Li, H., Zheng, B., Zhou, W., Liu, X., Dai, P., Li, K., Lin, X., 2017. Effects of combined application of nitrogen fertilizer and biochar on the nitrification and ammonia oxidizers in an intensive vegetable soil. AMB Express 7, 198. doi:10.1186/s13568-017-0498-7

Birnie, G.D., 1978. Centrifugal Separations inMolecular and Cell Biology. Butterworth & Co Publishers Ltd., Boston, MA.

Bolger, A.M., Lohse, M., Usadel, B., 2014. Trimmomatic: A flexible trimmer for Illumina sequence data. Bioinformatics 30, 2114–2120. doi:10.1093/bioinformatics/btu170

Bourke, J., Manley-Harris, M., Fushimi, C., Dowaki, K., Nunoura, T., Antal, M.J., 2007. Do All Carbonized Charcoals Have the Same Chemical Structure? 2. A Model of the Chemical Structure of Carbonized Charcoal. Industrial & Engineering Chemistry Research 46, 5954–5967. doi:10.1021/ie070415u

Briones, A.M., 2012. The secrets of El Dorado viewed through a microbial perspective. Frontiers in Microbiology 3, 1–6. doi:10.3389/fmicb.2012.00239

Bruun, E.W., Hauggaard-Nielsen, H., Ibrahim, N., Egsgaard, H., Ambus, P., Jensen, P.A., Dam-Johansen, K., 2011. Influence of fast pyrolysis temperature on biochar labile fraction and short-term carbon loss in a loamy soil. Biomass and Bioenergy 35, 1182–1189. doi:10.1016/j.biombioe.2010.12.008

Brzóska, K., Męczyńska, S., Kruszewski, M., 2006. Iron-sulfur cluster proteins: Electron transfer and beyond. Acta Biochimica Polonica 53, 685–691. doi:20061382 [pii]

Budai, A., Rasse, D.P., Lagomarsino, A., Lerch, T.Z., Paruch, L., 2016. Biochar persistence, priming and microbial responses to pyrolysis temperature series. Biology and Fertility of Soils 52, 749–761. doi:10.1007/s00374-016-1116-6

Buss, W., Mašek, O., Graham, M., Wüst, D., 2015. Inherent organic compounds in biochar-Their content, composition and potential toxic effects. Journal of Environmental Management 156, 150–157. doi:10.1016/j.jenvman.2015.03.035

Campbell, B.M., Thornton, P., Zougmoré, R., Van Asten, P., Lipper, L., Struik, P.C., Kuyper, T.W., 2014. Sustainable intensification: What is its role in climate smart agriculture? Current Opinion in Environmental Sustainability 8, 39–43. doi:10.1016/j.cosust.2014.07.002

Caporaso, J.G., Kuczynski, J., Stombaugh, J., Bittinger, K., Bushman, F.D., Costello, E.K., Fierer, N., Peña, A.G., Goodrich, J.K., Gordon, J.I., Huttley, G.A., Kelley, S.T., Knights, D., Koenig, J.E., Ley, R.E., Lozupone, C.A., McDonald, D., Muegge, B.D., Pirrung, M., Reeder, J., Sevinsky, J.R., Turnbaugh, P.J., Walters, W.A., Widmann, J., Yatsunenko, T., Zaneveld, J., Knight, R., 2010. QIIME allows analysis of high-throughput community sequencing data. Nature Methods 7, 335–336. doi:10.1038/nmeth.f.303

Carminati, A., Kaestner, A., Ippisch, O., Koliji, A., Lehmann, P., Hassanein, R., Vontobel, P., Lehmann, E., Laloui, L., Vulliet, L., Flühler, H., 2007. Water flow between soil aggregates. Transport in Porous Media 68, 219–236. doi:10.1007/s11242-006-9041-z

Carvalho, M.F., Ferreira, M.I.M., Moreira, I.S., Castro, P.M.L., Janssen, D.B., 2006. Degradation of fluorobenzene by Rhizobiales strain F11 via ortho cleavage of 4-fluorocatechol and catechol. Applied and Environmental Microbiology 72, 7413–7417. doi:10.1128/AEM.01162-06

Cayuela, M.L., Sánchez-Monedero, M.A., Roig, A., Hanley, K., Enders, A., Lehmann, J., 2013. Biochar and denitrification in soils: When, how much and why does biochar reduce N2O emissions? Scientific Reports 3, 1–7. doi:10.1038/srep01732

Cederlund, H., Wessén, E., Enwall, K., Jones, C.M., Juhanson, J., Pell, M., Philippot, L., Hallin, S., 2014. Soil carbon quality and nitrogen fertilization structure bacterial communities with predictable responses of major bacterial phyla. Applied Soil Ecology 84, 62–68. doi:10.1016/j.apsoil.2014.06.003

Chaumeil, P.-A., Mussig, A.J., Hugenholtz, P., Parks, D.H., 2019. GTDB-Tk: a toolkit to classify genomes with the Genome Taxonomy Database. Bioinformatics 1–3. doi:10.1093/bioinformatics/btz848

Chen, J., Strous, M., 2013. Denitrification and aerobic respiration, hybrid electron transport chains and co-evolution. Biochimica et Biophysica Acta - Bioenergetics 1827, 136–144. doi:10.1016/j.bbabio.2012.10.002

Chen, J., Sun, X., Li, L., Liu, X., Zhang, B., Zheng, J., Pan, G., 2016. Change in active microbial community structure, abundance and carbon cycling in an acid rice paddy soil with the addition of biochar. European Journal of Soil Science 67, 857–867. doi:10.1111/ejss.12388

Chen, Y., Murrell, J.C., 2010. When metagenomics meets stable-isotope probing: Progress and perspectives. Trends in Microbiology 18, 157–163. doi:10.1016/j.tim.2010.02.002

Clarke, K.R., 1993. Non-parametric multivariate analyses of changes in community structure. Austral Ecology 18, 117–143. doi:10.1111/j.1442-9993.1993.tb00438.x

Clarke, K.R., Gorley, R.N., 2006. PRIMER v6: User Manual/Tutorial. PRIMER-E, Plymouth UK 192 p. doi:10.1111/j.1442-9993.1993.tb00438.x

Clarke, K.R., Somerfield, P.J., Gorley, R.N., 2008. Testing of null hypotheses in exploratory community analyses: similarity profiles and biota-environment linkage. Journal of Experimental Marine Biology and Ecology 366, 56–69. doi:10.1016/j.jembe.2008.07.009

Clough, T.J., Condron, L.M., 2010. Biochar and the Nitrogen Cycle: Introduction. Journal of Environment Quality 39, 1218. doi:10.2134/jeq2010.0204

Colombo, C., Palumbo, G., He, J.Z., Pinton, R., Cesco, S., 2014. Review on iron availability in soil: Interaction of Fe minerals, plants, and microbes. Journal of Soils and Sediments 14, 538–548. doi:10.1007/s11368-013-0814-z

Coyotzi, S., Pratscher, J., Murrell, J.C., Neufeld, J.D., 2016. Targeted metagenomics of active microbial populations with stable-isotope probing. Current Opinion in Biotechnology 41, 1–8. doi:10.1016/j.copbio.2016.02.017

Crusoe, M.R., Alameldin, H.F., Awad, S., Boucher, E., Caldwell, A., Cartwright, R., Charbonneau, A., Constantinides, B., Edvenson, G., Fay, S., Fenton, J., Fenzl, T., Fish, J., Garcia-Gutierrez, L., Garland, P., Gluck, J., González, I., Guermond, S., Guo, J., Gupta, A., Herr, J.R., Howe, A., Hyer, A., Härpfer, A., Irber, L., Kidd, R., Lin, D., Lippi, J., Mansour, T., McA'Nulty, P., McDonald, E., Mizzi, J., Murray, K.D., Nahum, J.R., Nanlohy, K., Nederbragt, A.J., Ortiz-Zuazaga, H., Ory, J., Pell, J., Pepe-Ranney, C., Russ, Z.N., Schwarz, E., Scott, C., Seaman, J., Sievert, S., Simpson, J., Skennerton, C.T., Spencer, J., Srinivasan, R., Standage, D., Stapleton, J.A., Steinman, S.R., Stein, J., Taylor, B., Trimble, W., Wiencko, H.L., Wright, M., Wyss, B., Zhang, Q., Zyme, E., Brown, C.T., 2015. The khmer software package: enabling efficient nucleotide sequence analysis. F1000Research 4. doi:10.12688/f1000research.6924.1

Cuadrado, V., Gomila, M., Merini, L., Giulietti, A.M., Moore, E.R.B., 2010. Cupriavidus pampae sp. nov., a novel herbicide-degrading bacterium isolated from agricultural soil. International Journal of Systematic and Evolutionary Microbiology 60, 2606–2612. doi:10.1099/ijs.0.018341-0

Culman, S.W., Dupont, S.T., Glover, J.D., Buckley, D.H., Fick, G.W., Ferris, H., Crews, T.E., 2010. Long-term impacts of high-input annual cropping and unfertilized perennial grass production on soil properties and belowground food webs in Kansas,

USA. Agriculture, Ecosystems and Environment 137, 13–24. doi:10.1016/j.agee.2009.11.008

Dai, Z., Barberán, A., Li, Y., Brookes, P.C., Xu, J., 2017. Bacterial Community Composition Associated with Pyrogenic Organic Matter (Biochar) Varies with Pyrolysis Temperature and Colonization Environment. MSphere2 2, e00085-17. doi:10.1128/mSphere.00085-17

De Boer, W., Folman, L.B., Summerbell, R.C., Boddy, L., 2005. Living in a fungal world: Impact of fungi on soil bacterial niche development. FEMS Microbiology Reviews 29, 795–811. doi:10.1016/j.femsre.2004.11.005

Deenik, J.L., Diarra, A., Uehara, G., Campbell, S., Sumiyoshi, Y., Antal, M.J., 2011. Charcoal ash and volatile matter effects on soil properties and plant growth in an acid ultisol. Soil Science. doi:10.1097/SS.0b013e31821fbfea

Dempster, D.N., Gleeson, D.B., Solaiman, Z.M., Jones, D.L., Murphy, D. V., 2012. Decreased soil microbial biomass and nitrogen mineralisation with Eucalyptus biochar addition to a coarse textured soil. Plant and Soil 354, 311–324. doi:10.1007/s11104-011-1067-5

Deng, Y., Jiang, Y.-H., Yang, Y., He, Z., Luo, F., Zhou, J., 2012. Molecular ecological network analyses. BMC Bioinformatics 13, 113. doi:10.1186/1471-2105-13-113

Ding, G.C., Pronk, G.J., Babin, D., Heuer, H., Heister, K., Kögel-Knabner, I., Smalla, K., 2013. Mineral composition and charcoal determine the bacterial community structure in artificial soils. FEMS Microbiology Ecology 86, 15–25. doi:10.1111/1574-6941.12070

Ding, Y., Liu, Y.X., Wu, W.X., Shi, D.Z., Yang, M., Zhong, Z.K., 2010. Evaluation of biochar effects on nitrogen retention and leaching in multi-layered soil columns. Water, Air, and Soil Pollution 213, 47–55. doi:10.1007/s11270-010-0366-4

Docherty, K.M., Borton, H.M., Espinosa, N., Gebhardt, M., Gil-Loaiza, J., Gutknecht, J.L.M., Maes, P.W., Mott, B.M., Parnell, J.J., Purdy, G., Rodrigues, P.A.P., Stanish, L.F., Walser, O.N., Gallery, R.E., 2015. Key Edaphic Properties Largely Explain Temporal and Geographic Variation in Soil Microbial Communities across Four Biomes. PLOS ONE 10, e0135352. doi:10.1371/journal.pone.0135352

Ducey, T.F., Ippolito, J.A., Cantrell, K.B., Novak, J.M., Lentz, R.D., 2013. Addition of activated switchgrass biochar to an aridic subsoil increases microbial nitrogen cycling gene abundances. Applied Soil Ecology 65, 65–72. doi:10.1016/j.apsoil.2013.01.006

Dunford, E.A., Neufeld, J.D., 2010. DNA Stable-Isotope Probing (DNA-SIP) Video Link. J. Vis. Exp 42, e2027. doi:10.3791/2027

Dutta, T., Kwon, E., Bhattacharya, S.S., Jeon, B.H., Deep, A., Uchimiya, M., Kim, K.H., 2017. Polycyclic aromatic hydrocarbons and volatile organic compounds in biochar and biochar-amended soil: a review. GCB Bioenergy 9, 990–1004. doi:10.1111/gcbb.12363

Elzobair, K.A., Stromberger, M.E., Ippolito, J.A., Lentz, R.D., 2016. Contrasting effects of biochar versus manure on soil microbial communities and enzyme activities in an Aridisol. Chemosphere 142, 145–152. doi:10.1016/j.chemosphere.2015.06.044

Eren, A.M., Esen, O.C., Quince, C., Vineis, J.H., Morrison, H.G., Sogin, M.L., Delmont, T.O., 2015. Anvi'o: An advanced analysis and visualization platformfor 'omics data. PeerJ 2015, 1–29. doi:10.7717/peerj.1319

Eyice, Ö., Namura, M., Chen, Y., Mead, A., Samavedam, S., Schäfer, H., 2015. SIP metagenomics identifies uncultivated Methylophilaceae as dimethylsulphide degrading bacteria in soil and lake sediment. ISME Journal 9, 2336–2348. doi:10.1038/ismej.2015.37

Fan, F., Yin, C., Tang, Y., Li, Z., Song, A., Wakelin, S.A., Zou, J., Liang, Y., 2014. Probing potential microbial coupling of carbon and nitrogen cycling during decomposition of maize residue by13C-DNA-SIP. Soil Biology and Biochemistry 70, 12–21. doi:10.1016/j.soilbio.2013.12.002

FAO, 2017. The future of food and agriculture – Trends and challenges.

Faust, K., Raes, J., 2012. Microbial interactions: from networks to models. Nature Reviews Microbiology 10, 538–550. doi:10.1038/nrmicro2832

Feng, Y., Xu, Y., Yu, Y., Xie, Z., Lin, X., 2012. Mechanisms of biochar decreasing methane emission from Chinese paddy soils. Soil Biology and Biochemistry 46, 80–88. doi:10.1016/j.soilbio.2011.11.016

Fierer, N., Bradford, M.A., Jackson, R.B., 2007. Toward an ecological classification of soil bacteria. Ecology 88, 1354–64.

Fierer, N., Jackson, R.B., 2006. The diversity and biogeography of soil bacterial communities. PNAS 103, 626–31. doi:10.1073/pnas.0507535103

Fierer, N., Lennon, J.T., 2011. The generation and maintenance of diversity in microbial communities. American Journal of Botany 98, 439–448. doi:10.3732/ajb.1000498

Fox, A., Ikoyi, I., Torres-Sallan, G., Lanigan, G., Schmalenberger, A., Wakelin, S., Creamer, R., 2018. The influence of aggregate size fraction and horizon position on microbial community composition. Applied Soil Ecology 127, 19–29. doi:10.1016/j.apsoil.2018.02.023

Gallique, M., Bouteiller, M., Merieau, A., 2017. The Type VI Secretion System: A Dynamic System for Bacterial Communication? Frontiers in Microbiology 8, 1454. doi:10.3389/fmicb.2017.01454

Garnett, T., Appleby, M.C., Balmford, a, Bateman, I.J., Benton, T.G., Bloomer, P., Burlingame, B., Dawkins, M., Dolan, L., Fraser, D., Herrero, M., Hoffmann, I., Smith, P., Thornton, P.K., Toulmin, C., Vermeulen, S.J., Godfray, H.C.J., 2013. Sustainable Intensifi cation in Agriculture: Premises and Policies. Science Magazine 341, 33–34. doi:10.1126/science.1234485

Girvan, M.S., Bullimore, J., Pretty, J.N., Osborn, A.M., Ball, A.S., 2003. Soil Type Is the Primary Determinant of the Composition of the Total and Active Bacterial Communities in Arable Soils. Applied and Environmental Microbiology 69, 1800–1809. doi:10.1128/AEM.69.3.1800-1809.2003

Glaser, B., 2007. Prehistorically modified soils of central Amazonia: a model for sustainable agriculture in the twenty-first century. Philosophical Transactions of the Royal Society of London. Series B, Biological Sciences 362, 187–96. doi:10.1098/rstb.2006.1978

Glaser, B., Birk, J.J., 2012. State of the scientific knowledge on properties and genesis of Anthropogenic Dark Earths in Central Amazonia (terra preta de Índio). Geochimica et Cosmochimica Acta 82, 39–51. doi:10.1016/j.gca.2010.11.029

Glaser, B., Guggenberger, G., Zech, W., Ruivo, M.L., 2003. Soil organic matter stability in Amazonian Dark Earths. Amazonian Dark Earths: origin, properties, and management, in: Contribuicao de Analises de Quımica Organica e DNA Para o Entendimento Da Genese Das Terras Pretas Da Amazonia Central. Sao Paulo, Brazil: Sociedade de Arqueologia Brasileira.

Glaser, B., Haumaier, L., Guggenberger, G., Zech, W., 2001. The “Terra Preta” phenomenon: A model for sustainable agriculture in the humid tropics. Naturwissenschaften 88, 37–41. doi:10.1007/s001140000193

Gomez, J.D., Denef, K., Stewart, C.E., Zheng, J., Cotrufo, M.F., 2014. Biochar addition rate influences soil microbial abundance and activity in temperate soils. European Journal of Soil Science 65, 28–39. doi:10.1111/ejss.12097

Gordon, H., Haygarth, P.M., Bardgett, R.D., 2008. Drying and rewetting effects on soil

microbial community composition and nutrient leaching. Soil Biology and Biochemistry 40, 302–311. doi:10.1016/j.soilbio.2007.08.008

Graf, D.R.H., Jones, C.M., Hallin, S., 2014. Intergenomic comparisons highlight modularity of the denitrification pathway and underpin the importance of community structure for N2O emissions. PLoS ONE 9, 1–20. doi:10.1371/journal.pone.0114118

Griscom, B.W., Adams, J., Ellis, P.W., Houghton, R.A., Lomax, G., Miteva, D.A., Schlesinger, W.H., Shoch, D., Siikamäki, J. V., Smith, P., Woodbury, P., Zganjar, C., Blackman, A., Campari, J., Conant, R.T., Delgado, C., Elias, P., Gopalakrishna, T., Hamsik, M.R., Herrero, M., Kiesecker, J., Landis, E., Laestadius, L., Leavitt, S.M., Minnemeyer, S., Polasky, S., Potapov, P., Putz, F.E., Sanderman, J., Silvius, M., Wollenberg, E., Fargione, J., 2017. Natural climate solutions. Proceedings of the National Academy of Sciences 114, 11645–11650. doi:10.1073/pnas.1710465114

Gunina, A., Kuzyakov, Y., 2015. Sugars in soil and sweets for microorganisms: Review of origin, content, composition and fate. Soil Biology and Biochemistry 90, 87–100. doi:10.1016/j.soilbio.2015.07.021

Gurevich, A., Saveliev, V., Vyahhi, N., Tesler, G., 2013. QUAST: Quality assessment tool for genome assemblies. Bioinformatics 29, 1072–1075. doi:10.1093/bioinformatics/btt086

Hallam, S.J., McCutcheon, J.P., 2015. Microbes don't play solitaire: how cooperation trumps isolation in the microbial world. Environmental Microbiology Reports 7, 26–28. doi:10.1111/1758-2229.12248

Hallam, S.J., Mincer, T.J., Schleper, C., Preston, C.M., Roberts, K., Richardson, P.M., DeLong, E.F., 2006. Pathways of Carbon Assimilation and Ammonia Oxidation Suggested by Environmental Genomic Analyses of Marine Crenarchaeota. PLoS Biology 4, e95. doi:10.1371/journal.pbio.0040095

Hardy, B., Sleutel, S., Dufey, J.E., Cornelis, J.-T., 2019. The Long-Term Effect of Biochar on Soil Microbial Abundance, Activity and Community Structure Is Overwritten by Land Management. Frontiers in Environmental Science 7, 1–14. doi:10.3389/fenvs.2019.00110

Hargreaves, S.K., Williams, R.J., Hofmockel, K.S., 2015. Environmental Filtering of Microbial Communities in Agricultural Soil Shifts with Crop Growth. PLOS ONE 10, e0134345. doi:10.1371/journal.pone.0134345

Harter, J., Krause, H.-M., Schuettler, S., Ruser, R., Fromme, M., Scholten, T., Kappler, A., Behrens, S., 2014. Linking N2O emissions from biochar-amended soil to the

structure and function of the N-cycling microbial community. The ISME Journal 8, 660–674. doi:10.1038/ismej.2013.160

Harter, J., Weigold, P., El-Hadidi, M., Huson, D.H., Kappler, A., Behrens, S., 2016. Soil biochar amendment shapes the composition of N2O-reducing microbial communities. Science of the Total Environment 562, 379–390. doi:10.1016/j.scitotenv.2016.03.220

He, Y., Zhou, X., Jiang, L., Li, M., Du, Z., Zhou, G., Shao, J., Wang, X., Xu, Z., Bai, S.H., Wallace, H., Xu, C., 2017. Effects of biochar application on soil greenhouse gas fluxes: a meta-analysis. GCB Bioenergy 9, 743–755. doi:10.1111/gcbb.12376

Helen, D., Kim, H., Tytgat, B., Anne, W., 2016. Highly diverse nirK genes comprise two major clades that harbour ammonium-producing denitrifiers. BMC Genomics 17, 1–13. doi:10.1186/s12864-016-2465-0

Henry, S., Baudoin, E., Ló Pez-Gutiérrez, J.C., Martin-Laurent, F., Brauman, A., Philippot, L., 2004. Quantification of denitrifying bacteria in soils by nirK gene targeted real-time PCR. Journal of Microbiological Methods 59, 327–335. doi:10.1016/j.mimet.2004.07.002

Hernandez-Soriano, M.C., Kerré, B., Kopittke, P.M., Horemans, B., Smolders, E., 2016. Biochar affects carbon composition and stability in soil: A combined spectroscopy-microscopy study. Scientific Reports 6, 1–13. doi:10.1038/srep25127

Heylen, K., Vanparys, B., Wittebolle, L., Verstraete, W., Boon, N., Vos, P. De, 2006. Cultivation of Denitrifying Bacteria : Optimization of Isolation Conditions and Diversity Study Cultivation of Denitrifying Bacteria : Optimization of Isolation Conditions and Diversity Study †. Applied and Environmental Microbiology 72, 2637–2643. doi:10.1128/AEM.72.4.2637

Hink, L., Gubry-Rangin, C., Nicol, G.W., Prosser, J.I., 2018. The consequences of niche and physiological differentiation of archaeal and bacterial ammonia oxidisers for nitrous oxide emissions. ISME Journal 12, 1084–1093. doi:10.1038/s41396-017-0025-5

Ho, A., Di Lonardo, D.P., Bodelier, P.L.E., 2017. Revisiting life strategy concepts in environmental microbial ecology. FEMS Microbiology Ecology 93, 1–14. doi:10.1093/femsec/fix006

Hu, L., Cao, L., Zhang, R., 2014. Bacterial and fungal taxon changes in soil microbial community composition induced by short-term biochar amendment in red oxidized loam soil. World Journal of Microbiology and Biotechnology 30, 1085–1092. doi:10.1007/s11274-013-1528-5

Hyatt, D., Chen, G.L., LoCascio, P.F., Land, M.L., Larimer, F.W., Hauser, L.J., 2010. Prodigal: Prokaryotic gene recognition and translation initiation site identification. BMC Bioinformatics 11. doi:10.1186/1471-2105-11-119

Jeffery, S., Verheijen, F.G.A., Kammann, C., Abalos, D., 2016. Biochar effects on methane emissions from soils: A meta-analysis. Soil Biology and Biochemistry 101, 251–258. doi:10.1016/j.soilbio.2016.07.021

Jeffery, S., Verheijen, F.G.A., van der Velde, M., Bastos, A.C., 2011. A quantitative review of the effects of biochar application to soils on crop productivity using meta-analysis. Agriculture, Ecosystems and Environment 144, 175–187. doi:10.1016/j.agee.2011.08.015

Jenkins, J.R., Viger, M., Arnold, E.C., Harris, Z.M., Ventura, M., Miglietta, F., Girardin, C., Edwards, R.J., Rumpel, C., Fornasier, F., Zavalloni, C., Tonon, G., Alberti, G., Taylor, G., 2017. Biochar alters the soil microbiome and soil function: results of next-generation amplicon sequencing across Europe. GCB Bioenergy 9, 591–612. doi:10.1111/gcbb.12371

Jha, P., Biswas, A.K., Lakaria, B.L., Subba Rao, A., 2010. Biochar in agriculture - prospects and related implications. Current Science 99, 1218–1225. doi:10.2307/24068517

Jien, S.H., Wang, C.S., 2013. Effects of biochar on soil properties and erosion potential in a highly weathered soil. Catena 110, 225–233. doi:10.1016/j.catena.2013.06.021

Jones, C.M., Graf, D.R., Bru, D., Philippot, L., Hallin, S., 2013. The unaccounted yet abundant nitrous oxide-reducing microbial community: a potential nitrous oxide sink. The ISME Journal 7, 417–426. doi:10.1038/ismej.2012.125

Jones, R.T., Robeson, M.S., Lauber, C.L., Hamady, M., Knight, R., Fierer, N., 2009. A comprehensive survey of soil acidobacterial diversity using pyrosequencing and clone library analyses. The ISME Journal 3, 442–453. doi:10.1038/ismej.2008.127

Joseph, S., Anawar, H.M., Storer, P., Blackwell, P., Chia, C., Lin, Y., Munroe, P., Donne, S., Horvat, J., Wang, J., Solaiman, Z.M., 2015. Effects of Enriched Biochars Containing Magnetic Iron Nanoparticles on Mycorrhizal Colonisation, Plant Growth, Nutrient Uptake and Soil Quality Improvement. Pedosphere 25, 749–760. doi:10.1016/S1002-0160(15)30056-4

Jousset, A., Bienhold, C., Chatzinotas, A., Gallien, L., Gobet, A., Kurm, V., Küsel, K., Rillig, M.C., Rivett, D.W., Salles, J.F., Van Der Heijden, M.G.A., Youssef, N.H., Zhang, X., Wei, Z., Hol, G.W.H., 2017. Where less may be more: How the rare

biosphere pulls ecosystems strings. ISME Journal 11, 853–862. doi:10.1038/ismej.2016.174

Kandeler, E., Deiglmayr, K., Tscherko, D., Bru, D., Philippot, L., 2006. Abundance of narG, nirS, nirK, and nosZ genes of denitrifying bacteria during primary successions of a glacier foreland. Applied and Environmental Microbiology 72, 5957–5962. doi:10.1128/AEM.00439-06

Kanehisa, M., Sato, Y., Morishima, K., 2016. BlastKOALA and GhostKOALA: KEGG Tools for Functional Characterization of Genome and Metagenome Sequences. Journal of Molecular Biology 428, 726–731. doi:10.1016/j.jmb.2015.11.006

Kang, D.D., Froula, J., Egan, R., Wang, Z., 2015. MetaBAT, an efficient tool for accurately reconstructing single genomes from complex microbial communities. PeerJ 3, e1165. doi:10.7717/peerj.1165

Keiluweit, M., Nico, P.S., Johnson, M.G., Kleber, M., 2010. Dynamic Molecular Structure of Plant Biomass-Derived Black Carbon (Biochar). Environmental Science & Technology 44, 1247–1253. doi:10.1021/es9031419

Kelly, D.P., Wood, A.P., McDonald, I.R., 2000. Proposal for the reclassification of Thiobacillus novellus as Starkeya novella gen. nov., comb. nov., in the alpha-subclass of the Proteobacteria. International Journal of Systematic and Evolutionary Microbiology 50, 1797–1802. doi:10.1099/00207713-50-5-1797

Kent, W.J., 2002. BLAT — The BLAST -Like Alignment Tool. Genome Research 12, 656–664. doi:10.1101/gr.229202.

Khodadad, C.L.M., Zimmerman, A.R., Green, S.J., Uthandi, S., Foster, J.S., 2011. Taxa-specific changes in soil microbial community composition induced by pyrogenic carbon amendments. Soil Biology and Biochemistry 43, 385–392. doi:10.1016/j.soilbio.2010.11.005

King, G.M., 2007. Chemolithotrohic Bacteria: Distributions, Functions and Significance in Volcanic Environments. Microbes and Environments 22, 309–319. doi:10.1264/jsme2.22.309

Kolton, M., Graber, E.R., Tsehansky, L., Elad, Y., Cytryn, E., 2017. Biochar-stimulated plant performance is strongly linked to microbial diversity and metabolic potential in the rhizosphere. New Phytologist 213, 1393–1404. doi:10.1111/nph.14253

Kolton, M., Harel, Y.M., Pasternak, Z., Graber, E.R., Elad, Y., Cytryn, E., 2011. Impact of biochar application to soil on the root-associated bacterial community structure of fully developed greenhouse pepper plants. Applied and Environmental

Microbiology 77, 4924–4930. doi:10.1128/AEM.00148-11

Kopylova, E., Noé, L., Touzet, H., 2012. SortMeRNA: Fast and accurate filtering of ribosomal RNAs in metatranscriptomic data. Bioinformatics 28, 3211–3217. doi:10.1093/bioinformatics/bts611

Kozich, J.J., Westcott, S.L., Baxter, N.T., Highlander, S.K., Schloss, P.D., 2013. Development of a Dual-Index Sequencing Strategy and Curation Pipeline for Analyzing Amplicon Sequence Data on the MiSeq Illumina Sequencing Platform. Applied and Environmental Microbiology 79, 5112–5120. doi:10.1128/AEM.01043-13

Kuzyakov, Y., Bogomolova, I., Glaser, B., 2014. Biochar stability in soil: Decomposition during eight years and transformation as assessed by compound-specific 14C analysis. Soil Biology and Biochemistry 70, 229–236. doi:10.1016/j.soilbio.2013.12.021

Kuzyakov, Y., Subbotina, I., Chen, H., Bogomolova, I., Xu, X., 2009. Black carbon decomposition and incorporation into soil microbial biomass estimated by14C labeling. Soil Biology and Biochemistry 41, 210–219. doi:10.1016/j.soilbio.2008.10.016

Laghari, M., Naidu, R., Xiao, B., Hu, Z., Mirjat, M.S., Hu, M., Kandhro, M.N., Chen, Z., Guo, D., Jogi, Q., Abudi, Z.N., Fazal, S., 2016. Recent developments in biochar as an effective tool for agricultural soil management: a review. Journal of the Science of Food and Agriculture 96, 4840–4849. doi:10.1002/jsfa.7753

Laird, D.A., 2008. The Charcoal Vision: A Win-Win-Win Scenario for Simultaneously Producing Bioenergy, Permanently Sequestering Carbon, while Improving Soil and Water Quality. Agronomy Journal 100, 178–181. doi:10.2134/agronj2007.0161

Lal, R., 2015. Restoring soil quality to mitigate soil degradation. Sustainability 7, 5875–5895. doi:10.3390/su7055875

Lal, R., 2012. Climate Change and Soil Degradation Mitigation by Sustainable Management of Soils and Other Natural Resources. Agricultural Research 1, 199–212. doi:10.1007/s40003-012-0031-9

Lal, R., 2004. Soil carbon sequestration impacts on global climate change and food security. Science 304, 1623–7. doi:10.1126/science.1097396

Langmead, B., Salzberg, S.L., 2012. Fast gapped-read alignment with Bowtie 2. Nature Methods 9, 357–359. doi:10.1038/nmeth.1923

Langmead, B., Trapnell, C., Pop, M., Salzberg, S.L., 2009. Ultrafast and memory-efficient alignment of short DNA sequences to the human genome. Genome Biology 10. doi:10.1186/gb-2009-10-3-r25

Lanza, G., Rebensburg, P., Kern, J., Lentzsch, P., Wirth, S., 2016. Impact of chars and readily available carbon on soil microbial respiration and microbial community composition in a dynamic incubation experiment. Soil and Tillage Research 164, 18–24. doi:10.1016/j.still.2016.01.005

Lauber, C.L., Hamady, M., Knight, R., Fierer, N., 2009. Pyrosequencing-based assessment of soil pH as a predictor of soil bacterial community structure at the continental scale. Applied and Environmental Microbiology 75, 5111–5120. doi:10.1128/AEM.00335-09

Lauber, C.L., Ramirez, K.S., Aanderud, Z., Lennon, J., Fierer, N., 2013. Temporal variability in soil microbial communities across land-use types. The ISME Journal 7, 1641–1650. doi:10.1038/ismej.2013.50

Le Quéré, C., Moriarty, R., Andrew, R.M., Peters, G.P., Ciais, P., Friedlingstein, P., Jones, S.D., Sitch, S., Tans, P., Arneth, A., Boden, T.A., Bopp, L., Bozec, Y., Canadell, J.G., Chevallier, F., Cosca, C.E., Harris, I., Hoppema, M., Houghton, R.A., House, J.I., Jain, J.K., Johannessen, T., Kato, E., Keeling, R.F., Kitidis, V., Klein Goldewijk, K., Koven, C., Landa, C., Landschützer, P., Lenton, A., Lima, I.D., Marland, G., Mathis, J.T., Metzl, N., Nojiri, Y., Olsen, A., Ono, T., Peters, W., Pfeil, B., Poulter, B., Raupach, M.R., Regnier, P., Rödenbeck, C., Saito, S., Salisbury, J.E., Schuster, U., Schwinger, J., Séférian, R., Segschneider, J., Steinhoff, T., Stocker, B.D., Sutton, A.J., Takahashi, T., Tilbrook, B., Van Der Werf, G., Viovy, N., Wang, Y.-P., Wanninkhof, R., Wiltshire, A., Zeng, N., 2014. Global carbon budget 2014 Global Carbon Budget 2014 Title Page Abstract Instruments Data Provenance & Structure. Earth Syst. Sci. Data Discuss 6, 1–90. doi:10.5194/essdd-6-1-2014

Lee, T.K., Lee, J., Sul, W.J., Iwai, S., Chai, B., Tiedje, J.M., Park, J., 2011. Novel biphenyl-oxidizing bacteria and dioxygenase genes from a Korean tidal mudflat. Applied and Environmental Microbiology 77, 3888–3891. doi:10.1128/AEM.00023-11

Lehmann, J., Abiven, S., Kleber, M., Pan, G., Singh, B.P., Sohi, S., Zimmerman, A.R.A., 2015. Persistence of biochar in soil, in: Biochar for Environmental Management. Routledge, New York, NY, pp. 235–281.

Lehmann, J., Da Silva, J.P., Steiner, C., Nehls, T., Zech, W., Glaser, B., 2003. Nutrient availability and leaching in an archaeological Anthrosol and a Ferralsol of the Central Amazon basin: fertilizer, manure and charcoal amendments. Plant and Soil

249, 343–357.

Lehmann, J., Gaunt, J., Rondon, M., 2006. Bio-char Sequestration in Terrestrial Ecosystems – A Review. Mitigation and Adaptation Strategies for Global Change 11, 403–427. doi:10.1007/s11027-005-9006-5

Lehmann, J., Rillig, M.C., Thies, J., Masiello, C.A., Hockaday, W.C., Crowley, D., 2011. Biochar effects on soil biota - A review. Soil Biology and Biochemistry 43, 1812–1836. doi:10.1016/j.soilbio.2011.04.022

Lepleux, C., Turpault, M.P., Oger, P., Frey-Klett, P., Uroz, S., 2012. Correlation of the abundance of betaproteobacteria on mineral surfaces with mineral weathering in forest soils. Applied and Environmental Microbiology 78, 7114–7119. doi:10.1128/AEM.00996-12

Lewin, G.R., Carlos, C., Chevrette, M.G., Horn, H.A., McDonald, B.R., Stankey, R.J., Fox, B.G., Currie, C.R., 2016. Evolution and Ecology of *Actinobacteria* and Their Bioenergy Applications. Annual Review of Microbiology 70, 235–254. doi:10.1146/annurev-micro-102215-095748

Li, D., Liu, C.M., Luo, R., Sadakane, K., Lam, T.W., 2015. MEGAHIT: An ultra-fast single-node solution for large and complex metagenomics assembly via succinct de Bruijn graph. Bioinformatics 31, 1674–1676. doi:10.1093/bioinformatics/btv033

Li, D., Luo, R., Liu, C.M., Leung, C.M., Ting, H.F., Sadakane, K., Yamashita, H., Lam, T.W., 2016. MEGAHIT v1.0: A fast and scalable metagenome assembler driven by advanced methodologies and community practices. Methods 102, 3–11. doi:10.1016/j.ymeth.2016.02.020

Li, H., Handsaker, B., Wysoker, A., Fennell, T., Ruan, J., Homer, N., Marth, G., Abecasis, G., Durbin, R., 2009. The Sequence Alignment/Map format and SAMtools. Bioinformatics 25, 2078–2079. doi:10.1093/bioinformatics/btp352

Li, Q., Lei, Z., Song, X., Zhang, Z., Ying, Y., Peng, C., 2018. Biochar amendment decreases soil microbial biomass and increases bacterial diversity in Moso bamboo (Phyllostachys edulis) plantations under simulated nitrogen deposition. Environmental Research Letters 13, 0044029. doi:10.1088/1748-9326/aab53a

Li, Y., Yu, S., Strong, J., Wang, H., 2012. Are the biogeochemical cycles of carbon, nitrogen, sulfur, and phosphorus driven by the "FeIII-FeIIredox wheel" in dynamic redox environments? Journal of Soils and Sediments 12, 683–693. doi:10.1007/s11368-012-0507-z

Liang, B., Lehmann, J., Solomon, D., Kinyangi, J., Grossman, J., O'Neill, B., Skjemstad,

J.O., Thies, J., Luizão, F.J., Petersen, J., Neves, E.G., 2006. Black Carbon Increases Cation Exchange Capacity in Soils. Soil Science Society of America Journal 70, 1719. doi:10.2136/sssaj2005.0383

Liang, C., Da, E., Jesus, C., Duncan, D.S., Jackson, R.D., Tiedje, J.M., Balser, T.C., 2011. Soil microbial communities under model biofuel cropping systems in southern Wisconsin, USA: Impact of crop species and soil properties. Applied Soil Ecology 54, 24–31. doi:10.1016/j.apsoil.2011.11.015

Lienhard, P., Tivet, F., Chabanne, A., Dequiedt, S., Lelièvre, M., Sayphoummie, S., Leudphanane, B., Prévost-Bouré, N.C., Séguy, L., Maron, P.-A., Ranjard, L., 2013. No-till and cover crops shift soil microbial abundance and diversity in Laos tropical grasslands. Agronomy for Sustainable Development 33, 375–384. doi:10.1007/s13593-012-0099-4

Liu, X., Lee Burras, C., Kravchenko, Y.S., Duran, A., Huffman, T., Morras, H., Studdert, G., Zhang, X., Cruse, R.M., Yuan, X., 2012. Overview of Mollisols in the world: Distribution, land use and management. Canadian Journal of Soil Science 92, 383–402. doi:10.4141/cjss2010-058

Liu, Y., Zhu, J., Ye, C., Zhu, P., Ba, Q., Pang, J., Shu, L., 2018. Effects of biochar application on the abundance and community composition of denitrifying bacteria in a reclaimed soil from coal mining subsidence area. Science of The Total Environment 625, 1218–1224. doi:10.1016/j.scitotenv.2018.01.003

Lu, L., Yin, S., Liu, X., Zhang, W., Gu, T., Shen, Q., Qiu, H., 2013. Fungal networks in yield-invigorating and -debilitating soils induced by prolonged potato monoculture. Soil Biology and Biochemistry 65, 186–194. doi:10.1016/j.soilbio.2013.05.025

Lu, X., Seuradge, B.J., Neufeld, J.D., 2017. Biogeography of soil Thaumarchaeota in relation to soil depth and land usage. FEMS Microbiology Ecology 93, 1–11. doi:10.1093/femsec/fiw246

Luo, F., Zhong, J., Yang, Y., Scheuermann, R., Zhou, J., 2006. Application of random matrix theory to biological networks. Physics Letters A 357, 420–423. doi:10.1016/J.PHYSLETA.2006.04.076

Luo, Y., Durenkamp, M., De Nobili, M., Lin, Q., Brookes, P.C., 2011. Short term soil priming effects and the mineralisation of biochar following its incorporation to soils of different pH. Soil Biology and Biochemistry 43, 2304–2314. doi:10.1016/j.soilbio.2011.07.020

MacLean, A.M., MacPherson, G., Aneja, P., Finan, T.M., 2006. Characterization of the β-ketoadipate pathway in Sinorhizobium meliloti. Applied and Environmental

Microbiology 72, 5403–5413. doi:10.1128/AEM.00580-06

Männistö, M.K., Tiirola, M., Häggblom, M.M., 2007. Bacterial communities in Arctic fjelds of Finnish Lapland are stable but highly pH-dependent. FEMS Microbiology Ecology 59, 452–65.

Mathew, R.P., Feng, Y., Githinji, L., Ankumah, R., Balkcom, K.S., 2012. Impact of No-Tillage and Conventional Tillage Systems on Soil Microbial Communities. Applied and Environmental Soil Science 2012, 1–10. doi:10.1155/2012/548620

McMurdie, P.J., Holmes, S., 2013. phyloseq: An R package for reproducible interactive analysis and graphics of microbiome census data. PLoS ONE 8, e61217.

Meschewski, E., Holm, N., Sharma, B.K., Spokas, K., Minalt, N., Kelly, J.J., 2019. Pyrolysis biochar has negligible effects on soil greenhouse gas production, microbial communities, plant germination, and initial seedling growth. Chemosphere 228, 565–576. doi:10.1016/j.chemosphere.2019.04.031

Meyer, F., Paarmann, D., D'Souza, M., Olson, R., Glass, E., Kubal, M., Paczian, T., Rodriguez, A., Steven, R., Wilke, A., Wilkening, J., Edwards, R., 2008. The metagenomics RAST server—a public resource for the automatic phylo- genetic and functional analysis of metagenomes. BMC Bioinformatics 9, 386. doi:10.1186/1471-2105-9-386

Mia, S., Singh, B., Dijkstra, F.A., 2017. Aged biochar affects gross nitrogen mineralization and recovery: a 15N study in two contrasting soils. GCB Bioenergy 9, 1196–1206. doi:10.1111/gcbb.12430

Mills, H.J., Hunter, E., Humphrys, M., Kerkhof, L., Mcguinness, L., Huettel, M., Kostka, J.E., 2008. Characterization of Nitrifying, Denitrifying, and Overall Bacterial Communities in Permeable Marine Sediments of the Northeastern Gulf of Mexico. Applied and Environmental Microbiology 74, 4440–4453. doi:10.1128/AEM.02692-07

Mukherjee, A., Zimmerman, A.R., Harris, W., 2011. Surface chemistry variations among a series of laboratory-produced biochars. Geoderma 163, 247–255. doi:10.1016/j.geoderma.2011.04.021

Nadkarni, M.A., Martin, F.E., Jacques, N.A., Hunter, N., 2002. Determination of bacterial load by real-time PCR using a broad-range (universal) probe and primers set. Microbiology 148, 257–266. doi:10.1099/00221287-148-1-257

Naether, A., Foesel, B.U., Naegele, V., Wust, P.K., Weinert, J., Bonkowski, M., Alt, F., Oelmann, Y., Polle, A., Lohaus, G., Gockel, S., Hemp, A., Kalko, E.K. V,

Linsenmair, K.E., Pfeiffer, S., Renner, S., Schoning, I., Weisser, W.W., Wells, K., Fischer, M., Overmann, J., Friedrich, M.W., 2012. Environmental factors affect acidobacterial communities below the subgroup level in grassland and forest soils. Applied and Environmental Microbiology 78, 7398–7406. doi:10.1128/AEM.01325-12

Nannipieri, P., Ascher, J., Ceccherini, M.T., Landi, L., Pietramellara, G., Renella, G., 2003. Microbial diversity and soil functions. European Journal of Soil Science 54, 655–670. doi:10.2106/JBJS.I.01289

Naushad, H.S., Gupta, R.S., 2013. Phylogenomics and Molecular Signatures for Species from the Plant Pathogen-Containing Order Xanthomonadales. PLoS ONE 8. doi:10.1371/journal.pone.0055216

Nelson, M.B., Berlemont, R., Martiny, A.C., Martiny, J.B.H., 2015. Nitrogen cycling potential of a grassland litter microbial community. Applied and Environmental Microbiology 81, 7012–7022. doi:10.1128/AEM.02222-15

Newman, M.E.J., 2006. Modularity and community structure in networks. PNAS 1003, 8577–8582.

Nicolitch, O., Feucherolles, M., Churin, J.L., Fauchery, L., Turpault, M.P., Uroz, S., 2019. A microcosm approach highlights the response of soil mineral weathering bacterial communities to an increase of K and Mg availability. Scientific Reports 9, 1–13. doi:10.1038/s41598-019-50730-y

Noyce, G.L., Basiliko, N., Fulthorpe, R., Sackett, T.E., Thomas, S.C., 2015. Soil microbial responses over 2 years following biochar addition to a north temperate forest. Biology and Fertility of Soils 51, 649–659. doi:10.1007/s00374-015-1010-7

Noyce, G.L., Winsborough, C., Fulthorpe, R., Basiliko, N., 2016. The microbiomes and metagenomes of forest biochars. Scientific Reports 6, 26425. doi:10.1038/srep26425

O'Leary, N.A., Wright, M.W., Brister, J.R., Ciufo, S., Haddad, D., McVeigh, R., Rajput, B., Robbertse, B., Smith-White, B., Ako-Adjei, D., Astashyn, A., Badretdin, A., Bao, Y., Blinkova, O., Brover, V., Chetvernin, V., Choi, J., Cox, E., Ermolaeva, O., Farrell, C.M., Goldfarb, T., Gupta, T., Haft, D., Hatcher, E., Hlavina, W., Joardar, V.S., Kodali, V.K., Li, W., Maglott, D., Masterson, P., McGarvey, K.M., Murphy, M.R., O'Neill, K., Pujar, S., Rangwala, S.H., Rausch, D., Riddick, L.D., Schoch, C., Shkeda, A., Storz, S.S., Sun, H., Thibaud-Nissen, F., Tolstoy, I., Tully, R.E., Vatsan, A.R., Wallin, C., Webb, D., Wu, W., Landrum, M.J., Kimchi, A., Tatusova, T., DiCuccio, M., Kitts, P., Murphy, T.D., Pruitt, K.D., 2016. Reference sequence (RefSeq) database at NCBI: Current status, taxonomic expansion, and functional annotation. Nucleic Acids Research 44, D733–D745. doi:10.1093/nar/gkv1189

O'Neill, B., Grossman, J., Tsai, M.T., Gomes, J.E., Lehmann, J., Peterson, J., Neves, E., Thies, J.E., 2009. Bacterial community composition in Brazilian Anthrosols and adjacent soils characterized using culturing and molecular identification. Microbial Ecology 58, 23–35. doi:10.1007/s00248-009-9515-y

Oksanen, J., Blanchet, F.G., Friendly, M., Kindt, R., Legendre, P., Mcglinn, D., Minchin, P.R., O 'hara, R.B., Simpson, G.L., Solymos, P., Henry, M., Stevens, H., Szoecs, E., Wagner, H., Oksanen, M.J., 2018. Package "vegan."

Olesen, J.M., Bascompte, J., Dupont, Y.L., Jordano, P., 2007. The modularity of pollination networks. PNAS 104, 19891–19896.

Orellana, L.H., Rodriguez-R, L.M., Higgins, S., Chee-Sanford, J.C., Sanford, R.A., Ritalahti, K.M., Löffler, F.E., Konstantinidis, K.T., 2014. Detecting Nitrous Oxide Reductase (nosZ) Genes in Soil Metagenomes: Method Development and Implications for the Nitrogen Cycle. MBio 5, 19709–19714. doi:10.1128/mBio.01193-14

Orr, C., Ralebitso-Senior, T., 2014. Tracking N-cycling genes in biochar-supplemented ecosystems: A perspective. OA Microbiology 2, 1.

Orwin, K.H., Wardle, D.A., Greenfield, L.G., Setälä, H., 2006. Context dependent changes in the resistance and resilience of soil microbes to an experimental disturbance for three primary plant chronosequences. Oikos 112, 196–208.

Overbeek, R., Begley, T., Butler, R.M., Choudhuri, J. V., Chuang, H.Y., Cohoon, M., de Crécy-Lagard, V., Diaz, N., Disz, T., Edwards, R., Fonstein, M., Frank, E.D., Gerdes, S., Glass, E.M., Goesmann, A., Hanson, A., Iwata-Reuyl, D., Jensen, R., Jamshidi, N., Krause, L., Kubal, M., Larsen, N., Linke, B., McHardy, A.C., Meyer, F., Neuweger, H., Olsen, G., Olson, R., Osterman, A., Portnoy, V., Pusch, G.D., Rodionov, D.A., Rül;ckert, C., Steiner, J., Stevens, R., Thiele, I., Vassieva, O., Ye, Y., Zagnitko, O., Vonstein, V., 2005. The subsystems approach to genome annotation and its use in the project to annotate 1000 genomes. Nucleic Acids Research 33, 5691–5702. doi:10.1093/nar/gki866

Paine, R.T., 1995. A Conversation on Refining the Concept of Keystone Species. Conservation Biology 9, 962–964.

Palmer, K., Horn, M.A., 2012. Actinobacterial nitrate reducers and proteobacterial denitrifiers are abundant in N2O-metabolizing palsa peat. Applied and Environmental Microbiology 78, 5584–5596. doi:10.1128/AEM.00810-12

Park, D., Kim, H., Yoon, S., 2017. Nitrous Oxide Reduction by an Obligate Aerobic

Bacterium, Gemmatimonas aurantiaca Strain T-27. Applied and Environmental Microbiology 83, 1–12. doi:10.1128/AEM.00502-17

Parke, D., Ornston, L.N., 1986. Enzymes of the β-ketoadipate pathway are inducible in Rhizobium and Agrobacterium spp. and constitutive in Bradyrhizobium spp. Journal of Bacteriology 165, 288–292. doi:10.1128/jb.165.1.288-292.1986

Parks, D.H., Chuvochina, M., Chaumeil, P.-A., Rinke, C., Mussig, A.J., Hugenholtz, P., 2019. Selection of representative genomes for 24,706 bacterial and archaeal species clusters provide a complete genome-based taxonomy. BioRxiv 771964. doi:10.1101/771964

Parks, D.H., Chuvochina, M., Waite, D.W., Rinke, C., Skarshewski, A., Chaumeil, P.A., Hugenholtz, P., 2018. A standardized bacterial taxonomy based on genome phylogeny substantially revises the tree of life. Nature Biotechnology 36, 996. doi:10.1038/nbt.4229

Parks, D.H., Imelfort, M., Skennerton, C.T., Hugenholtz, P., Tyson, G.W., 2015. CheckM: Assessing the quality of microbial genomes recovered from isolates, single cells, and metagenomes. Genome Research 25, 1043–1055. doi:10.1101/gr.186072.114

Pascault, N., Ranjard, L., Kaisermann, A., Bachar, D., Christen, R., Terrat, S., Mathieu, O., Lévêque, J., Mougel, C., Henault, C., Lemanceau, P., Péan, M., Boiry, S., Fontaine, S., Maron, P.A., 2013. Stimulation of Different Functional Groups of Bacteria by Various Plant Residues as a Driver of Soil Priming Effect. Ecosystems 16, 810–822. doi:10.1007/s10021-013-9650-7

Paustian, K., Lehmann, J., Ogle, S., Reay, D., Robertson, G.P., Smith, P., 2016. Climate-smart soils. Nature 532, 49–57. doi:10.1038/nature17174

Pester, M., Schleper, C., Wagner, M., 2011. The Thaumarchaeota: an emerging view of their phylogeny and ecophysiology. Current Opinion in Microbiology 14, 300–306. doi:10.1016/j.mib.2011.04.007

Philippot, L., 2002. Denitrifying genes in Bacterial and Archeal genomes. Biochim Biophys Acta. 1577, 355–376. doi:10.1016/S0167-4781(02)00420-7

Philippot, L., Piutti, S., Martin-Laurent, F., Hallet, S., Germon, J.C., 2002. Molecular analysis of the nitrate-reducing community from unplanted and maize-planted soils. Applied and Environmental Microbiology 68, 6121–6128. doi:10.1128/AEM.68.12.6121-6128.2002

Pometto, A.L., Crawford, D.L., 1981. Enzymatic production of the lignin precursor trans-

[U-14C]cinnamic acid from l-[U-14C]phenylalanine using l-phenylalanine ammonia-lyase. Enzyme and Microbial Technology 3, 73–75. doi:10.1016/0141-0229(81)90040-5

Post, W.M., Kwon, K., 2000. Soil carbon sequestration and land-use change: processes and potential. Global Change Biology 6, 317–327. doi:10.1046/j.1365-2486.2000.00308.x

Power, M.E., Tilman, D., Estes, J.A., Menge, B.A., Bond, W.J., Scott Mills, L., Daily, G., Carlos Castilla, J., Lubchenco, J., 1996. Challenges in the Quest for Keystones. Paine Source: BioScience 46, 609–620.

Quilliam, R.S., Rangecroft, S., Emmett, B.A., Deluca, T.H., Jones, D.L., 2013. Is biochar a source or sink for polycyclic aromatic hydrocarbon (PAH) compounds in agricultural soils? GCB Bioenergy 5, 96–103. doi:10.1111/gcbb.12007

Quinlan, A.R., Hall, I.M., 2010. BEDTools: A flexible suite of utilities for comparing genomic features. Bioinformatics 26, 841–842. doi:10.1093/bioinformatics/btq033

Rabbi, S.M.F., Daniel, H., Lockwood, P. V., Macdonald, C., Pereg, L., Tighe, M., Wilson, B.R., Young, I.M., 2016. Physical soil architectural traits are functionally linked to carbon decomposition and bacterial diversity. Scientific Reports 6, 1–9. doi:10.1038/srep33012

Rho, M., Tang, H., Ye, Y., 2010. FragGeneScan: Predicting genes in short and error-prone reads. Nucleic Acids Research 38, 1–12. doi:10.1093/nar/gkq747

Rittl, T.F., Novotny, E.H., Balieiro, F.C., Hoffland, E., Alves, B.J.R., Kuyper, T.W., 2015. Negative priming of native soil organic carbon mineralization by oilseed biochars of contrasting quality. European Journal of Soil Science 66, 714–721. doi:10.1111/ejss.12257

Rodriguez-R, L.M., Gunturu, S., Tiedje, J.M., Cole, J.R., Konstantinidis, K.T., 2018. Nonpareil 3: Fast Estimation of Metagenomic Coverage and Sequence Diversity. MSystems 3, e00039-18.

Rodriguez-R, L.M., Konstantinidis, K.T., 2014. Nonpareil: A redundancy-based approach to assess the level of coverage in metagenomic datasets. Bioinformatics 30, 629–635. doi:10.1093/bioinformatics/btt584

Roesch, L.F., Fulthorpe, R.R., Riva, A., Casella, G., Hadwin, A.K., Kent, A.D., Daroub, S.H., Camargo, F.A., Farmerie, W.G., Triplett, E.W., 2007. Pyrosequencing enumerates and contrasts soil microbial diversity. The ISME Journal 1, 283–290. doi:10.1038/ismej.2007.53

Roesch, L.F.W., Fulthorpe, R.R., Riva, A., Casella, G., Hadwin, A.K.M., Kent, A.D., Daroub, S.H., Camargo, F.A.O., Farmerie, W.G., Triplett, E.W., 2007. Pyrosequencing enumerates and contrasts soil microbial diversity. ISME Journal 1, 283–290. doi:10.1038/ismej.2007.53

Rousk, J., Dempster, D.N., Jones, D.L., 2013. Transient biochar effects on decomposer microbial growth rates: Evidence from two agricultural case-studies. European Journal of Soil Science 64, 770–776. doi:10.1111/ejss.12103

Ruamps, L.S., Nunan, N., Chenu, C., 2011. Microbial biogeography at the soil pore scale. Soil Biology and Biochemistry 43, 280–286. doi:10.1016/j.soilbio.2010.10.010

Salles, J.F., Van Veen, J.A., Van Elsas, J.D., 2004. Multivariate Analyses of Burkholderia Species in Soil: Effect of Crop and Land Use History. Applied and Environmental Microbiology 70, 4012–4020. doi:10.1128/AEM.70.7.4012–4020.2004

Sekiya, N., Shiotsu, F., Abe, J., Morita, S., 2013. Distribution and Quantity of Root Systems of Field-Grown Erianthus and Napier Grass. American Journal of Plant Sciences 2013, 16–22. doi:10.4236/ajps.2013.412A1003

Shade, A., Jones, S.E., Caporaso, J.G., Handelsman, J., Knight, R., Fierer, N., Gilbert, J.A., 2014. Conditionally Rare Taxa Disproportionately Contribute to Temporal Changes in Microbial Diversity. MBio 5, 3–11. doi:10.1128/mBio.01371-14

Shannon, P., Markiel, A., Ozier, O., Baliga, N.S., Wang, J.T., Ramage, D., Amin, N., Schwikowski, B., Ideker, T., 2003. Cytoscape: A Software Environment for Integrated Models of Biomolecular Interaction Networks. Genome Research 13, 2498–2504.

Sharma, S.K., Ramesh, A., Sharma, M.P., Joshi, O.P., Govaerts, B., Steenwerth, K.L., Karlen, D.L., 2010. Microbial Community Structure and Diversity as Indicators for Evaluating Soil Quality, in: Biodiversity, Biofuels, Agroforestry, and Conservation Agriculture. pp. 317–358. doi:10.1007/978-90-481-9513-8_11

Sheng, Y., Zhu, L., 2018. Biochar alters microbial community and carbon sequestration potential across different soil pH. Science of the Total Environment 622–623, 1391–1399. doi:10.1016/j.scitotenv.2017.11.337

Shi, S., Nuccio, E.E., Shi, Z.J., He, Z., Zhou, J., Firestone, M.K., 2016. The interconnected rhizosphere: High network complexity dominates rhizosphere assemblages. Ecology Letters 19, 926–936. doi:10.1111/ele.12630

Shi, Y., Chai, L., Tang, C., Yang, Z., Zhang, H., Chen, R., Chen, Y., Zheng, Y., 2013. Characterization and genomic analysis of kraft lignin biodegradation by the beta-proteobacterium Cupriavidus basilensis B-8. Biotechnology for Biofuels 6, 1–14. doi:10.1186/1754-6834-6-1

Sinsabaugh, R.L., Manzoni, S., Moorhead, D.L., Richter, A., 2013. Carbon use efficiency of microbial communities: Stoichiometry, methodology and modelling. Ecology Letters 16, 930–939. doi:10.1111/ele.12113

Six, J., Bossuyt, H., Degryze, S., Denef, K., 2004. A history of research on the link between (micro)aggregates, soil biota, and soil organic matter dynamics. Soil and Tillage Research 79, 7–31. doi:10.1016/j.still.2004.03.008

Six, J., Elliott, E.T., Paustian, K., 2000. Soil macroaggregate turnover and microaggregate formation: A mechanism for C sequestration under no-tillage agriculture. Soil Biology and Biochemistry 32, 2099–2103. doi:10.1016/S0038-0717(00)00179-6

Smith, C.R., Blair, P.L., Boyd, C., Cody, B., Hazel, A., Hedrick, A., Kathuria, H., Khurana, P., Kramer, B., Muterspaw, K., Peck, C., Sells, E., Skinner, J., Tegeler, C., Wolfe, Z., 2016. Microbial community responses to soil tillage and crop rotation in a corn/soybean agroecosystem. Ecology and Evolution 6, 8075–8084. doi:10.1002/ece3.2553

Smith, J.L., Collins, H.P., Bailey, V.L., 2010. The effect of young biochar on soil respiration. Soil Biology and Biochemistry 42, 2345–2347. doi:10.1016/j.soilbio.2010.09.013

Smith, P., Bustamante, M., Ahammad, H., Clark, H., Dong, H., Elsiddig, E.A., Haberl, H., Harper, R., House, J., Jafari, M., Masera, O., Mbow, C., Ravindranath, N.H., Rice, C.W., Robledo Abad, C., Romanovskaya, A., Sperling, F., Tubiello, F., 2014. Agriculture, Forestry and Other Land Use (AFOLU), Climate Change 2014: Mitigation of Climate Change. Contribution of Working Group III to the Fifth Assessment Report of the Intergovernmental Panel on Climate Change. Cambridge, United Kingdom and New York, NY, USA. doi:10.1017/cbo9781107415416.017

Smith, P., Martino, D., Cai, Z., Gwary, D., Janzen, H., Kumar, P., McCarl, B., Ogle, S., O'Mara, F., Rice, C., Scholes, B., Sirotenko, O., Howden, M., McAllister, T., Pan, G., Romanenkov, V., Schneider, U., Towprayoon, S., Wattenbach, M., Smith, J., 2008. Greenhouse gas mitigation in agriculture. Philosophical Transactions of the Royal Society B: Biological Sciences 363, 789–813. doi:10.1098/rstb.2007.2184

Sorrenti, G., Masiello, C.A., Dugan, B., Toselli, M., 2016. Biochar physico-chemical properties as affected by environmental exposure. Science of the Total Environment

563–564, 237–246. doi:10.1016/j.scitotenv.2016.03.245

Sparks, D., Page, A., Helmke, P., Loeppert, R., Soltanpour, P., Tabatabai, M., Johnston, C., Summer, M., 1996. Methods of Soil Analysis Part 3 Chemical Methods, Soil Science Society of America. Soil Science Society of America, Inc., Madison, Wisconsin.

Starkenburg, S.R., Chain, P.S.G., Sayavedra-Soto, L. a, Hauser, L., Land, M.L., Larimer, F.W., Malfatti, S. a, Klotz, M.G., Bottomley, P.J., Arp, D.J., Hickey, W.J., 2006. Genome sequence of the chemolithoautotrophic nitrite-oxidizing bacterium *Nitrobacter winogradskyi* Nb-255. Applied and Environmental Microbiology 72, 2050–2063. doi:10.1128/AEM.72.3.2050

Steinbeiss, S., Gleixner, G., Antonietti, M., 2009. Effect of biochar amendment on soil carbon balance and soil microbial activity. Soil Biology and Biochemistry 41, 1301–1310. doi:10.1016/j.soilbio.2009.03.016

Stieglmeier, M., Mooshammer, M., Kitzler, B., Wanek, W., Zechmeister-Boltenstern, S., Richter, A., Schleper, C., 2014. Aerobic nitrous oxide production through N-nitrosating hybrid formation in ammonia-oxidizing archaea. ISME Journal 8, 1135–1146. doi:10.1038/ismej.2013.220

Su, P., Lou, J., Brookes, P.C., Luo, Y., He, Y., Xu, J., 2017. Taxon-specific responses of soil microbial communities to different soil priming effects induced by addition of plant residues and their biochars. Journal of Soils and Sediments 17, 674–684. doi:10.1007/s11368-015-1238-8

Suliman, W., Harsh, J.B., Abu-Lail, N.I., Fortuna, A.M., Dallmeyer, I., Garcia-Perez, M., 2016. Influence of feedstock source and pyrolysis temperature on biochar bulk and surface properties. Biomass and Bioenergy 84, 37–48. doi:10.1016/j.biombioe.2015.11.010

Tan, G., Wang, H., Xu, N., Liu, H., Zhai, L., 2018. Biochar amendment with fertilizers increases peanut N uptake, alleviates soil N 2 O emissions without affecting NH 3 volatilization in field experiments. Environmental Science and Pollution Research 25, 8817–8826. doi:10.1007/s11356-017-1116-6

Thies, J.E., Rillig, M.C., Graber, E.R., 2015. Biochar effects on the abundance, activity and diversity of the soil biota, in: Biochar for Environmental Management: Science, Technology and Implementation. pp. 327–390.

Tilman, D., Cassman, K.G., Matson, P.A., Naylor, R., Polasky, S., 2002. Agricultural sustainability and intensive production practices. Nature 418, 671–677. doi:10.1038/nature01014

Tong, H., Hu, M., Li, F., Chen, M., Lv, Y., 2015. Burkholderiales participating in pentachlorophenol biodegradation in iron-reducing paddy soil as identified by stable isotope probing. Environmental Sciences: Processes and Impacts 17, 1282–1289. doi:10.1039/c4em00530a

Torsvik, V., Øvreås, L., Thingstad, T.F., 2002. Prokaryotic Diversity—Magnitude, Dynamics, and Controlling Factors. Science 296, 1064–1066.

Tylianakis, J.M., Tscharntke, T., Lewis, O.T., 2007. Habitat modification alters the structure of tropical host–parasitoid food webs. Nature 445, 202–205. doi:10.1038/nature05429

United Nations, 2017. World Population Prospects The 2017 Revision. doi:10.1017/CBO9781107415324.004

Uyttebroek, M., Breugelmans, P., Janssen, M., Wattiau, P., Joffe, B., Karlson, U., Ortega-Calvo, J.J., Bastiaens, L., Ryngaert, A., Hausner, M., Springael, D., 2006. Distribution of the Mycobacterium community and polycyclic aromatic hydrocarbons (PAHs) among different size fractions of a long-term PAH-contaminated soil. Environmental Microbiology 8, 836–847. doi:10.1111/j.1462-2920.2005.00970.x

Ventura, M., Canchaya, C., Tauch, A., Chandra, G., Fitzgerald, G.F., Chater, K.F., Van Sinderen, D., 2007. Genomics of Actinobacteria: Tracing the Evolutionary History of an Ancient Phylum. Microbiology and Molecular Biology Reviews 71, 495–548. doi:10.1128/MMBR.00005-07

Verastegui, Y., Cheng, J., Engel, K., Kolczynski, D., Mortimer, S., Lavigne, J., Montalibet, J., Romantsov, T., Hall, M., McConkey, B.J., Rose, D.R., Tomashek, J.J., Scott, B.R., Charles, T.C., Neufeld, J.D., 2014. Multisubstrate Isotope Labeling and Metagenomic Analysis of Active Soil Bacterial Communities. MBio 5, e01157-14. doi:10.1128/mBio.01157-14

Vitousek, P.M., Aber, J.D., Howarth, R.H., Likens, G.E., Matson, P.A., Schindler, D.W., Schlesinger, W.H., Tilman, D.G., 1997. Human alteration of the global nitrogen cycle: Source and consequences. Ecol Appl 7, 737–750. doi:10.1038/nn1891

Wang, J., Pan, X., Liu, Y., Zhang, X., Xiong, Z., 2012. Effects of biochar amendment in two soils on greenhouse gas emissions and crop production. Plant and Soil 360, 287–298. doi:10.1007/s11104-012-1250-3

Wang, Q., Garrity, G.M., Tiedje, J.M., Cole, J.R., 2007. Naïve Bayesian classifier for rapid assignment of rRNA sequences into the new bacterial taxonomy. Applied and

Environmental Microbiology 73, 5261–5267. doi:10.1128/AEM.00062-07

Warwick, R.M., Clarke, K.R., Suharsono, 1990. A statistical analysis of coral community responses to the 1982-83 El Niño in the Thousand Islands, Indonesia. Coral Reefs 8, 171–179.

Wickham, H., 2009. ggplot2 by Hadley Wickham. Media 35, 211. doi:10.1007/978-0-387-98141-3

Wickham, H., 2007. Reshaping Data with the reshape Package. Journal of Statistical Software 21, 1–20. doi:10.1016/S0142-1123(99)00007-9

Wickham, H., François, R., Henry, L., Müller, K., 2019. dplyr: A Grammar of Data Manipulation. R Package Version 0.8.1.

Wiedemeier, D.B., Abiven, S., Hockaday, W.C., Keiluweit, M., Kleber, M., Masiello, C.A., McBeath, A. V., Nico, P.S., Pyle, L.A., Schneider, M.P.W., Smernik, R.J., Wiesenberg, G.L.B., Schmidt, M.W.I., 2015. Aromaticity and degree of aromatic condensation of char. Organic Geochemistry 78, 135–143. doi:10.1016/j.orggeochem.2014.10.002

Wilke, C.O., 2017. cowplot: Streamlined Plot Theme and Plot Annotations for "ggplot2."

Wilpiszeski, R.L., Aufrecht, J.A., Retterer, S.T., Sullivan, M.B., Graham, D.E., Pierce, E.M., Zablocki, O.D., Palumbo, A. V., Elias, D.A., 2019. Soil Aggregate Microbial Communities: Towards Understanding Microbiome Interactions at Biologically Relevant Scales. Applied and Environmental Microbiology 85, 1–18. doi:10.1128/AEM.00324-19

Wobbrock, J.O., Findlater, L., Gergle, D., Higgins, J.J., 2011. The Aligned Rank Transform for Nonparametric Factorial Analyses Using Only ANOVA Procedures, in: ACM Conference on Human Factors in Computing Systems (CHI '11). ACM Press, New York, pp. 143–146.

Wolińska, A., Kuźniar, A., Zielenkiewicz, U., Izak, D., Szafranek-Nakonieczna, A., Banach, A., Błaszczyk, M., 2017. Bacteroidetes as a sensitive biological indicator of agricultural soil usage revealed by a culture-independent approach. Applied Soil Ecology 119, 128–137. doi:10.1016/j.apsoil.2017.06.009

Xu, H.-J., Wang, X.-H., Li, H., Yao, H.-Y., Su, J.-Q., Zhu, Y.-G., 2014. Biochar Impacts Soil Microbial Community Composition and Nitrogen Cycling in an Acidic Soil Planted with Rape. Environmental Science & Technology 48, 9391–9399. doi:10.1021/es5021058

Xu, H.J., Wang, X.H., Li, H., Yao, H.Y., Su, J.Q., Zhu, Y.G., 2014. Biochar impacts soil microbial community composition and nitrogen cycling in an acidic soil planted with rape. Environmental Science and Technology 48, 9391–9399. doi:10.1021/es5021058

Xu, N., Tan, G., Wang, H., Gai, X., 2016. Effect of biochar additions to soil on nitrogen leaching, microbial biomass and bacterial community structure. European Journal of Soil Biology 74, 1–8. doi:10.1016/j.ejsobi.2016.02.004

Yang, P., Dirk van Elsas, J., 2018. Mechanisms and ecological implications of the movement of bacteria in soil. Applied Soil Ecology 129, 112–120. doi:10.1016/j.apsoil.2018.04.014

Youngblut, N.D., Buckley, D.H., 2014. Intra-genomic variation in G + C content and its implications for DNA stable isotope probing. Environmental Microbiology Reports 6, 767–775. doi:10.1111/1758-2229.12201

Yu, J., Deem, L.M., Crow, S.E., Deenik, J., Ryan Penton, C., 2019. Comparative metagenomics reveals enhanced nutrient cycling potential after 2 years of biochar amendment in a tropical oxisol. Applied and Environmental Microbiology 85, 1–17. doi:10.1128/AEM.02957-18

Yu, J., Deem, L.M., Crow, S.E., Deenik, J.L., Penton, C.R., 2018. Biochar application influences microbial assemblage complexity and composition due to soil and bioenergy crop type interactions. Soil Biology and Biochemistry 117, 97–107. doi:10.1016/j.soilbio.2017.11.017

Yu, Z., Chen, L., Pan, S., Li, Y., Kuzyakov, Y., Xu, J., Brookes, P., Luo, Y., 2018. Feedstock determines biochar-induced soil priming effects by stimulating the activity of specific microorganisms. European Journal of Soil Science 69, 521–534. doi:10.1111/ejss.12542

Yuan, C., Lei, J., Cole, J., Sun, Y., 2015. Reconstructing 16S rRNA genes in metagenomic data. Bioinformatics 31, i35–i43. doi:10.1093/bioinformatics/btv231

Zhang, M., Riaz, M., Zhang, L., El-Desouki, Z., Jiang, C., 2019. Biochar induces changes to basic soil properties and bacterial communities of different soils to varying degrees at 25 mm rainfall: More effective on acidic soils. Frontiers in Microbiology 10. doi:10.3389/fmicb.2019.01321

Zhang, Q.Z., Dijkstra, F.A., Liu, X.R., Wang, Y.D., Huang, J., Lu, N., 2014. Effects of biochar on soil microbial biomass after four years of consecutive application in the north China Plain. PLoS ONE 9, 1–8. doi:10.1371/journal.pone.0102062

Zhao, L., Cao, X., Mašek, O., Zimmerman, A., 2013. Heterogeneity of biochar properties as a function of feedstock sources and production temperatures. Journal of Hazardous Materials 256–257, 1–9. doi:10.1016/j.jhazmat.2013.04.015

Zhao, M., Sun, B., Wu, L., Gao, Q., Wang, F., Wen, C., Wang, M., Liang, Y., Hale, L., Zhou, J., Yang, Y., 2016. Zonal Soil Type Determines Soil Microbial Responses to Maize Cropping and Fertilization. MSystems 1, e00075-16. doi:10.1128/mSystems.00075-16

Zheng, H., Wang, Z., Deng, X., Herbert, S., Xing, B., 2013. Impacts of adding biochar on nitrogen retention and bioavailability in agricultural soil. Geoderma 206, 32–39. doi:10.1016/j.geoderma.2013.04.018

Zheng, J., Chen, J., Pan, G., Liu, X., Zhang, X., Li, L., Bian, R., Cheng, K., Jinwei, Z., 2016. Biochar decreased microbial metabolic quotient and shifted community composition four years after a single incorporation in a slightly acid rice paddy from southwest China. Science of the Total Environment 571, 206–217. doi:10.1016/j.scitotenv.2016.07.135

Zhou, J., Deng, Y., Luo, F., He, Z., Tu, Q., Zhi, X., 2010. Functional molecular ecological networks. MBio 1, e00169-10. doi:10.1128/mBio.00169-10.Editor

Zhou, J., Deng, Y., Luo, F., He, Z., Yang, Y., 2011. Phylogenetic molecular ecological network of soil microbial communities in response to elevated CO2. MBio 2, e00122-11. doi:10.1128/mBio.00122-11.Editor

Zhu, X., Burger, M., Doane, T. a, Horwath, W.R., 2013. Ammonia oxidation pathways and nitrifier denitrification are significant sources of N 2 O and NO under low oxygen availability. Pnas 110, 6328–6333. doi:10.1073/pnas.1219993110/-/DCSupplemental.www.pnas.org/cgi/doi/10.1073/pnas.1219993110

Ziels, R.M., Sousa, D.Z., Stensel, H.D., Beck, D.A.C., 2018. DNA-SIP based genome-centric metagenomics identifies key long-chain fatty acid-degrading populations in anaerobic digesters with different feeding frequencies. ISME Journal 12, 112–123. doi:10.1038/ismej.2017.143

Zimmerman, A.R., 2010. Abiotic and microbial oxidation of laboratory-produced black carbon (biochar). Environmental Science and Technology 44, 1295–1301. doi:10.1021/es903140c

APPENDIX A

MICROBIAL COMMUNITY STRUCTURE AND SOIL METADATA RESULTS SUPPORTING FINDINGS OF CHAPTER 3

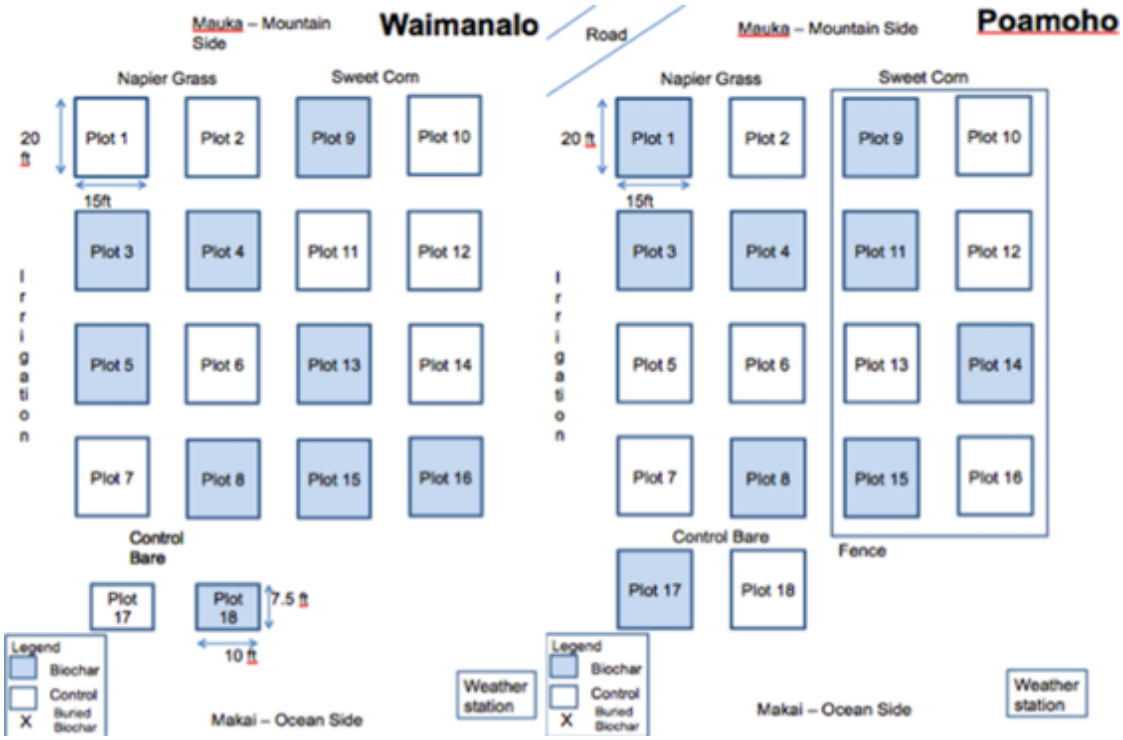


Figure A1. Layout of plots at each site. At both sites a randomized block design was used, crop-type was the block and presence or absence of biochar was the fixed factor.

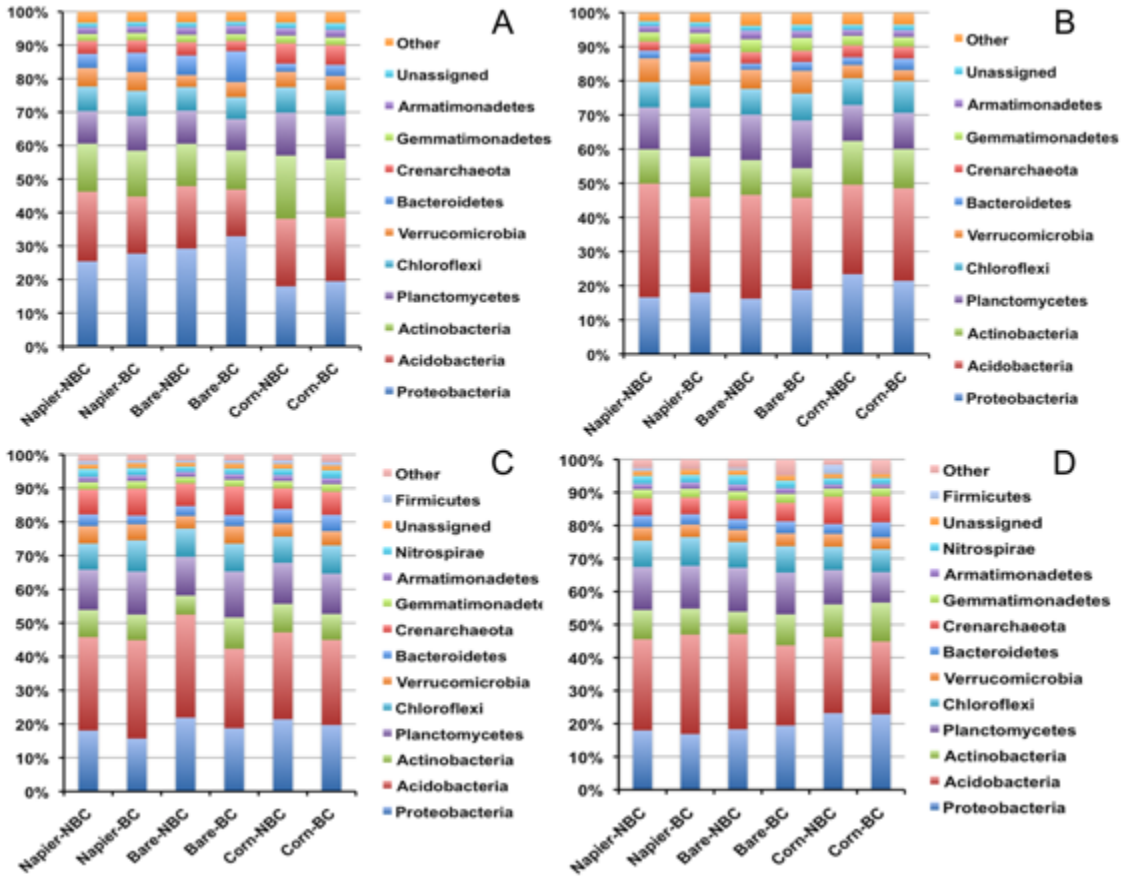


Figure A2. Relative abundance of phyla in the Oxisol during (A) pre-plant and (B) pre-harvest and in the Mollisol during (C) pre-plant and (D) pre-harvest. Following crop type are the treatment abbreviations: NBC: Control and BC: biochar. Other are all other phyla with relative abundance that compose <1% of the community.

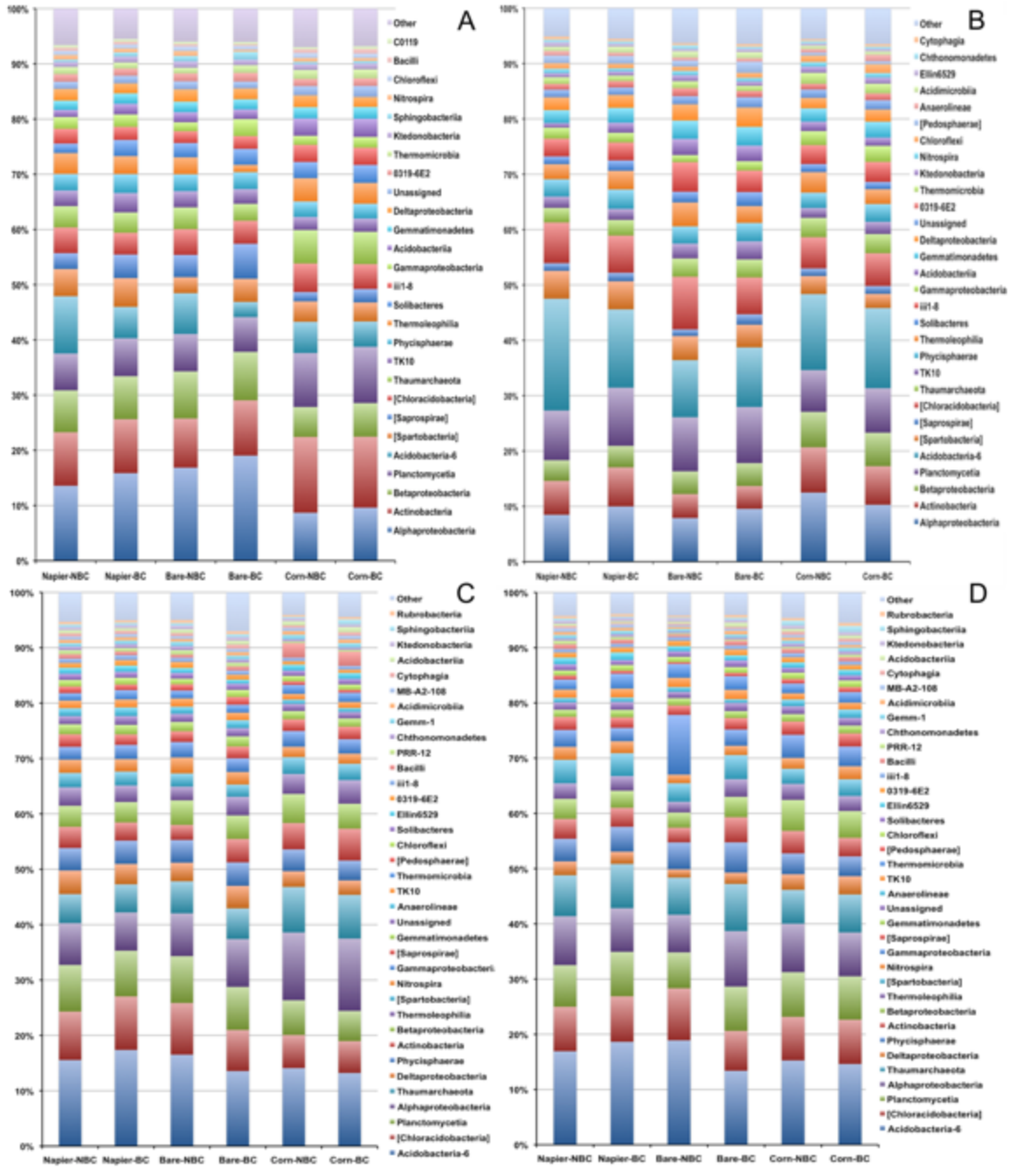


Figure A3. Relative abundance of taxa (class-level) according to soil type and sampling time. (Top Left: Oxisol Pre-plant, Top Right: Oxisol Pre-harvest, Bottom Left: Mollisol Pre-plant, Bottom Right: Mollisol Pre-harvest).

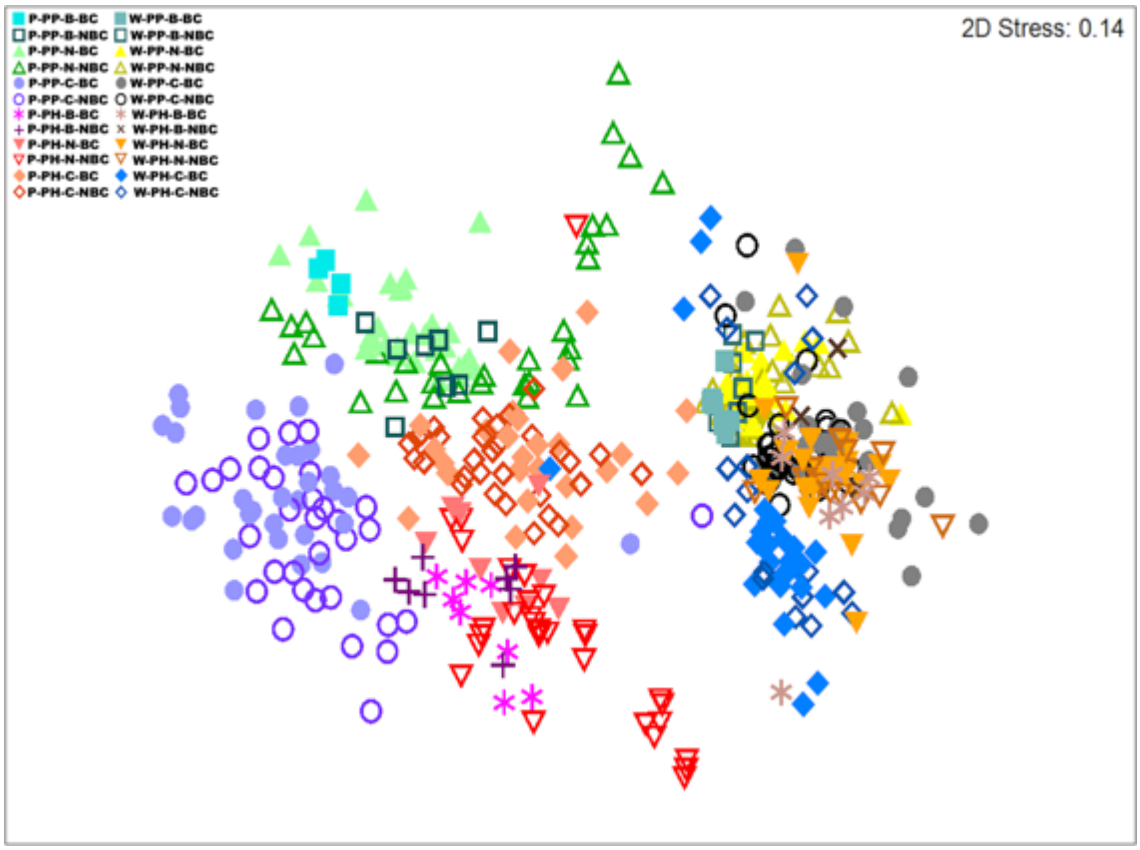


Figure A4. Non-metric multi-dimensional scaling (nMDS) plot depicting differences in bacterial community composition. Communities are broadly clustered according to soil type, Oxisol (P) and Mollisol (W); Time of sampling, pre-plant (PP) and pre-harvest (PH); Cropping system, bare (B), napiergrass (N) corn (C); Treatment, biochar (BC) and no biochar (NBC).

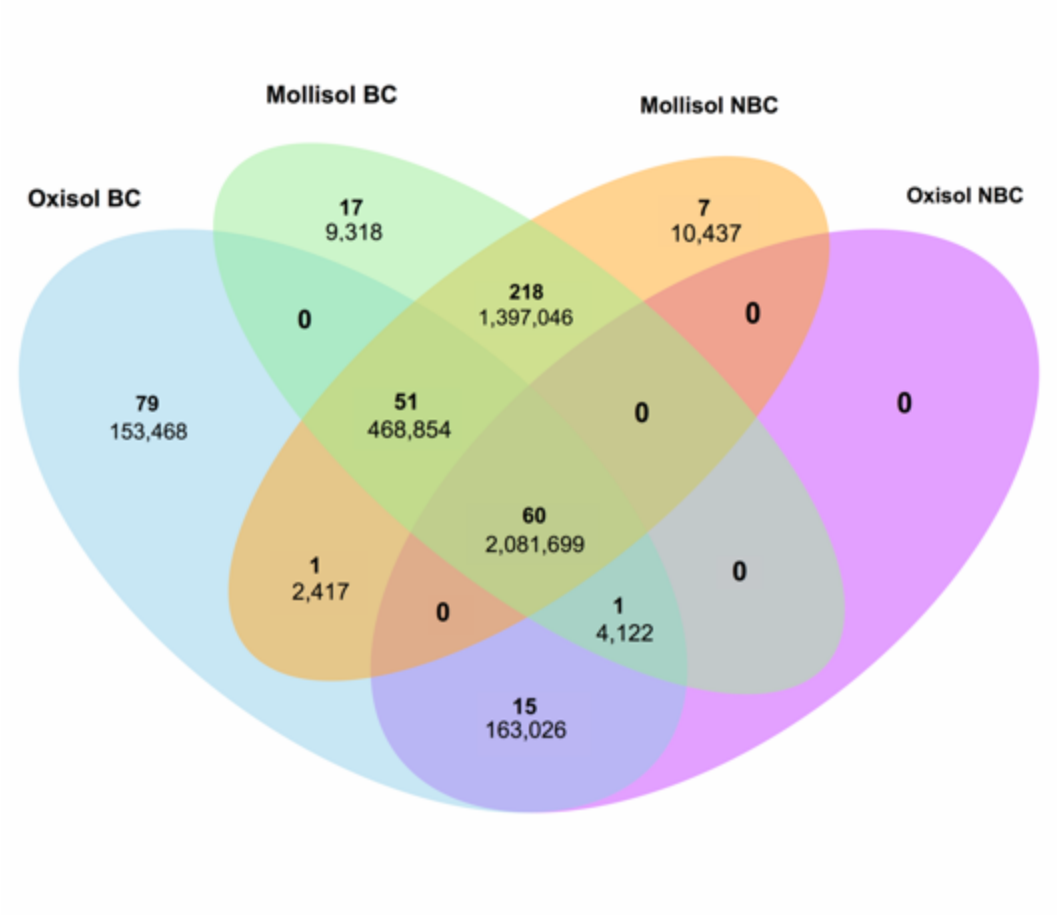


Figure A5. Venn diagram of unique and shared OTUs shared by soil type and biochar treatment. The top number is the OTU count and bottom number is the corresponding number of sequences. OTUs were included at a stringent cutoff of 90% occurrence among replicates within each group, reducing the dataset to 449 OTUs encompassing 4,290,387 sequences (66.9% of the non-singleton/doubleton dataset).

Table A1. Mean values and standard error of measured soil chemical properties.

Soil Type	Time	Treat	pH	Ca mg kg^{-1}	Na mg kg^{-1}	K mg kg^{-1}	Mg mg kg^{-1}	Water	%C	%N
Oxisol	Pre-Plant	Nap-BC	6.84 ± 0.18	1624.3 ± 170.1	ND	352.1 ± 25.1	127.2 ± 4.9	33.5 ± 1.6	1.76 ± 0.04	0.17 ± 0.002
		Nap-NBC	6.61 ± 0.27	2125.1 ± 471.6	ND	275.3 ± 32.8	111.0 ± 3.7	34.0 ± 1.3	1.26 ± 0.02	0.16 ± 0.002
		Corn-BC	6.40 ± 0.21	1822.7 ± 233.6	115.7 ± 8.7	439.8 ± 26.6	108.0 ± 3.3	ND	1.95 ± 0.06	0.19 ± 0.001
		Corn-NBC	6.36 ± 0.10	2077.8 ± 152.0	110.4 ± 4.8	400.6 ± 24.0	111.8 ± 3.5	ND	1.43 ± 0.02	0.19 ± 0.003
		Bare-BC	6.74 ± 0.16	1462.2 ± 203.2	ND	235.1 ± 13.9	105.5 ± 4.9	35.3 ± 3.8	2.24 ± 0.01	0.21 ± 0.001
		Bare-NBC	6.41 ± 0.25	1528.5 ± 226.5	105.6 ± 0.0	322.4 ± 5.6	116.2 ± 2.6	29.2 ± 1.2	1.55 ± 0.02	0.19 ± 0.001
	Pre-Harvest	Nap-BC	6.75 ± 0.12	1598.78 ± 140.31	116.00 ± 2.70	548.28 ± 41.13	238.19 ± 24.36	23.52 ± 0.29	1.96 ± 0.07	0.17 ± 0.002
		Nap-NBC	6.86 ± 0.13	1750.82 ± 141.81	121.23 ± 10.39	590.02 ± 62.92	175.55 ± 21.81	22.92 ± 0.55	1.20 ± 0.01	0.15 ± 0.002
		Corn-BC	6.22 ± 0.15	1203.76 ± 61.97	117.35 ± 6.58	715.56 ± 60.13	183.02 ± 9.43	34.45 ± 0.65	1.77 ± 0.05	0.17 ± 0.005
		Corn-NBC	6.11 ± 0.14	1212.68 ± 36.57	126.17 ± 9.43	644.34 ± 42.19	177.23 ± 21.38	34.87 ± 0.52	1.26 ± 0.02	0.16 ± 0.003
		Bare-BC	6.71 ± 0.04	1478.82 ± 144.16	173.51 ± 10.16	349.80 ± 17.13	283.32 ± 41.38	25.28 ± 0.03	1.94 ± 0.004	0.18 ± 0.001
		Bare-NBC	6.06 ± 0.36	1116.99 ± 207.71	124.75 ± 0.85	421.79 ± 8.49	205.91 ± 17.20	23.90 ± 1.41	1.41 ± 0.007	0.18 ± 0.00
Mollisol	Pre-Plant	Nap-BC	6.03 ± 0.06	4420.2 ± 80.9	126.5 ± 4.5	488.3 ± 21.7	688.9 ± 13.5	35.4 ± 1.0	2.23 ± 0.08	0.17 ± 0.001
		Nap-NBC	6.07 ± 0.08	4270.3 ± 80.4	118.6 ± 3.8	471.4 ± 26.4	646.6 ±18.8	30.4 ± 1.8	1.42 ± 0.02	0.17 ± 0.004
		Corn-BC	6.54 ± 0.17	4531.3 ± 116.1	116.2 ± 4.0	543.5 ± 17.1	683.7 ± 17.9	ND	2.09 ± 0.07	0.18 ± 0.003
		Corn-NBC	6.28 ± 0.15	4517.6 ± 115.6	102.2 ± 2.3	566.7 ± 44.4	665.1 ± 7.9	ND	1.46 ± 0.02	0.17 ± 0.004
		Bare-BC	5.93 ± 0.12	4460.4 ± 45.7	124.3 ± 6.2	466.0 ± 2.3	697.1 ± 14.6	ND	2.05 ± 0.02	0.18 ± 0.00
		Bare-NBC	5.93 ± 0.14	4672.6 ± 0.0	123.8 ± 3.2	521.8 ± 23.8	754.0 ± 11.9	ND	1.59 ± 0.02	0.18 ± 0.001
	Pre-Harvest	Nap-BC	6.78 ± 0.04	3865.57 ± 83.00	153.16 ± 3.39	933.23 ± 86.47	1420.36 ± 27.23	34.77 ± 0.97	2.73 ± 0.07	0.16 ± 0.002
		Nap-NBC	6.82 ± 0.05	3925.94 ± 41.46	155.33 ± 2.98	820.69 ± 83.68	1479.63 ± 25.06	32.62 ± 1.86	1.39 ± 0.03	0.15 ± 0.002
		Corn-BC	6.71 ± 0.05	4058.92 ± 80.31	180.87 ± 7.83	1063.24 ± 67.39	1489.85 ± 20.69	34.26 ± 1.11	1.69 ± 0.02	0.15 ± 0.001
		Corn-NBC	6.79 ± 0.18	4030.82 ± 154.09	183.16 ± 12.47	1206.47 ± 231.17	1409.77 ± 47.22	32.17 ± 1.98	1.21 ± 0.02	0.14 ± 0.002
		Bare-BC	6.71 ± 0.10	4096.57 ± 40.34	156.63 ± 25.31	874.79 ± 77.60	1615.37 ± 67.17	35.92 ± 2.41	1.82 ± 0.03	0.16 ± 0.001
		Bare-NBC	6.83 ± 0.19	3675.00 ± 5.00	141.10 ± 5.30	878.00 ± 124.00	1489.00 ± 23.00	37.19 ± 1.59	1.45 ± 0.03	0.15 ± 0.004

Treat: treatment; Ca: calcium; Na: sodium; K: potassium; Mg: magnesium; C: carbon; N: nitrogen; ND: not determined

Table A2. Permutational ANOVA (PERMANOVA) of microbial community between soil, cropping system, sampling period, biochar treatment, and the interactions.

Factors						
Name	Abbrev.	Type	Levels			
Site	Si	Fixed	2			
Crop	Cr	Fixed	3			
Time	Ti	Fixed	2			
Treatment	Tr	Fixed	2			
Source	df	SS	MS	Pseudo-F	P(perm)	Unique perms
Si	1	1.10E+05	1.10E+05	79.764	0.001	999
Cr	2	25410	12705	9.1992	0.001	995
Ti	1	24097	24097	17.448	0.001	996
Tr	1	2726.4	2726.4	1.974	0.019	998
SixCr	2	15280	7640.1	5.5319	0.001	999
SixTi	1	12939	12939	9.3686	0.001	998
SixTr	1	2785.2	2785.2	2.0167	0.018	998
CrxTi	2	31491	15746	11.401	0.001	998
CrxTr	2	5028.6	2514.3	1.8205	0.009	995
TixTr	1	2122.1	2122.1	1.5365	0.066	998
SixCrxTi	2	18676	9337.9	6.7612	0.001	997
SixCrxTr	2	5551.6	2775.8	2.0098	0.003	996
SixTixTr	1	2441.8	2441.8	1.768	0.041	999
CrxTixTr	2	3499.7	1749.8	1.267	0.111	995
SixCrxTixTr	2	3317.6	1658.8	1.2011	0.155	999
Res	459	6.34E+05	1381.1			
Total	482	1.00E+06				

Table A3. ANOVA table of aligned rank transformed diversity indices according to soil type, biochar treatment, cropping system, and sampling time.
[1]Significance is denoted by asterisks, *** (p <0.001), ** (p <0.01), *(p<0.05).

Variables	**Margalef's Richness**		**Pielou's Evenness**		**Shannon Diversity**	
	F-value	p-value	F-value	p-value	F-value	p-value
Site	190.64	<2.22E-16***	242.40	<2.20E-16***	216.23	<2.20E-16***
Biochar	0.58	0.45	1.53	0.22	0.79	0.38
Crop	34.34	1.27E-14***	5.68	3.65E-03**	33.93	1.81E-14***
Time	126.06	<2.22E-16***	112.21	<2.20E-16***	144.75	<2.20E-16***
Site:Biochar	6.91	8.86E-03**	0.74	0.39	7.40	6.78E-03**
Site:Crop	0.76	0.47	1.25	0.29	0.56	0.57
Biochar:Crop	16.41	1.31E-07***	7.68	5.23E-04***	16.65	1.04E-07***
Site:time	7.83	5.35E-0.3**	13.97	2.09E-04***	15.26	1.08E-04***
Biochar:time	5.28	0.02*	14.43	1.65E-04***	8.37	3.99E-03**
Crop:Time	118.13	<2.22E-16***	64.50	<2.20E-16***	114.23	<2.20E-16***
Site:Biochar:Crop	1.38	0.25	3.61	0.03*	2.22	0.11
Site:Biochar:Time	1.71	0.19	8.35	4.05E-03**	3.97	0.04*
Site:Crop:Time	1.05	0.35	7.25	7.91E-04***	0.32	0.73
Biochar:Crop:Time	1.24	0.29	0.82	0.44	1.38	0.25
Site:Biochar:Crop:Time	0.14	0.87	5.19	5.93E-03**	0.13	0.87

Table A4. Permutational dispersion (PERMDISP) test of homogeneity of dispersion with corresponding t-test results comparing biochar and no biochar treatments under each crop/soil type group.

		Pre-Plant		Pre-Harvest	
Soil Type	Treat	Mean	T-test	Mean	T-test
Oxisol	Nap-BC	33.0 ± 0.6	**T=5.44 p=0.001**	34.0 ± 0.5	**T= 5.57 p=0.002**
	Nap-NBC	38.4 ± 0.8		39.0 ± 0.5	
	Corn-BC	39.5 ± 0.6	T=0.13 p=0.897	38.6 ± 0.5	**T=2.65 p= 0.014**
	Corn-NBC	39.4 ± 0.7		37.1 ± 0.3	
	Bare-BC	22.9 ± 0.4	**T=2.89 p=0.032**	33.7 ± 0.4	T= 1.32 p= 0.164
	Bare-NBC	29.6 ± 1.6		34.6 ± 0.6	
Mollisol	Nap-BC	30.6 ± 0.6	**T=2.65 p=0.019**	35.8 ± 0.6	T= 0.46 p= 0.738
	Nap-NBC	32.8 ± 0.6		35.4 ± 0.5	
	Corn-BC	37.9 ± 0.5	**T=2.26 p=0.038**	36.0 ± 1.0	T= 1.56 p= 0.196
	Corn-NBC	36.3 ± 0.4		38.2 ± 0.8	
	Bare-BC	27.7 ± 0.6	T=1.09 p=0.253	35.3 ± 1.4	T= 1.51 p= 0.681
	Bare-NBC	28.6 ± 0.6		31.5 ± 0.9	

Nap: Napier; BC: Biochar; NBC: No biochar

Table A5. Detailed lineage for module hubs and connectors from Figure 2.2. Lineage is based on 97% similarity to references in the 2013 Greengenes database. In order from left to right are class, order, family and genus classification.

Classification	Treat	OTU	Lineage
Network Hubs	Oxisol-BC	1121483	Actinobacteria, Actinomycetales
	Mollisol-NBC	614944	Gammaproteobacteria, Xanthomonadales, Xanthomonadaceae
Module Hubs	Oxisol-BC	1105814	Alphaproteobacteria, Rhizobiales, Bradyrhizobiaceae, Bradyrhizobium
		1014728	Sphingobacteriia, Sphingobacteriales, Sphingobacteriaceae
		637184	Acidobacteria-6, iii1-15
		338196	iii1-8, DS-18
		566964	0319-6E2
	Oxisol-NBC	2714250	Acidobacteria-6, iii1-15
		156976	iii1-8, DS-18
		209467	iii1-8, DS-18
		705844	TK10, B07_WMSP1
	Mollisol-BC	614944	Gammaproteobacteria, Xanthomonadales, Xanthomonadaceae
		654742	Alphaproteobacteria, Sphingomonadales, Sphingomonadaceae, Kaistobacter
		728640	Acidobacteria-6, iii1-15
		4389260	Planctomycetia, Gemmatales, Gemmataceae, Gemmata
		637184	Acidobacteria-6, iii1-15
		1834768	Gammaproteobacteria, Xanthomonadales, Xanthomonadaceae, Stenotrophomonas
		892000	Acidobacteria-6, iii1-15
	Mollisol-NBC	717396	Acidobacteria-6, iii1-15
		1669790	0319-6E2
		313245	Acidobacteria-6, iii1-15
Connectors	Oxisol-BC	646107	[Chloracidobacteria], PK29
		4276843	BRC1, PRR-11
		4293581	Acidobacteria-6, iii1-15, mb2424
		848824	Sphingobacteriia, Sphingobacteriales, Sphingobacteriaceae
		4442148	Acidobacteria-6, iii1-15
		725677	Planctomycetia, Pirellulales, Pirellulaceae, Pirellula
		113500	Acidobacteria-6, iii1-15, mb2424
		1126307	Acidimicrobiia, Acidimicrobiales
		250522	Alphaproteobacteria, Rhizobiales
		226049	Solibacteres, Solibacterales, Solibacteraceae, CandidatusSolibacter
		1068902	Actinobacteria, Actinomycetales, Nocardioidaceae, Aeromicrobium
		816631	Acidobacteria-6, iii1-15
		565399	[Saprospirae], [Saprospirales], Chitinophagaceae, Chitinophagaceae
		219282	Betaproteobacteria, Ellin6067
		735782	[Chloracidobacteria], RB41
		1044436	Deltaproteobacteria, Syntrophobacterales, Syntrophobacteraceae
		706798	Actinobacteria, Actinomycetales, Pseudonocardiaceae, Saccharopolyspora
		1038865	Sphingobacteriia, Sphingobacteriales, Sphingobacteriaceae
		1105574	Betaproteobacteria, Burkholderiales, Oxalobacteraceae
		367606	[Chloracidobacteria], 11-24
		128177	Ellin6529
		1064235	Planctomycetia, Planctomycetales, Planctomycetaceae, Planctomyces

	217349	BD7-11
	647619	Thaumarchaeota, Nitrososphaerales, Nitrososphaeraceae, CandidatusNitrososphaera
	246619	Planctomycetia, Planctomycetales, Planctomycetaceae, Planctomyces
	541741	Acidobacteria-6, iii1-15
	855996	Gemmatimonadetes, N1423WL
	112952	Ellin6529
	993307	Planctomycetia, Pirellulales, Pirellulaceae, Pirellula
	547110	Phycisphaerae, WD2101
	247867	Phycisphaerae, WD2101
	587032	Planctomycetia, Gemmatales, Gemmataceae
Mollisol-BC	1111883	Gemm-1
Mollisol-NBC	940737	Betaproteobacteria, Burkholderiales, Comamonadaceae
	222350	Alphaproteobacteria, Rhizobiales, Hyphomicrobiaceae, Rhodoplanes
	839513	Chthonomonadetes, SJA-22
	151011	Planctomycetia, Gemmatales, Gemmataceae
	654742	Alphaproteobacteria, Sphingomonadales, Sphingomonadaceae, Kaistobacter
	1105574	Betaproteobacteria, Burkholderiales, Oxalobacteraceae
	816631	Acidobacteria-6, iii1-15
	131339	Anaerolineae, SBR1031, A4b
	213829	MB-A2-108

Table A6. Network properties of 100 randomized networks of the Oxisol and Mollisol control and biochar networks.

	Oxisol Control	**Oxisol Biochar**	**Mollisol Control**	**Mollisol Biochar**
Network Indexes	100 Random Networks Indexes	100 Random Networks Indexes	100 Random Networks Indexes	100 Random Networks Indexes
Average clustering coefficient (avgCC)	0.067 +/- 0.014	0.069 +/- 0.012	0.042 +/- 0.010	0.048 +/- 0.008
Average path distance (GD)	3.274 +/- 0.050	3.331 +/- 0.044	3.805 +/- 0.073	3.698 +/- 0.051
Geodesic efficiency (E)	0.347 +/- 0.004	0.337 +/- 0.003	0.296 +/- 0.004	0.301 +/- 0.003
Harmonic geodesic distance (HD)	2.881 +/- 0.032	2.971 +/- 0.031	3.378 +/- 0.045	3.323 +/- 0.034
Centralization of degree (CD)	0.184 +/- 0.000	0.146 +/- 0.000	0.174 +/- 0.000	0.129 +/- 0.000
Centralization of betweenness (CB)	0.230 +/- 0.028	0.167 +/- 0.017	0.332 +/- 0.030	0.206 +/- 0.022
Centralization of stress centrality (CS)	0.694 +/- 0.087	0.591 +/- 0.064	0.918 +/- 0.112	0.649 +/- 0.082
Centralization of eigenvector centrality (CE)	0.317 +/- 0.026	0.278 +/- 0.023	0.458 +/- 0.017	0.325 +/- 0.022
Density (D)	0.031 +/- 0.000	0.024 +/- 0.000	0.013 +/- 0.000	0.013 +/- 0.000
Reciprocity	1.000 +/- 0.000	1.000 +/- 0.000	1.000 +/- 0.000	1.000 +/- 0.000
Transitivity (Trans)	0.067 +/- 0.011	0.076 +/- 0.009	0.045 +/- 0.007	0.052 +/- 0.006
Connectedness (Con)	0.956 +/- 0.032	0.956 +/- 0.028	0.886 +/- 0.036	0.922 +/- 0.028
Efficiency	0.975 +/- 0.001	0.981 +/- 0.001	0.990 +/- 0.000	0.990 +/- 0.000
Hierarchy	0.000 +/- 0.000	0.000 +/- 0.000	0.000 +/- 0.000	0.000 +/- 0.000
Lubness	1.000 +/- 0.000	1.000 +/- 0.000	1.000 +/- 0.000	1.000 +/- 0.000
Modularity (Leading Eigenvector)	0.441 +/- 0.009	0.425 +/- 0.008	0.553 +/- 0.008	0.515 +/- 0.007

APPENDIX B

CROP DATA, METAGENOMIC STATISTICS AND RESULTS SUPPORTING FINDS OF CHAPTER 4

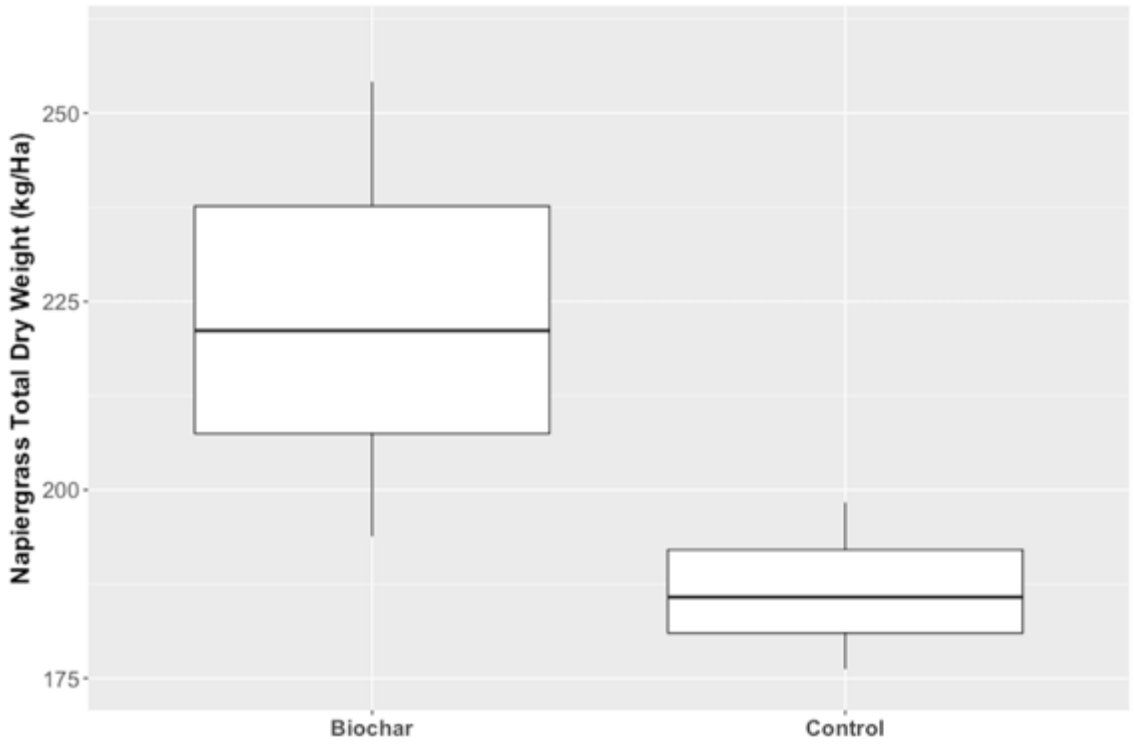


Figure B1. Boxplots representing napiergrass crop yield harvested December 2015. The median of the four replicate plots is marked by the bold bars; the first and third quartile are represented by the upper and lower boundaries of the boxes; the upper and lower whiskers represent the 1.5 interquartile range.

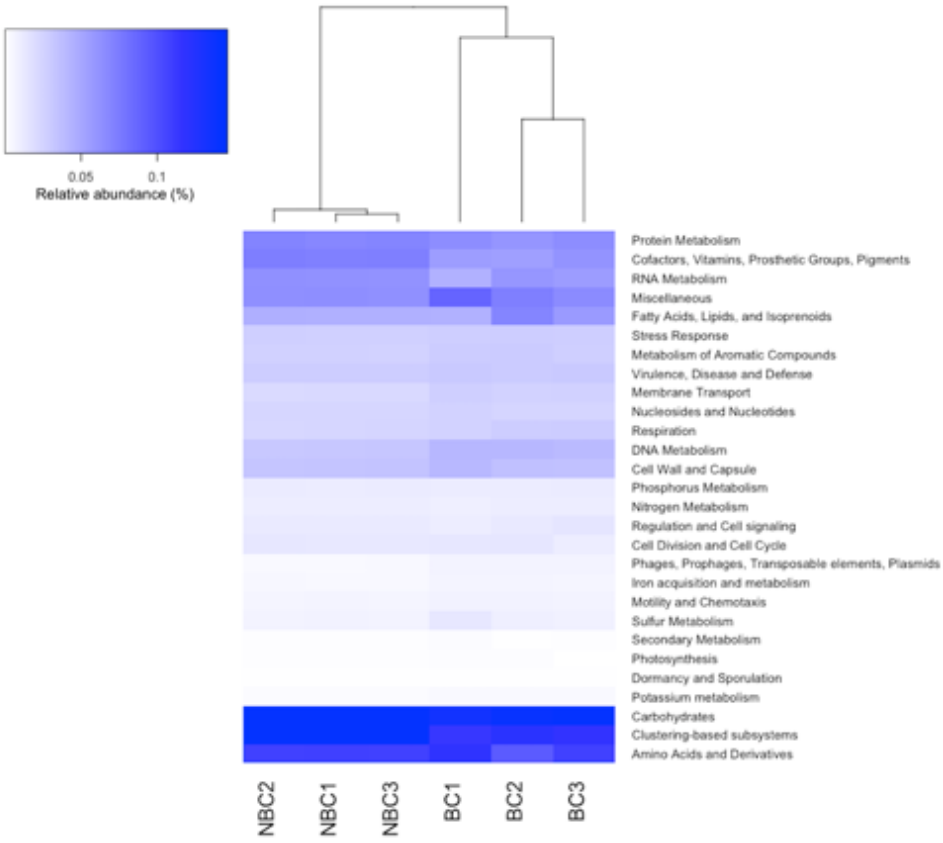


Figure B2. Clustering of samples and replicates based on SEED subsystem relative abundance. Each column represents a sample and each row represents a level 1 SEED subsystem. The abundance of the subsystems, normalized by the total number of reads in the sample, is represented by the color intensity. Clustering was carried out to group samples using Euclidean distance.

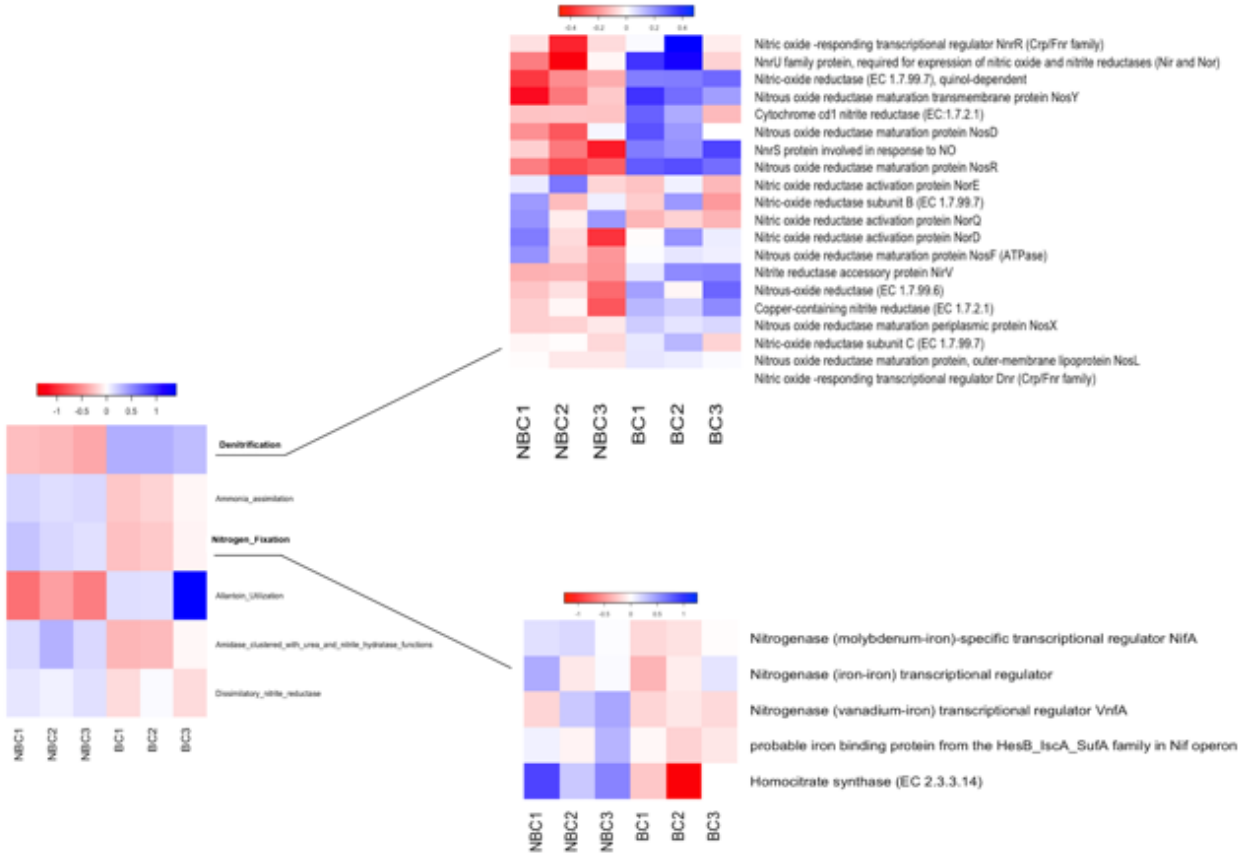


Figure B3. Significant changes in abundance of select pathways related to N metabolism. The heatmap to the left represents the change in abundance at the level-3 subsystem classification (rows) for each microcosm metagenome (columns). Heatmaps on the right represent $\log_2$(biochar/control) at the function-level (rows) for the denitrification pathway (top-right) and nitrogen fixation pathway (bottom-right). Color code is based on the magnitude of change and scale values indicate the $\log_2$-fold change (see scale on the top of each heatmap).

Table B1. Sequencing and assembly statistics for each soil metagenome. Samples were sequenced on the Illumina NextSeq-500 instrument. Sample replicates are the same library sequenced on independent lanes of the Illumina instrument, i.e. technical replicates.

Sample	Size (x 10^6)		Merged	Assembly[a]			Taxonomic Composition (%)				
	Raw	Trimmed		# Contigs (Kbp)	N_{50}	Largest Contig (Kbp)	Bacterial	Archaeal	Eukaryotic	Viral	Unclassified
NBC1.rep1	13.02	11.85	NBC1	445	931	73.1	99.03	0.46	0.36	0.02	0.13
NBC1.rep2	13.15	11.93									
NBC1.rep3	12.92	11.70									
NBC1.rep4	12.73	11.39									
NBC2.rep1	12.01	10.97	NBC2	374	908	66.9	98.93	0.48	0.44	0.02	0.13
NBC2.rep2	12.11	11.02									
NBC2.rep3	11.89	10.81									
NBC2.rep4	11.74	10.57									
NBC3.rep1	12.62	11.51	NBC3	380	905	68.2	99.69	0.53	0.63	0.03	0.12
NBC3.rep2	12.66	11.50									
NBC3.rep3	12.50	11.34									
NBC3.rep4	12.42	11.17									
BC1.rep1	45.94	41.92	BC1	2542	1188	736	99.05	0.27	0.53	0.04	0.10
BC1.rep2	46.11	41.96									
BC1.rep3	45.47	41.31									
BC1.rep4	45.60	40.95									
BC2.rep1	49.10	44.98	BC2	2708	1206	675	99.08	0.28	0.50	0.04	0.10
BC2.rep2	49.60	45.26									
BC2.rep3	48.61	44.31									
BC2.rep4	48.53	43.79									
BC3.rep1	15.34	14.02	BC3	789	1005	163	99.09	0.27	0.50	0.04	0.09
BC3.rep2	15.51	14.13									
BC3.rep3	15.20	13.82									
BC3.rep4	15.27	13.74									

[a] Statistics reported are based on contigs longer than 500bp

Table B2. Statistics of metagenomes analyzed through MG-RAST

Characteristics	BC1	BC2	BC3	NBC1	NBC2	NBC3
# Sequences (1E+6)	6.90	7.41	2.44	1.78	1.61	1.78
Avg. Length (bp)	649	650	573	538	523	519
# QC failed seqs (1E+3)	750 (10.9%)	816 (11.0%)	270 (11.1%)	186 (10.5%)	168 (10.4%)	185 (10.3%)
# rRNA gene seqs	6,158	6,432	2,341	1,737	1,801	1,998
# seqs w/ predicted proteins of known function (1E+6)	4.46 (72.5%)	4.78 (72.5%)	1.57 (72.5%)	1.15 (72.1%)	1.03 (71.1%)	1.12 (70.0%)
# seqs w/ predicted proteins of unknown function (1E+6)	1.68 (27.4%)	1.81 (27.5%)	0.595 (27.4%)	0.441 (27.8%)	0.415 (28.8%)	0.478 (29.9%)

Table B3. Alpha diversity estimates of samples used in this study based on rRNA gene-encoded reads.

	Genus		
Sample	Margalef's Richness	Pielou's Evenness	Shannon Diversity
NBC1	40.17	0.7619	4.853
NBC2	40.57	0.7652	4.876
NBC3	40.38	0.7699	4.907
BC1	37.04	0.7860	5.015
BC2	37.00	0.7859	5.017
BC3	39.38	0.7789	4.963
Paired t-test	T = -3.24 p-value = 0.08334	T=3.90 p-value = 0.06	T= 3.68 p-value = 0.067

Table B4. Differentially abundant SEED subsystems (levels 1 – 3) between biochar-amended and control metagenomes.

Level 1	Level 2	Level 3	Mean number of reads	Enriched Group	Log2 fold change	P-value (B-H adjusted)
Amino Acids and Derivatives	Arginine; urea cycle, polyamines	Putrescine_utilization_pathways	1299.53	Control	0.726	3.88E-11
		Arginine_Deiminase_Pathway	651.47	Control	0.378	4.45E-02
	Branched-chain amino acids	HMG_CoA_Synthesis	4927.93	Control	1.891	1.26E-123
		Branched-Chain_Amino_Acid_Biosynthesis	8759.65	Control	0.731	4.93E-27
		Leucine_Degradation_and_HMG-CoA_Metabolism	11395.04	Biochar	1.428	2.84E-18
		Valine_degradation	17325.37	Biochar	1.919	1.58E-02
	Glutamine, glutamate, aspartate, asparagine; ammonia assimilation	Aspartate_aminotransferase	61.95	Control	0.681	3.11E-02
	Histidine Metabolism	Histidine_Degradation	4329.11	Control	0.266	3.53E-03
	Lysine, threonine, methionine, and cysteine	Threonine_and_Homoserine_Biosynthesis	14081.27	Control	0.263	5.20E-11
	NULL	Creatine_and_Creatinine_Degradation	5615.85	Control	0.248	2.77E-04
Carbohydrates	Central carbohydrate metabolism	Ethylmalonyl-CoA_pathway_of_C2_assimilation	1036.75	Control	0.577	1.53E-08
		Dehydrogenase_complexes	6969.69	Control	1.277	4.48E-05
		Methylglyoxal_Metabolism	8801.06	Control	0.203	1.45E-02
		Soluble_methane_monooxygenase_(sMMO)	87.87	Control	0.741	1.59E-02
	CO2 fixation	Photorespiration_(oxidative_C2_cycle)	10773.93	Control	0.471	6.91E-07
		CO2_uptake,_carboxysome	250.03	Biochar	0.429	1.46E-02
		Carboxysome	2180.14	Biochar	0.175	3.90E-02
		Melibiose_Utilization	737.81	Biochar	4.637	2.03E-04

	Di- and oligosaccharides	Sucrose_utilization	47.73	Biochar	2.333	1.58E-02
	Fermentation	Butanol_Biosynthesis	33362.06	Control	0.374	1.77E-05
		Fermentations:_Lactate	1654.25	Control	0.227	1.24E-02
	Monosaccharides	Fructose_utilization	1470.30	Biochar	1.273	6.32E-117
		2-Ketogluconate_Utilization	68.63	Biochar	1.121	6.64E-05
		Hexose_Phosphate_Uptake_System	69.56	Biochar	1.418	1.30E-04
		D-gluconate_and_ketogluconates_metabolism	2199.28	Control	0.248	4.17E-04
		L-rhamnose_utilization	3348.06	Control	0.510	1.30E-03
		D-galactonate_catabolism	459.79	Biochar	0.451	1.98E-02
		L-Arabinose_utilization	2835.62	Biochar	0.501	3.67E-02
	NULL	VC0266	31.64	Biochar	0.762	2.33E-02
	One-carbon Metabolism	One-carbon_metabolism_by_tetrahydropterines	2570.48	Control	0.323	3.83E-04
	Organic acids	Malonate_decarboxylase	45.62	Biochar	1.780	2.23E-07
		Methylcitrate_cycle	472.06	Biochar	1.319	2.66E-04
	Polysaccharides	Glycogen_metabolism	1405.53	Biochar	2.769	9.86E-08
		Cellulosome	233.21	Biochar	0.692	1.86E-03
	Sugar alcohols	Ethanolamine_utilization	468.55	Biochar	0.360	5.13E-05
		Inositol_catabolism	2395.04	Control	0.251	1.04E-04
		Mannitol_Utilization	306.69	Control	0.342	7.59E-03
Cell Wall and Capsule	Capsular and extracellular polysacchrides	Capsular_Polysaccharide_(CPS)_of_Campylobacter	51.01	Biochar	5.969	5.85E-12
		Vibrio_Polysaccharide_(VPS)_Biosynthesis	602.20	Biochar	2.450	6.50E-04
		Xanthan_Exopolysaccharide_Biosynthesis_and_Export	34.68	Biochar	1.122	1.35E-03

		dTDP-rhamnose_synthesis	1764.78	Control	0.528	4.58E-03
		Pseudaminic_Acid_Biosynthesis	45.26	Biochar	0.886	5.54E-03
		Capsular_heptose_biosynthesis	1100.76	Biochar	1.007	4.20E-02
	Cell wall of Mycobacteria	mycolic_acid_synthesis	4482.82	Biochar	2.709	4.57E-03
	Gram-Negative cell wall components	Lipopolysaccharide_assembly	786.63	Biochar	1.405	2.39E-68
		Outer_membrane	807.61	Biochar	0.737	2.24E-03
		Lipid_A_modifications	112.41	Biochar	1.046	4.83E-03
	NULL	Peptidoglycan_Biosynthesis	21068.14	Control	0.572	4.36E-05
		Recycling_of_Peptidoglycan_Amino_Sugars	262.80	Biochar	1.394	9.66E-03
Clustering-based subsystems	Carbohydrates	Putative_sugar_ABC_transporter_(ytf_cluster)	80.91	Biochar	2.951	1.16E-05
	Catabolism of an unknown compound	CBSS-262316.1.peg.2929	1044.04	Control	1.056	1.65E-19
	Choline bitartrate degradation, putative	CBSS-344610.3.peg.2335	3902.65	Control	0.263	2.28E-04
	Clustering-based subsystems	Putative_diaminopropionate_ammonia-lyase_cluster	3706.99	Biochar	0.541	6.28E-06
	CRISPRs and associated hypotheticals	CBSS-216592.1.peg.3534	28.30	Biochar	3.118	4.38E-03
	Cytochrome biogenesis	CBSS-196164.1.peg.1690	6484.47	Control	0.283	1.10E-03
		CBSS-196164.1.peg.461	4484.78	Control	0.160	1.71E-02
	Fatty acid metabolic cluster	CBSS-246196.1.peg.364	11806.19	Control	6.270	0.00E+00
		COG1399	8379.16	Biochar	0.393	3.72E-03
	Flagella protein?	CBSS-323098.3.peg.2823	41.70	Biochar	0.824	3.06E-02
	Hypothetical associated with RecF	Hypothetical_Coupled_to_RecF	350.67	Biochar	3.535	6.23E-03

	Hypothetical lipase related to Phosphatidate metabolism	CBSS-316407.3.peg.1371	289.78	Biochar	3.338	1.28E-51
	Isoprenoid/cell wall biosynthesis: PREDICTED UNDECAPRENYL DIPHOSPHATE PHOSPHATASE	CBSS-83331.1.peg.3039	3321.63	Biochar	2.910	8.33E-54
	Lysine, threonine, methionine, and cysteine	CBSS-84588.1.peg.1247	676.20	Biochar	1.750	9.31E-18
		YeiH	85.71	Biochar	1.343	6.60E-11
	Methylamine utilization	Glutamate-mediated_methylamine_utilization_pathway	2530.03	Control	0.161	1.80E-02
	Monosaccharides	Unspecified_monosaccharide_transport_cluster	366.81	Control	0.876	2.01E-02
	NULL	CBSS-196620.1.peg.2477	4339.69	Control	5.863	2.36E-180
		Butyrate_metabolism_cluster	8024.87	Control	14.630	1.06E-100
		CBSS-211586.1.peg.3133	334.67	Control	2.739	5.01E-85
		CBSS-83333.1.peg.946	775.54	Biochar	2.441	1.36E-79
		CBSS-342610.3.peg.1794	396.11	Biochar	6.732	5.51E-61
		CBSS-316273.3.peg.2709	287.91	Control	6.848	9.85E-46
		EC49-61	1520.37	Biochar	2.544	1.33E-34
		CBSS-288681.3.peg.1039	405.16	Biochar	9.151	2.93E-27
		CBSS-314269.3.peg.1840	7095.49	Control	0.560	5.60E-26
		Putative_sulfate_assimilation_cluster	165.52	Control	2.788	1.05E-23
		Cell_division-ribosomal_stress_proteins_cluster	7651.05	Control	2.596	6.50E-18
		CBSS-176299.4.peg.1996B	5088.37	Control	0.584	1.49E-16

		Cluster_co-expressed_with_butyrate_metabolism_cluster	98.00	Biochar	7.464	2.85E-16
		CBSS-312309.3.peg.1965	1341.45	Control	0.871	3.05E-16
		CBSS-176280.1.peg.1561	847.89	Biochar	2.273	9.38E-15
		CBSS-138119.3.peg.2719	77.29	Biochar	7.173	1.12E-14
		CBSS-316273.3.peg.448	874.06	Biochar	0.995	5.08E-13
		Cluster_with_phosphopentomutase_paralog	940.80	Control	0.585	8.31E-11
		CBSS-393124.3.peg.2657	1329.38	Control	0.765	4.69E-10
		CBSS-290633.1.peg.1906	247.46	Biochar	0.852	6.19E-10
		USS-DB-6	138.58	Biochar	0.850	2.36E-08
		Bacterial_Cell_Division	8536.99	Biochar	0.957	5.48E-07
		CBSS-257314.1.peg.752	1027.13	Biochar	4.978	1.80E-06
		CBSS-316273.3.peg.2378	100.85	Biochar	1.254	3.62E-06
		Aerotolerance_operon_in_Bacteroides_and_potentially_orthologous_operons_in_other_organisms	606.67	Biochar	0.453	4.64E-06
		CBSS-630.2.peg.3360	1301.26	Biochar	0.347	6.01E-06
		CBSS-316273.3.peg.227	966.84	Control	1.535	7.08E-06
		Cluster_containing_CofD-like_protein_and_co-occuring_with_DNA_repair	223.79	Control	0.651	9.49E-06
		Bacterial_RNA-metabolizing_Zn-dependent_hydrolases	9208.80	Control	0.187	2.69E-04
		DNA_gyrase_subunits	4799.47	Control	0.398	3.08E-04
		CBSS-316057.3.peg.3521	1467.33	Biochar	0.199	3.83E-04
		CBSS-176279.3.peg.1262	94.40	Control	0.936	6.15E-04
		Glutaredoxin_3_containing_cluster	114.15	Biochar	3.619	1.47E-03
		CBSS-176279.3.peg.868	4102.88	Control	0.372	1.71E-03
		CBSS-316407.3.peg.2816	71.30	Biochar	0.769	2.73E-03

		LMPTP_YwlE_cluster	2368.55	Biochar	3.003	3.09E-03
		CBSS-235.1.peg.567	5177.42	Control	0.175	3.83E-03
		Conjugative_transfer_related_cluster	858.84	Control	0.649	4.03E-03
		CBSS-316273.3.peg.922	108.06	Biochar	0.805	6.89E-03
		Conserved_gene_cluster_associated_with_Met-tRNA_formyltransferase	9709.53	Control	0.381	1.50E-02
		CBSS-160492.1.peg.550	43.82	Biochar	1.022	3.79E-02
		Glutaredoxin_3_containing_cluster_2	253.42	Biochar	0.873	4.11E-02
	Protein export?	CBSS-393121.3.peg.2760	4052.62	Control	1.198	1.01E-110
	proteosome related	Cluster-based_Subsystem_Grouping_Hypotheticals_-_perhaps_Proteosome_Related	1464.92	Control	0.421	8.92E-14
	Putrescine/GABA utilization cluster-temporal,to add to SSs	GABA_and_putrescine_metabolism_from_cluters	2607.13	Control	0.939	1.82E-02
	Recombination related cluster	CBSS-198094.1.peg.4426	505.27	Control	2.698	7.05E-65
	Ribosomal Protein L28P relates to a set of uncharacterized proteins	A_Gram-positive_cluster_that_relates_ribosomal_protein_L28P_to_a_set_of_uncharacterized_proteins	686.90	Biochar	1.479	1.89E-03
	Ribosome-related cluster	A_Gammaproteobacteria_Cluster_Relating_to_Translation	6137.52	Control	1.392	2.66E-02
	Sarcosine oxidase	Sarcosine_oxidase_subunits	102.29	Control	8.947	4.93E-27
	Sulfatases and sulfatase modifying factor 1 (and a hypothetical)	Sulfatases_and_sulfatase_modifying_factor_1	533.69	Biochar	0.668	3.50E-03
	TldD cluster	CBSS-354.1.peg.2917	1765.06	Biochar	0.928	1.57E-34

	Translation	CBSS-243265.1.peg.198	927.41	Control	1.695	6.20E-29
		CBSS-326442.4.peg.1852	3400.22	Control	0.331	2.19E-02
	Tricarboxylate transporter	CBSS-49338.1.peg.459	5518.17	Control	0.344	4.61E-05
Cofactors, Vitamins, Prosthetic Groups, Pigments	Biotin	Biotin_biosynthesis	1921.05	Biochar	1.234	7.34E-114
	Folate and pterines	YgfZ	42127.81	Control	0.730	6.59E-09
		YgfZ-Iron	6260.98	Control	0.288	2.35E-04
		Methanopterin_biosynthesis2	203.39	Biochar	0.585	3.08E-04
		p-Aminobenzoyl-Glutamate_Utilization	76.58	Biochar	0.697	1.02E-03
		Pterin_biosynthesis	315.33	Biochar	2.610	1.15E-02
	NAD and NADP	NAD_and_NADP_cofactor_biosynthesis_global	5277.91	Biochar	0.731	4.51E-09
		NAD_consumption	3884.34	Control	0.149	4.63E-04
	Pyridoxine	Pyridoxin_(Vitamin_B6)_Biosynthesis	9698.51	Control	1.332	7.38E-04
	Quinone cofactors	Menaquinone_Biosynthesis_via_Futalosine_--_gjo	631.43	Control	0.296	3.75E-04
	Riboflavin, FMN, FAD	Riboflavin,_FMN_and_FAD_metabolism	6557.91	Control	0.490	1.98E-04
		riboflavin_to_FAD	1874.57	Control	0.670	6.96E-04
	Tetrapyrroles	Heme_and_Siroheme_Biosynthesis	4767.12	Control	0.393	3.50E-22
		Heme_biosynthesis_orphans	390.54	Control	0.739	1.37E-02
DNA Metabolism	DNA recombination	RuvABC_plus_a_hypothetical	3529.85	Control	0.220	1.70E-03
	DNA repair	DNA_repair,_bacterial_DinG_and_relatives	787.58	Biochar	9.268	8.05E-46
		DNA_repair,_bacterial_MutL-MutS_system	1885.43	Biochar	0.656	1.69E-23
		DNA_repair,_bacterial_photolyase	74.40	Control	8.469	5.68E-23
		DNA_repair,_bacterial	6927.65	Biochar	0.457	2.53E-06

		DNA_repair,_bacterial_RecFOR_pathway	5759.12	Control	0.578	4.93E-04
	DNA replication	DNA_topoisomerases,_Type_II,_ATP-dependent	2677.43	Biochar	6.817	2.05E-201
		DNA-replication	27361.48	Biochar	0.480	3.26E-05
	DNA uptake, competence	Gram_Positive_Competence	73.66	Biochar	2.817	3.98E-12
		Late_competence	143.25	Control	2.771	3.21E-11
		DNA_processing_cluster	530.35	Biochar	1.526	4.68E-03
	NULL	Restriction-Modification_System	641.05	Biochar	3.286	3.61E-15
		DNA_phosphorothioation	34.97	Biochar	1.459	6.25E-05
		Type_I_Restriction-Modification	1148.54	Control	0.419	6.82E-05
		DNA_structural_proteins,_bacterial	797.33	Biochar	0.306	2.03E-04
Dormancy and Sporulation	NULL	Persister_Cells	28.95	Biochar	1.971	4.77E-07
		Spore_pigment_biosynthetic_cluster_in_Actinomycetes	153.61	Control	0.494	2.73E-03
		Sporulation_gene_orphans	93.69	Control	0.562	4.85E-03
Fatty Acids, Lipids, and Isoprenoids	Fatty acids	Phospholipid_and_Fatty_acid_biosynthesis_related_cluster	649.60	Biochar	0.923	4.51E-10
		Fatty_Acid_Biosynthesis_FASI	367.73	Control	0.775	1.57E-08
		Fatty_acid_metabolism_cluster	11531.86	Biochar	3.381	1.41E-02
	Isoprenoids	Polyprenyl_Diphosphate_Biosynthesis	861.95	Biochar	3.974	1.70E-216
		Myxoxanthophyll_biosynthesis_in_Cyanobacteria	39.18	Biochar	1.390	3.71E-02
	NULL	Polyhydroxybutyrate_metabolism	32905.19	Control	0.806	1.52E-47
	Phospholipids	Sphingolipid_biosynthesis	759.55	Control	11.541	1.02E-52
		Glycerolipid_and_Glycerophospholipid_Metabolism_in_Bacteria	17173.20	Biochar	0.410	2.82E-19
	Triacylglycerols	Triacylglycerol_metabolism	262.84	Biochar	1.699	2.20E-03
	NULL	Hemin_transport_system	376.17	Biochar	3.053	1.24E-06

Iron acquisition and metabolism		Iron_Scavenging_cluster_in_Thermus	79.16	Biochar	1.119	2.89E-05
		Heme,_hemin_uptake_and_utilization_systems_in_GramNegatives	1088.05	Biochar	0.924	2.46E-04
		Heme,_hemin_uptake_and_utilization_systems_in_GramPositives	264.88	Control	0.918	3.34E-03
		Transport_of_Iron	3914.42	Biochar	0.815	5.05E-03
	Siderophores	Vibrioferrin_synthesis	28.64	Biochar	1.446	6.69E-05
		Siderophore_Pyoverdine	381.28	Biochar	0.412	2.91E-03
Membrane Transport	ABC transporters	ABC_transporter_oligopeptide_(TC_3.A.1.5.1)	3040.15	Control	0.318	3.54E-07
		ABC_transporter_dipeptide_(TC_3.A.1.5.2)	2351.24	Control	0.211	2.61E-03
		ABC_transporter_peptide_(TC_3.A.1.5.5)	49.73	Biochar	1.112	4.58E-03
		Periplasmic-Binding-Protein-Dependent_Transport_System_for_α-Glucosides	608.79	Control	0.367	3.79E-02
		ABC_transporter_branched-chain_amino_acid_(TC_3.A.1.4.1)	6069.28	Control	0.158	4.03E-02
	NULL	Ton_and_Tol_transport_systems	10676.60	Biochar	0.880	2.28E-35
		ECF_class_transporters	792.39	Control	0.792	5.74E-09
		Citrate_Utilization_System_(CitAB,_CitH,_and_tctABC)	148.47	Control	1.546	1.84E-08
	Protein and nucleoprotein secretion system, Type IV	Conjugative_transfer	1104.09	Biochar	0.678	8.88E-09
		Vir-like_type_4_secretion_system	274.66	Biochar	1.304	1.44E-02
	Protein secretion system, Type I	Type_I_protein_secretion_systems	120.36	Biochar	0.935	6.38E-06
	Protein secretion system, Type II	Predicted_secretion_system_W_clustering_with_cell_division_proteins	1244.46	Biochar	1.054	2.81E-16

		General_Secretion_Pathway	1491.91	Biochar	0.338	5.48E-07
	Protein secretion system, Type III	Type_III_secretion_systems	150.70	Biochar	0.898	2.14E-03
		Type_III_secretion_system	54.55	Biochar	1.504	4.90E-02
	Protein secretion system, Type V	Type_Vc_secretion_systems	58.93	Biochar	0.677	1.75E-02
	Protein secretion system, Type VI	Type_VI_secretion_systems	1305.69	Biochar	0.801	3.60E-04
	Protein secretion system, Type VII (Chaperone/Usher pathway, CU)	sigma-Fimbriae	47.04	Biochar	1.210	6.89E-05
	Protein translocation across cytoplasmic membrane	HtrA_and_Sec_secretion	4068.69	Biochar	0.961	7.29E-85
		ESAT-6_proteins_secretion_system_in_Firmicutes	57.88	Control	0.513	4.95E-02
	Sugar Phosphotransferase Systems, PTS	Fructose_and_Mannose_Inducible_PTS	2379.82	Biochar	0.269	1.72E-02
	Uni- Sym- and Antiporters	Multi-subunit_cation_antiporter	703.80	Biochar	0.569	2.05E-05
		Proton-dependent_Peptide_Transporters	428.34	Biochar	0.587	1.68E-04
Metabolism of Aromatic Compounds	Metabolism of central aromatic intermediates	4-Hydroxyphenylacetic_acid_catabolic_pathway	1672.86	Control	0.639	2.21E-06
		Salicylate_and_gentisate_catabolism	2512.92	Biochar	1.500	2.84E-03
		Catechol_branch_of_beta-ketoadipate_pathway	937.03	Biochar	1.782	2.17E-02
	NULL	Benzoate_transport_and_degradation_cluster	3753.18	Biochar	0.594	6.69E-05
		carbazol_degradation_cluster	100.60	Biochar	3.843	3.10E-03
		Chlorobenzoate_degradation	932.89	Biochar	0.584	2.99E-09
		Quinate_degradation	127.67	Biochar	0.845	1.92E-02

	Peripheral pathways for catabolism of aromatic compounds	Naphtalene_and_antracene_degradation	337.92	Biochar	0.369	2.24E-02
Miscellaneous	Plant-Prokaryote DOE project	COG0277	5044.38	Biochar	4.822	0.00E+00
		COG0451	2367.02	Biochar	0.802	6.69E-45
		At3g21300	5899.87	Control	0.938	3.07E-41
		At2g33980_At1g28960	793.38	Control	1.240	2.89E-18
		Experimental_-_Histidine_Degradation	2436.63	Control	0.529	9.18E-15
		Experimental-Ubiquinone_BiosynthesisVDC	4633.43	Biochar	0.701	9.43E-08
		At5g63420	2545.48	Control	0.390	1.50E-07
		YrdC-YciO-Sua5_protein_family	13752.40	Control	0.197	7.05E-06
		At4g38090	155.30	Biochar	0.792	8.55E-05
		Experimental-PTPS	1702.76	Biochar	0.216	3.60E-04
		At5g38900	398.22	Biochar	0.338	1.59E-03
		Single-Rhodanese-domain_proteins	144.05	Biochar	0.634	2.55E-03
		DMT_transporter	3036.52	Biochar	1.534	2.84E-03
		At3g50560	3229.38	Biochar	0.482	3.38E-03
		Iron-sulfur_cluster_assembly	3577.07	Biochar	1.779	6.65E-03
		At1g24340	227.06	Control	0.389	1.15E-02
		At1g01770	233.23	Biochar	0.416	1.78E-02
		PROSC	17702.66	Biochar	0.188	1.78E-02
		COG2302	3548.68	Biochar	0.164	2.23E-02
		At1g10830	51.14	Biochar	2.553	2.50E-02
		Experimental-COG2515	236.27	Control	0.453	2.78E-02
		At1g52510_AT4G12830_(COG0596)	265.59	Biochar	0.705	3.08E-02

		Scaffold_proteins_for_[4Fe-4S]_cluster_assembly_(MRP_family)	3764.74	Control	0.189	4.45E-02
Motility and Chemotaxis	Flagellar motility in Prokaryota	Flagellum	5612.33	Biochar	0.666	1.70E-15
		Flagellum_in_Campylobacter	326.04	Biochar	2.295	2.42E-05
Nitrogen Metabolism	NULL	Denitrification	997.37	Biochar	0.746	3.83E-26
		Ammonia_assimilation	11724.03	Control	0.355	2.91E-04
		Nitrogen_fixation	283.08	Control	0.439	2.11E-03
		Allantoin_Utilization	1038.80	Biochar	1.384	1.15E-02
		Amidase_clustered_with_urea_and_nitrile_hydratase_functions	86.61	Control	0.545	1.48E-02
		Dissimilatory_nitrite_reductase	2066.32	Control	0.215	4.31E-02
Nucleosides and Nucleotides	NULL	Adenosyl_nucleosidases	151.28	Biochar	4.084	6.96E-41
		Hydantoin_metabolism	3036.30	Control	0.398	2.24E-06
	Purines	Xanthine_Metabolism_in_Bacteria	259.68	Control	2.347	3.89E-50
		Purine_Utilization	3741.83	Control	1.383	1.51E-12
	Pyrimidines	De_Novo_Pyrimidine_Synthesis	10154.41	Biochar	0.563	4.50E-24
		Novel_non-oxidative_pathway_of_Uracil_catabolism	1327.09	Biochar	1.357	7.65E-07
Phages, Prophages, Transposable elements, Plasmids	Gene Transfer Agent (GTA)	Gene_Transfer_Agent	372.87	Biochar	1.142	1.32E-07
	Phages, Prophages	r1t-like_streptococcal_phages	813.67	Biochar	2.464	3.21E-23
	Plasmid related functions	Plasmid-encoded_T-DNA_transfer	791.12	Biochar	1.262	5.68E-12
	Transposable elements	Conjugative_transposon,_Bacteroidales	107.62	Biochar	2.670	7.79E-12
		Tn552	863.84	Biochar	5.113	1.29E-05
Phosphorus Metabolism	NULL	P_uptake_(cyanobacteria)	9329.58	Control	0.732	9.32E-07
		Phosphate-binding_DING_proteins	24.81	Biochar	1.589	6.09E-03

		Phosphonate_metabolism	160.40	Biochar	1.046	3.67E-02
Potassium Metabolism	NULL	Glutathione-regulated_potassium-efflux_system_and_associated_functions	795.47	Biochar	0.463	1.27E-09
		Potassium_homeostasis	5556.33	Biochar	0.349	3.33E-09
Protein Metabolism	Protein biosynthesis	tRNA_aminoacylation,_Glu_and_Gln	3875.62	Biochar	0.844	8.66E-60
		tRNA_aminoacylation,_Asp_and_Asn	3924.24	Control	0.334	2.66E-15
		tRNA_aminoacylation,_Pro	1046.92	Control	0.283	1.00E-05
		Translation_termination_factors_bacterial	3174.36	Biochar	0.678	4.65E-04
		Ribosome_SSU_bacterial	7015.94	Control	0.252	5.38E-03
		Trans-translation_by_stalled_ribosomes	1099.60	Control	3.369	5.55E-03
		tRNA_aminoacylation,_Val	1730.94	Control	0.214	7.46E-03
		tRNA_aminoacylation,_Leu	1564.64	Control	0.246	1.85E-02
		Universal_GTPases	11757.08	Control	1.091	2.28E-02
		tRNA_aminoacylation,_Arg	1180.97	Control	0.190	3.90E-02
		Translation_elongation_factor_G_family	177.68	Control	0.371	4.46E-02
	Protein degradation	Putative_TldE-TldD_proteolytic_complex	2017.18	Control	0.655	1.43E-15
		Protein_degradation	1462.49	Biochar	0.273	8.02E-05
		Metalloendopeptidases_(EC_3.4.24.-)	41.14	Biochar	2.939	1.88E-03
		Proteasome_archaeal	507.64	Control	0.700	3.25E-03
		Metallocarboxypeptidases_(EC_3.4.17.-)	360.27	Control	0.285	2.58E-02
	Protein folding	Protein_chaperones	5892.51	Control	1.015	2.48E-93
		Periplasmic_disulfide_interchange	731.22	Control	1.398	3.73E-02
		GroEL_GroES	3661.57	Control	0.300	4.48E-02

	Protein processing and modification	Protein_Acetylation_and_Deacetylation_in_Bacteria	7029.75	Control	0.311	9.71E-07
		Inteins	430.29	Control	0.394	1.61E-03
		G3E_family_of_P-loop_GTPases_(metallocenter_biosynthesis)	10419.93	Control	0.300	1.20E-02
	Selenoproteins	Selenocysteine_metabolism	1695.03	Control	0.324	6.77E-08
		Glycine_reductase,_sarcosine_reductase_and_betaine_reductase	14041.02	Control	0.166	1.23E-05
Regulation and Cell signaling	NULL	Stringent_Response,_(p)ppGpp_metabolism	2987.45	Biochar	1.825	6.33E-108
		DNA-binding_regulatory_proteins,_strays	413.44	Biochar	1.114	2.59E-21
		Coenzyme_F420_synthesis	1717.67	Control	0.593	2.64E-21
		Trans-envelope_signaling_system_VreARI_in_Pseudomonas	95.99	Biochar	2.137	3.92E-06
		WhiB_and_WhiB-type_regulatory_proteins_	144.66	Control	0.755	7.08E-06
		Global_Two-component_Regulator_PrrBA_in_Proteobacteria	215.61	Biochar	0.665	6.82E-05
		Cell_envelope-associated_LytR-CpsA-Psr_transcriptional_attenuators	150.17	Control	0.639	4.50E-03
		Pseudomonas_quinolone_signal_PQS	40.13	Biochar	2.220	8.72E-03
		HPr_catabolite_repression_system	588.04	Biochar	0.518	2.62E-02
	Quorum sensing and biofilm formation	Acyl_Homoserine_Lactone_(AHL)_Autoinducer_Quorum_Sensing_	21.57	Biochar	2.243	9.93E-04
Respiration	ATP synthases	F0F1-type_ATP_synthase	4031.01	Control	0.149	4.11E-02
		Terminal_cytochrome_oxidases	2397.92	Biochar	0.298	2.13E-03

	Electron accepting reactions	Ubiquinone_Menaquinone-cytochrome_c_reductase_complexes	1400.21	Control	0.200	1.82E-02
	Electron donating reactions	CO_Dehydrogenase	6206.32	Control	0.567	9.61E-16
		Respiratory_Complex_I	10530.63	Control	0.220	3.32E-07
		NiFe_hydrogenase_maturation	213.45	Biochar	1.883	4.44E-03
		Respiratory_dehydrogenases_1	7437.16	Biochar	0.770	5.68E-03
		Succinate_dehydrogenase	393.80	Control	0.288	1.82E-02
	NULL	Soluble_cytochromes_and_functionally_related_electron_carriers	3189.36	Biochar	3.166	9.46E-05
		Biogenesis_of_cytochrome_c_oxidases	443.59	Biochar	0.657	4.08E-02
RNA Metabolism	RNA processing and modification	rRNA_modification_Archaea	234.54	Control	5.174	2.47E-81
		mnm5U34_biosynthesis_bacteria	6674.40	Control	1.230	8.53E-24
		RNA_pseudouridine_syntheses	3697.87	Biochar	0.597	2.29E-05
		RNA_3'-terminal_phosphate_cyclase	104.59	Biochar	0.983	1.05E-03
		eukaryotic_rRNA_modification_and_related_functions	356.96	Control	0.822	1.10E-03
		tRNA_modification_yeast_cytoplasmic	1274.58	Biochar	0.898	1.36E-02
		rRNA_modification_Bacteria	7723.40	Biochar	0.374	2.24E-02
		Polyadenylation_bacterial	7894.07	Control	0.321	3.79E-02
		RNA_processing_and_degradation,_bacterial	4430.07	Control	0.189	4.85E-02
	Transcription	RNA_polymerase_bacterial	4820.15	Control	0.386	5.86E-03
Secondary Metabolism	Aromatic amino acids and derivatives	Cinnamic_Acid_Degradation	437.78	Control	1.072	4.97E-02
	Bacterial cytostatics, differentiation factors and antibiotics	Nonribosomal_peptide_synthetases_(NRPS)_in_Frankia_sp._Ccl3	103.66	Control	0.772	2.38E-03

	Biosynthesis of phenylpropanoids	Phenylpropanoids_general_biosynthesis	476.95	Control	0.600	4.76E-05
Stress Response	Heat shock	Heat_shock_dnaK_gene_cluster_extended	9462.52	Biochar	0.561	6.69E-05
	NULL	SigmaB_stress_responce_regulation	1106.91	Control	0.249	2.83E-03
		Phage_shock_protein_(psp)_operon	246.82	Control	0.384	5.43E-03
		Flavohaemoglobin	322.48	Control	0.422	1.40E-02
	Osmotic stress	Osmoregulation	740.20	Biochar	0.371	9.92E-04
		Ectoine_biosynthesis_and_regulation	71.38	Control	0.759	1.39E-02
	Oxidative stress	Glutathione_analogs:_mycothiol	992.06	Control	0.947	2.65E-09
		Regulation_of_Oxidative_Stress_Response	10738.87	Control	0.190	1.51E-03
		Glutaredoxins	802.66	Biochar	0.454	6.08E-03
		Glutathione:_Non-redox_reactions	1174.26	Biochar	0.570	7.54E-03
		Redox-dependent_regulation_of_nucleus_processes	3693.11	Control	1.274	1.37E-02
		Rubrerythrin	726.28	Biochar	0.258	1.42E-02
Sulfur Metabolism	NULL	Galactosylceramide_and_Sulfatide_metabolism	4191.94	Biochar	5.729	1.18E-42
		Thioredoxin-disulfide_reductase	1304.12	Biochar	0.433	1.90E-06
	Organic sulfur assimilation	Alkanesulfonate_assimilation	3680.08	Control	1.063	2.33E-75
		Utilization_of_glutathione_as_a_sulphur_source	972.83	Control	0.187	1.47E-02
		Taurine_Utilization	595.09	Biochar	1.286	1.92E-02
Virulence, Disease and Defense	Adhesion	Mediator_of_hyperadherence_YidE_in_Enterobacteria_and_its_conserved_region	99.93	Biochar	0.628	3.74E-03
	Bacteriocins, ribosomally synthesized antibacterial peptides	Tolerance_to_colicin_E2	135.20	Biochar	0.887	6.55E-08

	Detection	MLST	5606.24	Control	1.502	4.93E-113
	Invasion and intracellular resistance	Listeria_surface_proteins:_Internalin-like_proteins	38.09	Biochar	1.854	6.76E-05
	NULL	C_jejuni_colonization_of_chick_caeca	7954.31	Biochar	0.359	3.59E-05
		Streptococcus_agalactiae_virulome	27.87	Biochar	3.527	2.74E-03
		Bacterial_cyanide_production_and_tolerance_mechanisms	1036.02	Biochar	0.496	6.31E-03
		Streptococcus_pyogenes_Virulome	152.24	Biochar	0.424	1.46E-02
	Resistance to antibiotics and toxic compounds	BlaR1_Family_Regulatory_Sensor-transducer_Disambiguation	4525.03	Biochar	3.941	0.00E+00
		Cobalt-zinc-cadmium_resistance	18685.28	Biochar	0.161	1.73E-19
		Mercuric_reductase	1671.15	Control	0.556	4.09E-15
		Resistance_to_fluoroquinolones	5619.87	Control	1.727	2.36E-10
		Copper_homeostasis	1370.17	Biochar	0.464	3.32E-07
		The_mdtABCD_multidrug_resistance_cluster	706.21	Biochar	0.462	3.95E-07
		Arsenic_resistance	541.25	Control	0.350	1.07E-04
		Copper_homeostasis:_copper_tolerance	577.17	Biochar	2.730	1.71E-03
		Resistance_to_Vancomycin	144.58	Control	0.423	7.20E-03
		Multidrug_Resistance_Efflux_Pumps	5655.27	Biochar	0.523	1.61E-02

APPENDIX C

METAGENOMIC AND STATISTICS AND GENOMIC BINNIG RESULTS

SUPPORTING FINDINGS OF CHAPTER 5

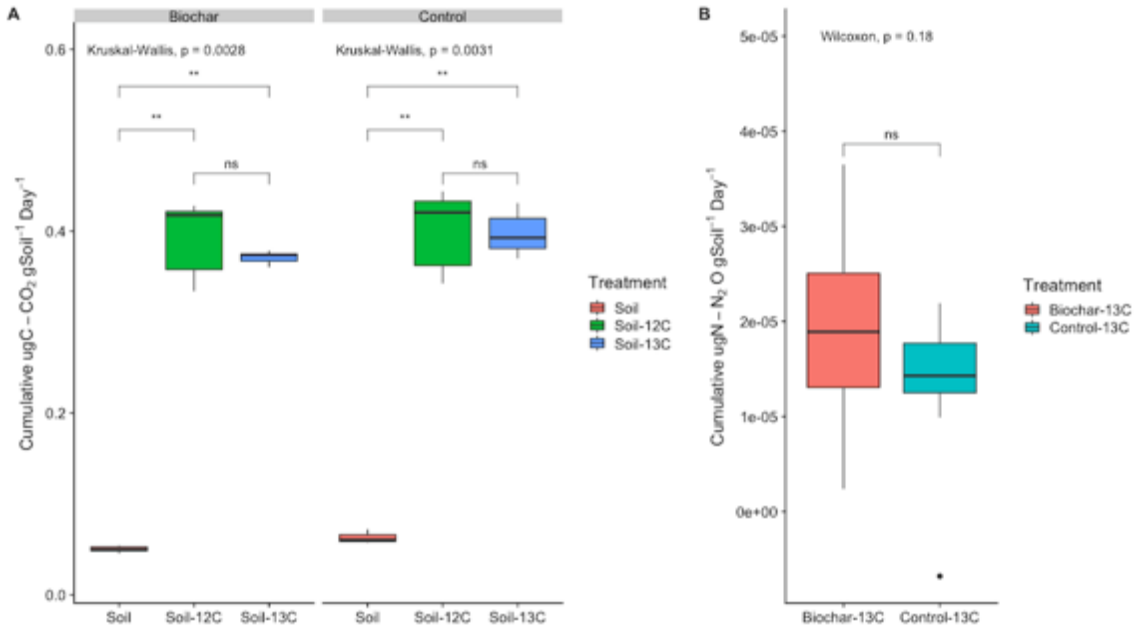


Figure C1. Cumulative gas production rate for microcosms receiving ^{13}C-perennial ryegrass over a 14-day incubation period. Boxplots represent the median, first and third percentiles, range of microcosm (A) CO_2 and (B) N_2O gas production rate (n = 12). ***, $P < 0.001$; **, $P < 0.01$, *, $P < 0.05$.

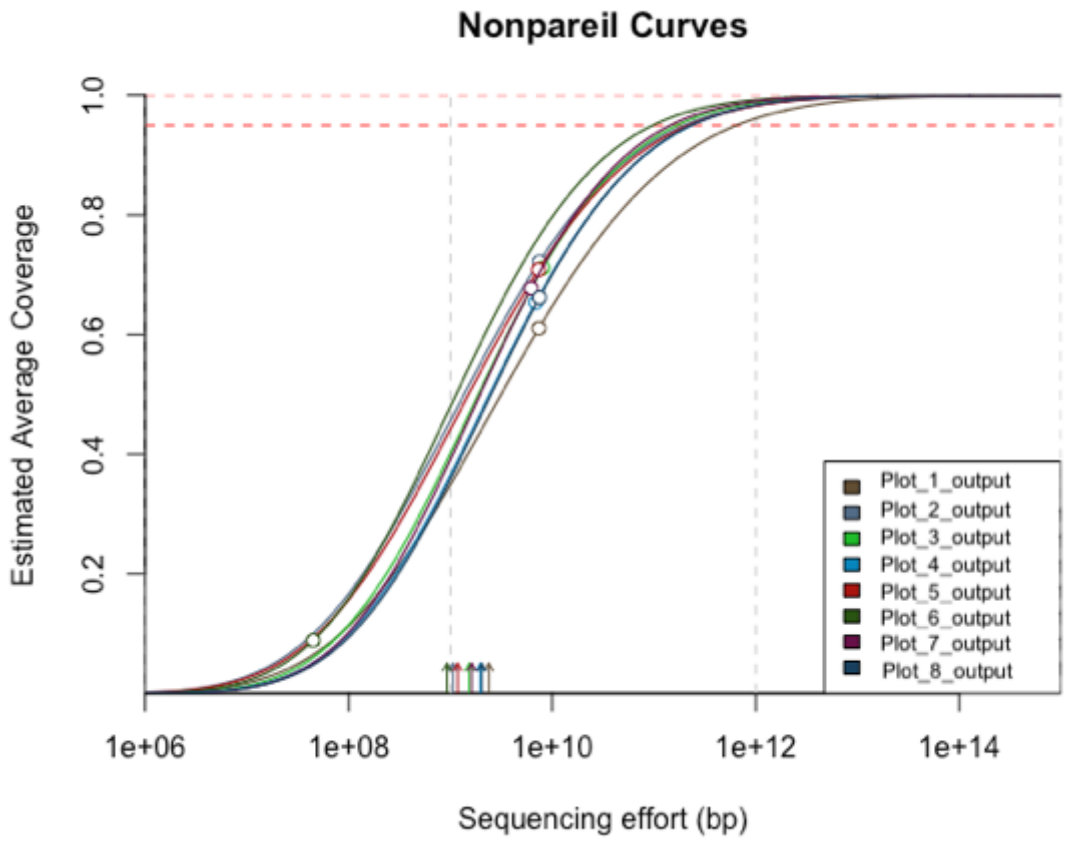


Figure C2. Average coverage of DNA-SIP metagenomes. Estimated from the portion of nonunique reads as a function of the size of subsamples randomly drawn from metagenomes of biochar-amended and control soils. Solid lines indicate the fitted models based on subsampling, the open circles mark the actual size and estimated coverage of the metagenomic dataset, red and pink dashed-line indicates the 95% and 100% average coverage levels, respectively.

Table C1. Soil properties per plot in microcosms incubated with ^{13}C-labeled perennial ryegrass.

		Biochar-amended				Control			
		Plot 1	Plot 3	Plot 4	Plot 8	Plot 2	Plot 5	Plot 6	Plot 7
Soil chemicals	Ca (mg/kg)	1201.2 ± 292.8	1651.1 ± 25.6	1243.0 ± 47.0	2024.5 ± 365.1	2070.0 ± 10.0	1711.6 ± 4.4	1099.0 ± 359.0	1432.8 ± 180.8
	Na (mg/kg)	32.8 ± 3.9	46.1 ± 2.1	30.6 ± 2.2	37.9 ± 3.3	31.1 ± 3.7	37.5 ± 9.9	30.0 ± 3.4	40.8 ± 3.8
	Mg (mg/kg)	214.6 ± 26.4	285.0 ± 10.1	225.9 ± 46.1	273.0 ± 8.1	185.5 ± 32.5	230.2 ± 35.8	229.9 ± 70.1	236.6 ± 35.4
	K (mg/kg)	972.1 ± 17.9	671.9 ± 35.3	1175.0 ± 107.0	923.3 ± 68.7	1050.0 ± 164.0	789.0 ± 203.0	661.0 ± 119.0	653.6 ± 49.6
	C (%)*	1.84 ± 0.31^{ab}	2.15 ± 0.45^{ab}	1.96 ± 0.14^{ab}	2.39 ± 0.02^{a}	1.31 ± 0.03^{b}	1.41± 0.04^{b}	1.38 ± 0.04^{b}	1.38 ± 0.02^{b}
	N (%)	0.17 ± 0. 1	0.17 ± 0. 1	0.17 ± 0.00	0.20 ± 0.01	0.16 ± 0.00	0.16 ± 0.00	0.17 ± 0.00	0.17 ± 0.01
	pH	6.66 ± 0.54	6.99 ± 0.13	6.55 ± 0.01	6.81 ± 0.20	7.40 ± 0.06	6.78 ± 0.10	5.99 ± 0.52	6.46 ± 0.00
	Moisture (%)*	43.56 ± 0.66^{a}	33.55 ± 0.42^{b}	35.40 ± 1.34^{b}	34.17 ± 1.32^{b}	34.33 ± 2.28^{b}	34.90 ± 1.78^{b}	34.08 ± 1.46^{b}	34.08 ± 1.21^{b}

* $p<0.05$, ** $p<0.01$, *** $p<0.001$: One way ANOVA, letters indicate Students Newman-Keul post hoc test

Table C2. Significant and nearly significant results differentially abundant KO terms between biochar-amended and control metagenomes.

KO term	Base Mean	log2Fold Change	Lfc SE	stat	pvalue	padj	KEGG Family	Gene
K00370	363.29	-0.432	0.105	-4.128	3.66E-05	0.03	02020 Two-component system [PATH:ko02020]	narG; narZ; nxrA; nitrate reductase / nitrite oxidoreductase; alpha subunit
K11891	163.55	0.528	0.123	4.275	1.91E-05	0.03	02025 Biofilm formation - Pseudomonas aeruginosa [PATH:ko02025]	impL; vasK; icmF; type VI secretion system protein ImpL
K07347	127.71	0.632	0.153	4.132	3.59E-05	0.03	05133 Pertussis [PATH:ko05133]	fimD; fimC; mrkC; htrE; cssD; outer membrane usher protein
K03286	63.82	0.602	0.155	3.882	1.04E-04	0.06	02000 Transporters [BR:ko02000]	TC.OOP; OmpA-OmpF porin; OOP family
K11904	223.03	0.626	0.162	3.854	1.16E-04	0.06	02044 Secretion system [BR:ko02044]	vgrG; type VI secretion system secreted protein VgrG
K06994	1887.60	-0.384	0.103	-3.747	1.79 E-04	0.07	99996 General function prediction only	K06994; putative drug exporter of the RND superfamily
K03336	326.03	-0.340	0.091	-3.752	1.76 E-04	0.07	00562 Inositol phosphate metabolism [PATH:ko00562]	iolD; 3D-(3;5/4)-trihydroxycyclohexane-1;2-dione acylhydrolase (decyclizing)
K09118	369.50	-0.454	0.124	-3.661	2.51 E-04	0.08	99997 Function unknown	K09118; uncharacterized protein

K11896	125.59	0.466	0.128	3.635	2.78 E-04	0.08	02044 Secretion system [BR:ko02044]	impG; vasA; type VI secretion system protein ImpG
K04768	183.95	-0.432	0.122	-3.551	3.83 E-04	0.09	99981 Carbohydrate metabolism	acuC; acetoin utilization protein AcuC
K03466	1705.56	-0.292	0.082	-3.565	3.64 E-04	0.09	03036 Chromosome and associated proteins [BR:ko03036]	ftsK; spoIIIE; DNA segregation ATPase FtsK/SpoIIIE; S-DNA-T family

Table C3. Characteristics of medium- and high-quality genome bins. Metrics were calculated from CheckM.

Genome Bin I.D.	Average Bin[a] Coverage	Taxonomy[b] (Family-level)	Completeness (%)	Contamination (%)	GC (%)	Size (Mbp)	Coding Density
Biochar-amended soil							
Bin.1_13	9.69	Micrococcaceae	58.62	0	67.5	2.46	91.1
Bin.1_14_1	7.52	Rhizobiaceae	50.86	5.17	64.5	4.14	89.33
Bin.1_17	7.23	Streptomycetaceae	60.28	6.36	71.8	5.90	88.74
Bin.1_18	9.34	Xanthomonadaceae	70.34	3.45	70.5	2.58	91.75
Bin.1_21	38.19	Streptomycetaceae	71.84	5.17	73.1	8.93	88.71
Bin.1_22	16.18	Dermatophilaceae	89.79	3.88	71.8	3.68	91.72
Bin.1_23	15.71	Streptosporangiaceae	67.83	9.05	71.6	8.72	92.46
Bin.1_3	8.40	20CM-4-69-9	84.20	3.74	70.1	3.79	93.92
Bin.1_31_1	8.50	Kribbellaceae	65.16	9.48	68.9	6.79	93.17
Bin.1_32	21.03	Catenulisporaceae	50.63	0	70.7	7.97	89.85
Bin.1_33	9.15	2-12-FULL-66-21	75.34	2.59	68.3	4.73	91.99
Bin.1_35	62.33	Streptomycetaceae	61.34	3.06	71.1	4.86	90.95
Bin.1_36	26.46	Gemmatimonadaceae	90.69	2.75	69.9	3.77	92.86
Bin.1_37	10.67	Sphingomonadaceae	55.63	5.91	64.1	1.84	92.15
Bin.1_6_1	15.22	Micromonosporaceae	71.05	9.65	69.5	5.78	91.92
Bin.3_15	8.74	Burkholderiaceae	79.99	2.52	68.0	4.66	88.90
Bin.3_16	112.83	Streptomycetaceae	56.71	2.79	71.1	6.49	90.81
Bin.3_19	29.67	Streptomycetaceae	88.73	6.45	71.0	10.9	89.54
Bin.3_21	9.38	Gemmatimonadaceae	83.15	3.85	70.2	3.68	91.43
Bin.3_22_1	14.32	Pseudonocardiaceae	60.34	2.59	72.2	5.01	91.22
Bin.3_25	8.30	Mycobacteriaceae	77.85	1.44	68.3	5.03	89.08
Bin.3_28_1	11.83	Dermatophilaceae	50.52	9.42	71.7	1.96	92.53
Bin.3_29	18.84	Micromonosporaceae	79.98	4.30	70.1	7.30	91.71
Bin.3_37	9.01	Mycobacteriaceae	66.18	1.75	68.7	4.19	90.12
Bin.3_38	23.85	Gemmatimonadaceae	89.78	2.75	69.9	3.73	92.75
Bin.3_6	16.81	Xanthomonadaceae	58.62	6.90	67.9	2.44	93.66
Bin.3_8	9.73	Nocardioidaceae	63.95	0	72.9	3.64	93.21
Bin.3_9	14.00	Rhizobiaceae	91.14	3.42	63.1	5.06	88.75
Bin.4_12_3	9.94	Sphingomonadaceae	50.34	6.03	64.0	1.94	92.31
Bin.4_17_1	41.92	Micromonosporaceae	82.48	6.25	70.2	6.73	92.29
Bin.4_18_1	12.46	Streptosporangiaceae	56.66	9.48	71.5	10.1	93.89
Bin.4_20	71.86	Streptomycetaceae	67.70	2.36	70.8	8.76	90.22
Bin.4_3	12.46	Gemmatimonadaceae	85.65	4.4	69.6	4.27	91.77
Bin.4_31	11.82	Gemmatimonadaceae	88.09	7.74	70.3	3.54	91.90
Bin.4_6_1	7.88	Catenulisporaceae	63.79	8.62	70.7	8.21	90.71
Bin.4_9_1_1	9.32	Xanthobacteraceae	68.09	9.32	64.7	4.30	89.11
Bin.4_30_1_1	12.04	Rhodanobacteraceae	92.08	0.94	69.2	3.14	90.43
Bin.8_14	20.20	Haliangiaceae	90.45	3.39	68.3	9.81	93.72
Bin.8_16	17.27	Polyangiaceae	94.91	5.18	66.2	11.9	91.83
Bin.8_18	34.94	Streptomycetaceae	64.47	0	70.5	11.3	88.38
Bin.8_36	34.44	Micromonosporaceae	86.21	3.28	70.3	7.13	92.28
Bin.8_4	16.69	Xanthomonadaceae	79.31	1.72	68.9	4.43	87.29
Bin.8_40	15.16	Dermatophilaceae	87.07	3.80	71.7	3.54	91.67
Bin.8_42	11.74	Gemmatimonadaceae	89.85	2.75	70.2	4.10	91.37
Bin.8_45	78.91	Streptomycetaceae	50.86	1.72	71.1	6.84	90.94
Bin.8_6	31.06	Gemmatimonadaceae	90.49	2.2	69.9	3.75	92.85
Bin.8_9_1_1	8.79	Polyangiaceae	73.39	8.92	67.2	8.26	94.33
Bin.8_17_1_1	8.84	Rhodanobacteraceae	73.45	6.90	69.4	3.21	90.73
Bin.8_41_1_1	46.53	Streptosporangiaceae	56.19	8.62	71.7	8.16	92.64
Control soil							
Bin.2_15	9.78	Streptomycetaceae	63.98	2.90	71.9	6.57	88.73
Bin.2_16	9.89	Microbacteriaceae	62.56	1.35	71.5	2.11	91.89
Bin.2_17	7.22	o_20CM-4-69-9	62.41	9.48	72.2	2.37	94.19
Bin.2_2	48.68	Pseudonocardiaceae	58.91	2.59	71.8	9.92	91.81
Bin.2_21	13.78	Micromonosporaceae	77.19	7.89	71.1	7.32	90.66
Bin.2_23_2	20.43	Streptosporangiaceae	69.68	6.97	71.2	7.47	93.38
Bin.2_23_3	21.83	Streptosporangiaceae	59.04	0.69	71.1	4.12	93.03

Bin.2_24	26.22	Micromonosporaceae	96.48	1.93	69.1	7.45	91.71
Bin.2_3	11.48	QHCE01	95.33	1.26	58.5	3.05	90.84
Bin.2_31	154.23	Streptomycetaceae	71.86	0.54	70.7	8.02	89.48
Bin.2_36	8.93	Pseudonocardiaceae	50.34	3.45	72.1	8.71	90.84
Bin.2_7	13.36	Sphingomonadaceae	88.96	8.83	64.4	2.29	93.71
Bin.5_1	12.81	Nocardioidaceae	90.78	5.04	72.5	4.71	92.4
Bin.5_13	40.30	Dermatophilaceae	74.23	0.63	71.9	3.26	91.73
Bin.5_19	15.38	Gemmatimonadaceae	91.97	2.75	70.2	4.04	91.54
Bin.5_20	164.13	Streptomycetaceae	57.76	1.72	71.2	6.20	91.03
Bin.5_27	12.34	Micromonosporaceae	83.74	6.06	71.3	4.26	91.08
Bin.5_30	22.91	Streptosporangiaceae	76.90	9.33	71.6	8.29	92.52
Bin.5_34	17.65	Micrococcaceae	55.17	3.45	67.4	2.70	91.36
Bin.5_5	28.65	Gemmatimonadaceae	90.69	2.75	69.9	3.77	91.91
Bin.6_1_1	21.92	Streptomycetaceae	85.81	9.65	70.0	11.0	87.19
Bin.6_17	10.33	Dermatophilaceae	55.57	1.09	71.3	2.03	92.07
Bin.6_18	7.72	Sphingomonadaceae	90.50	4.27	64.9	2.34	93.07
Bin.6_19	8.01	Micrococcaceae	72.40	2.01	68.6	2.74	91.35
Bin.6_2	8.65	Gemmatimonadaceae	73.43	2.20	69.5	2.97	91.59
Bin.6_3	8.27	Acidobacteriaceae	90.30	1.94	58.3	5.17	89.72
Bin.6_6	12.51	Gemmatimonadaceae	85.93	4.72	69.6	3.81	92.05
Bin.6_9	75.61	Catenulisporaceae	88.53	3.86	70.9	9.53	90.18
Bin.7_11	10.13	Streptomycetaceae	52.25	5.70	71.7	5.29	88.12
Bin.7_12	30.29	Streptosporangiaceae	81.48	7.75	71.3	9.15	92.13
Bin.7_13	29.74	Gemmatimonadaceae	88.68	2.20	69.9	3.71	92.85
Bin.7_14	8.84	Mycobacteriaceae	76.00	1.42	68.3	5.18	89.09
Bin.7_19_2	20.78	Streptomycetaceae	50.86	8.19	71.2	10.9	89.14
Bin.7_20	23.97	Dermatophilaceae	89.76	5.89	71.7	3.72	91.77
Bin.7_21	12.05	Burkholderiaceae	87.47	0.31	68.0	4.83	88.69

[a] Bin coverage is calculated using perl script. Bin coverage is weighted by the length

[b] Taxonomy determined using GTDB-Tk at the family level